Bacterial communities associated with chronic rhinosinusitis and the impact of mucin degradation on *Staphylococcus aureus* physiology

A DISSERTATION

SUBMITTED TO THE FACULTY OF THE

UNIVERSITY OF MINNESOTA

BY

Sarah Kathleen Lucas

IN PARTIAL FULFILLMENT OF THE REQUIREMENTS

FOR THE DEGREE OF

DOCTOR OF PHILOSOPHY

Advisor: Ryan C. Hunter

August 2020

Acknowledgements

First, this thesis was made possible by the support of the Microbiology, Immunology, and Cancer Biology graduate program, and the faculty and staff of the Department of Microbiology & Immunology at the University of Minnesota. The contribution of the research community and resources available to me at the University of Minnesota cannot be overstated, and I feel very fortunate to have had the opportunity to work within a community that upholds high scholarly standards and are also a pleasure to be around. I would like to extend my deepest gratitude to several individuals for their support during my doctoral training:

My advisor, Dr. Ryan Hunter: Thank you for the confidence you had in me, especially in the times when I scarcely believed in myself. Thank you for your patience, and for being the first true mentor I ever had.

My labmates: it was a pleasure to conduct research alongside you all. My daily sounding boards for far-out ideas, and encouragement to jump into experiments and just "see what happens".

The members of my thesis committee: Gary Dunny, Mark Herzberg, and Dan Knights. Thanks for all the great feedback in our meetings. Your comments on my work over the years have always been constructive. There would be times in our annual meetings where I would find great motivation in your enthusiasm of the data I presented. I hope I have absorbed some of your wisdom these past few years.

Dylan White, Elise Breed, and Mark Daniel: thank you for your friendship and camaraderie over the years. Your willingness to grab a beer together at Stub and Herbs at the end of a long day made a world of difference.

My family, Mom, Dad, Andrea, and Conrad: thank you for being a strong support system for me. For sharing in all the ups and downs that happen. For still reacting with shock every Minnesota winter when I convey the weekly weather report.

Monica DiMuzio and Jessica Myers: You two are my rocks. My best friends since grade school. Thank you for your almost daily support. Our friendship has seen a lot of "education".

And last, but not least, my husband Dr. Christopher Fernandez: I am so fortunate to be married to someone I admire and love as much as you. Thank for being my home wherever our geographical home may be.

Table of Contents

List of Tables ..... **iv**

List of Figures ..... **v**

Chapter 1: Introduction **1**

Chronic rhinosinusitis: epidemiology, etiology, and treatment 2

Bacteriology of Chronic Rhinosinusitis 7

New hypotheses: Mucin-microbe interactions in CRS 14

Chapter 2: 16S rRNA gene sequencing reveals site-specific signatures of the upper and lower airways of cystic fibrosis patients† 17

Summary 18

Introduction 19

Materials and Methods 21

Results 24

Discussion 31

Acknowledgements 34

Figures 35

Chapter 3: The microbiome of chronic rhinosinusitis in a cystic fibrosis patient cohort at University of Minnesota 40

Summary 41

Introduction 42

Materials and Methods 44

Results 47

Discussion 50

Acknowledgements 51

Tables 52

Figures 55

Chapter 4: Anaerobic mucin degrading bacterial communities differentiate the microbiome in chronic rhinosinusitis and can impact physiology of nasal pathobiont *Staphylococcus aureus*..... 59

Summary..... 60
Introduction..... 62
Materials and Methods..... 65
Results..... 71
Discussion..... 80
Acknowledgements..... 85
Tables..... 87
Figures..... 92

Chapter 5: Conclusion..... 100

Summary of research..... 101
Future Directions..... 104
Concluding Remarks..... 106

Bibliography..... 109

Appendices..... 131

Appendix A: Supplementary Information for Chapter 2 - 16S rRNA gene sequencing reveals site-specific signatures of the upper and lower airways of cystic fibrosis patients †..... 132
Appendix B: Bioorthogonal non-canonical amino acid tagging reveals translationally active subpopulations of the cystic fibrosis lung microbiota†..... 143

List of Tables

Table 3.1 CF-CRS patient clinical information 52
Table 3.2 Prevalence and abundance of ASVs of top 20 genera in CF-CRS samples 53
Table 4.1 Demographic and clinical data for FESS patients 87
Table 4.2 Prevalence and average relative abundance of anaerobe features* in CRS and non-CRS samples..... 88

List of Figures

Figure 2.1 Bacterial Load in Sinus and Lung Samples. 35
Figure 2.2 Bacterial community composition of the upper and lower airways. 36
Figure 2.3 Alpha diversity of CF maxillary sinuses differs from CF lung sputum. 37
Figure 2.4 Ordination of weighted Unifrac distances. 38
Figure 2.5 BugBase analysis of PICRUSt-predicted metagenomes. 39
Figure 3.1 CF-CRS sinus communities differentiate by Proteobacteria or Firmicutes. ... 56
Figure 3.2 DPCoA of bacterial community composition with clinical factors..... 57
Figure 3.3. Shannon diversity and dominant *Pseudomonas* or *Staphylococcus*. 58
Figure 4.1 Bacterial diversity differs between CRS and non-CRS samples..... 92
Figure 4.2 Relative abundance of Bacterial phyla in CRS and non-CRS samples. 93
Figure 4.3 Predicted CAZy enzyme classes for CRS and non-CRS samples. 94
Figure 4.4 Anaerobic mucin enrichment cultures of CRS sinus mucus. 95
Figure 4.5 *S. aureus* growth on mucin under aerobic and anaerobic conditions. 96
Figure 4.6. *S. aureus* growth on CFS from CRS mucin-degrading communities. 97
Figure 4.7. RNA-seq reveals impact of mucin degradation and fermentation on *S. aureus* transcription. 99

Chapter 1: Introduction

Chronic rhinosinusitis: epidemiology, etiology, and treatment

Epidemiology

Rhinosinusitis (RS) is an inflammatory syndrome affecting 6-15% of the general population (Fokkens et al., 2020; National Center for Health Statistics, 2019). RS encompasses a wide range of sinonasal symptoms including nasal congestion or discharge, facial pain or pressure, loss of the sense of smell, polyposis, mucopurulent discharge, and edema or obstruction of the sinuses and nasal cavity (Fokkens et al., 2020; Orlandi et al., 2016). Chronic rhinosinusitis (CRS) is the persistence of symptoms beyond 12 weeks and has a prevalence of 5% of the general population (Hoggard et al., 2017). The costs of CRS are substantial at the individual and population levels (Bhattacharyya, 2011). This debilitating disease causes a significant decline in quality of life, including a reduction in physical wellbeing, and loss of the ability to work (Fokkens et al., 2020; Orlandi et al., 2016). Individuals with CRS experience a significantly greater number of primary care visits compared to the general population (Bhattacharyya, 2011). The estimated economic burden of CRS in the United States to be $22 billion USD in direct and indirect costs, translating to $8,200-$10,500 per patient (Smith et al., 2015).

Etiology

Although CRS has been researched for decades, its etiology remains unclear. Early studies favored an infection model of disease, whereby a pathogenic microorganism is causal to CRS. Until recently, the sinuses were considered sterile, and any presence of microorganisms to be pathogenic (Cook and Haber, 1987; Hamad et al., 2009; Sobin et al., 2009). A 1981 study by Itzhak Brook was the first the document aerobic and anaerobic

microbiology in the healthy human sinuses. Since then, it is now accepted that microbial life exists in the upper respiratory tracts of individuals with and without respiratory disease. Additionally, the prevalence of canonical pathogens such as *Staphylococcus aureus* in the upper respiratory tract of up to 50% healthy individuals without any sinonasal symptoms has been confounding (Bassis et al., 2014; Gorwitz et al., 2008; Wertheim et al., 2005). More recently, hypotheses implicating genetic, atopic, and inflammatory processes in immune barrier dysfunction have become more prominent (Hoggard et al., 2017; Lam et al., 2015). The most inclusive models suggest both barrier disruption and microbial pathogenesis to be intertwined in the development of CRS, however mechanisms of host-microbial feedback in the progression to a state of chronic inflammation have not been characterized.

Genetic susceptibility constitutes at least one basis for CRS development. Several syndromes with established genetic components have CRS as a clinical consequence, including primary ciliary dyskinesia, and cystic fibrosis (CF) (Hsu et al., 2013). It is estimated that 90% of people with CF have CRS, making it an important comorbidity to study in this population (Chaaban et al., 2013; Hamilos, 2016). Indeed, even carriers of mutations in the CFTR gene (whose gene product absence or dysfunction is responsible for CF) are at higher risk of CRS development (Wang et al., 2005), underlying the importance of homeostatic mechanisms maintaining barrier function at respiratory mucosal surfaces. Sinonasal pathogen colonization has been linked to lung infections that are the primary cause of most morbidity and mortality in the CF population, suggesting both microbial and inflammatory processes in the sinuses are integral to the health of a unified

airway (Illing and Woodworth, 2014). Chapters 2 and 3 of this dissertation focus on CF-associated CRS, and explore the relationship between pulmonary and CRS microbiota.

Aside from genetic factors, the majority of hypotheses for CRS etiology focus on prolonged abnormal inflammatory response, responsiveness to treatments, and associated environmental stimuli such as allergens, toxins, and microorganisms. The most frequently used method for categorizing CRS is based on the presence or absence of nasal polyps, termed CRSwNP and CRSsNP, respectively (Fokkens et al., 2020). This is the context in which most current etiological theories are framed, however, there is no current explanation that completely supports the division of cases into these two subtypes. Regardless, obstruction of the upper airway passages is universal to both CRSwNP and CRSsNP.

Efforts to define disease "endotypes" consider the additional involvement of immune barrier dysfunction in CRS (Fokkens et al., 2020; Lam et al., 2015). Defects in physical properties of the mucosal layer, mucociliary clearance, antimicrobial peptide production and cell surface receptor function, and integrity of epithelial cell tight junctions are considered in this model, and it is most inclusive to CRSwNP and CRSsNP. Allergy and atopic disease may likely constitute another disease endotype, however the association is still poorly defined (Marcus et al., 2019).

Finally, there is consensus that bacterial infection is an integral component to pathogenesis in CRS. It is still unclear whether the dysfunctional inflammatory response, sinus blockage, and reduced mucociliary clearance in CRS result in, or are caused by shifts in sinus bacteria. Current hypotheses include single pathogen virulence (e.g.

Staphylococcus aureus superantigen expression), bacterial biofilm formation, and microbiome dysbiosis (Foreman et al., 2011; Hoggard, Biswas, et al., 2017; Ou et al., 2014). It is likely the development of CRS is multifactorial, involving both infection and host-inflammatory components.

Treatment

Antibiotics are a mainstay of rhinosinusitis (RS) treatment. In a five-year study, antibiotics were prescribed in 80% of all outpatient visits with a diagnosis of RS, and 50% of CRS visits (S. Smith et al., 2013). During that period RS/CRS made up 11% of all adult clinic visits resulting in an antibiotic prescription, the highest of any other measured diagnosis (S. Smith et al., 2013). These data are remarkable, because a number of medical consensus reports do not recommend antibiotics as part of standard clinical care for RS (Fokkens et al., 2020; Orlandi et al., 2016), and the use of antibiotics in CRS is controversial (Hoggard, Mackenzie, et al., 2017). Several clinical trials have shown limited evidence for the efficacy of antibiotics in the treatment of CRS. One review found that antibiotics benefitted the patient only when prescribed post-surgery (Lim et al., 2008). Other studies have shown antibiotics improve patient outcomes only in culture-directed scenarios where a known antibiotic-susceptible pathogen was identified, and symptoms such as purulent secretions, site pain, and fever point to acute bacterial infection (Huang and Govindaraj, 2013; Lim et al., 2008). Hypotheses for reduced efficacy of antibiotic treatment in CRS include inflammation-mediated blockage of the sinuses - reducing access to the infection site, polymicrobial biofilm formation, and antibiotic resistance mechanisms (Kennedy and Borish, 2013).

In contrast to current recommendations for antibiotic treatment of CRS, there is evidence for the efficacy of treatments that reduce inflammation and relieve sinonasal blockage. Topical steroids and hypertonic saline rinses have both been associated with CRS symptom relief (Huang and Govindaraj, 2013; Rudmik et al., 2012). Functional endoscopic sinus surgery (FESS) employed to remove polyps, physically debride the sinuses, and open up the sinonasal cavity has also been shown to have largely positive outcomes for CRS patients who have failed prior medical interventions (Chester et al., 2008). The higher rates of effectiveness of these treatments underscores the convergence of etiological hypotheses on sinus blockage and inflammation as major drivers of this disease.

The high prevalence and heterogeneity of CRS call for the development of new treatments. One concern is the contribution of antibiotic use for RS and CRS to the global public health issue of antibiotic resistance, however clinical perspectives on antibiotic use for the treatment of RS and CRS are beginning to change (Essack and Pignatari, 2013; Kennedy and Borish, 2013). Although more proven, FESS is an invasive procedure, and between 17-25% of CRS patients will require further surgical treatment within 10 years of undergoing FESS (T. L. Smith et al., 2019). This thesis presents an improved understanding of the microbial ecology in CRS, which may guide the development of more strategic treatment of pathogenic bacteria in CRS.

Bacteriology of Chronic Rhinosinusitis

The Bacterial contribution to CRS

Unifying all potential causes of CRS is the resulting mucus stasis, which contrasts the constant movement of mucus out of the healthy respiratory system. Mucociliary clearance, facilitated by the synchronized beating of cilia lining the pseudostratified epithelium of the airways, allows the constant movement of particulates - including microorganisms - to be shuttled out of the airways. In CRS, this process becomes dysfunctional, leading to microenvrionmental perturbations that both impact and are potentially influenced by microorganisms present in this niche. Bacterial proliferation and virulence, polymicrobial biofilm formation, or changes in the diversity of bacteria (presence and abundance), are all considered potential pathogenic mechanisms in CRS that are not mutually exclusive (Hoggard, Mackenzie, et al., 2017). While the bacteriology of healthy and CRS sinuses is increasingly well described, the role of bacteria in CRS pathogenesis remains unclear, and our ability to understand the disease is constrained when observations are limited to a single timepoint in a cross-sectional study design.

Early culture work

Early culture-based studies contextualized any bacterial presence in the sinuses to be pathogenic, and often focused on the recovery and *in vitro* characterization of a causative pathogenic organism. Bacteria commonly recovered in these studies included *Staphylococcus aureus*, *Moraxella* spp., *Haemophilus influenzae,* and *Pseudomonas aeruginosa* (Hoggard, Mackenzie, et al., 2017). These organisms remain the most

frequently identified pathogens in CRS by culture, however, numerous culture-based surveys have expanded our knowledge of sinus-associated bacteria to include more members of the aerobic and facultative anaerobic genera *Staphylococcus, Haemophilus, Pseudomonas, Streptococcus,* and *Corynebacterium* (Bhattacharyya and Kepnes, 1999; Brown et al., 1998; Finegold et al., 2002; Hauser et al., 2015; Kaspar et al., 2015; Nadel et al., 1998). A study by Kaspar et al. found 139 different bacterial species in a cohort of 16 non-CRS and 18 CRS patients, and showed *Streptococcus epidermidis, S. aureus, Propionibacterium acnes, Propionibacterium avidum, Propionibacterium granulosum, Corynebacterium accolens, Corynebacterium tuberculostearicum,* and *Finegoldia magna,* comprised the most frequently isolated organisms, regardless of disease state (Kaspar et al., 2015). The greatest diversity was seen in the genus *Corynebacterium*, with 23 different species identified. The study stressed a lack of bacterial identification associated with CRS status, and confirmed high inter-subject variability seen in other studies. Indeed, asymptomatic prevalence of *S. aureus* in the sinonasal cavity of adults is estimated ~50% (Bassis et al., 2014; Gorwitz et al., 2008; Wertheim et al., 2005). Occurrence of these organisms in both healthy and CRS subjects suggests that the potential for virulence of any single organism depends on factors controlled by the infection microenvironment such as available nutrients and co-colonizing organisms. These parameters are difficult to approximate *in vitro*.

In an effort to describe bacteriology unique to CRS, a hypothesis emerged that anaerobic bacteria were prevalent and associated with pathogenesis. Besides the recognized inflammation and reduction in mucociliary clearance, characterization of the

physical and chemical aspects of the CRS sinus environment, including oxygen consumption by aerobic organisms and innate immune cells, hypoxia-induced mucus hypersecretion, and increased sinus pressure, support the idea that the CRS sinuses provide a low-oxygen niche for anaerobe proliferation. The association of anaerobes with chronic infections is not unprecedented and has been described at other epithelial sites. For example, Flynn et al. demonstrated mucin-degrading consortia can be isolated from CF sputum, and mucin-degradation byproducts can augment growth of *P. aeruginosa* (Flynn et al., 2016). Additionally, in chronic wounds, anaerobe co-occurrence with common wound pathogens such as *S. aureus* has also been described (Choi et al., 2018; Wolcott et al., 2016).

Several studies support a role for anaerobic bacteria in CRS. In a 2011 review, 18 studies using culture-based techniques found that anaerobes comprised 8-93% of isolates from 32-100% of patients tested (Brook, 2011). Variability in recovery may be the result of differences in sampling and/or culture technique, but also may indicate that the presence of anaerobic bacteria may have a temporal relationship with CRS disease progression. In one of the only longitudinal microbiology surveys of CRS to date, Brook and colleagues evaluated sinus aspirates in five patients with repeated failures of antibiotic management over the course of 34-50 days, nearing the threshold for defined chronic disease (12 weeks) (I Brook et al., 1996). Results suggested that failure to respond to antibiotic therapy was associated with the presence of antibiotic resistant aerobic bacteria, and the emergence of *Fusobacterium nucleatum*, pigmented *Prevotella*, *Porphyromonas* spp., and *Peptostreptococcus* spp. in the subsequent aspirate. Symptoms in these patients were only

resolved through the administration of an antibiotic cocktail with activity against these organisms, or surgical sinus drainage. In one of the most detailed studies of the diversity of anaerobic organisms in CRS, Finegold and colleagues found that while antibiotic treatment failure was more associated with aerobic bacteria *S. aureus* and *P. aeruginosa*, the recurrence of CRS symptoms after successful treatment were twice as frequent when anaerobes were present at greater than 10^3 colony forming units (Finegold et al., 2002). Interestingly, Brook and Frazier found that anaerobes were associated with CRS patients who had not had previous sinus surgery (Itzhak Brook and Frazier, 2001). Taken together, these results suggest that selective pressures exist in the establishment of CRS that promote growth of anaerobic bacteria. Without surgical management anaerobes may establish synergistic polymicrobial communities that become difficult to eradicate.

Similar to the aerobic culture results, differential identification of anaerobes associated with CRS is still confounded by their regular isolation from non-CRS sinuses. Kasper et al. described isolation of species from *Finegoldia, Fusobacterium, Prevotella, Veillonella, Anaerococcus, Parvimonas, Clostridium, and Peptoniphilus* from the sinuses regardless of CRS status (Kaspar et al., 2015). The high similarity of bacterial taxa found in both CRS and non-CRS sinuses calls for new approaches to determine their pathogenic contribution of bacteria in this niche.

The Sequencing Perspective

Clinical culture remains the gold standard for pathogen identification and guidance of antibiotic administration in sinusitis cases, however, clinical cultures fail to grow

bacteria in up to 45% of CRS cases, suggesting that cultivability is a barrier to bacterial identification (Hauser et al., 2015; Mantovani et al., 2010). Use of culture-independent methods that depend on nucleic acids for identification of microorganisms relieves the culture constraint and is demonstrably better at capturing bacterial diversity among human-associated microbiota. A frequently used method of molecular identification is targeted sequencing of the variable regions of the 16S rRNA gene, which are able to phylogenetically differentiate bacteria. In CRS, 16S rRNA gene sequencing (16S) identifies up to an order of magnitude greater bacterial taxa compared to culture alone (Bassiouni et al., 2015; Hauser et al., 2015; Ramakrishnan et al., 2015). Even in the ambitious culture-based study by Kasper et al., 16S recovered more unique bacterial taxa, albeit species resolution was accomplished less often. This increased ability to identify bacteria in the CRS niche allows for better approximation of bacterial diversity.

In agreement with culture-based studies, 16S surveys demonstrate high interpatient variability in microbial community composition and identify the most prevalent genera in sinus communities regardless of disease status are *Staphylococcus, Corynebacterium,* and *Propionibacterium*. Without the constraint of cultivation, detection of anaerobic bacteria in the sinuses is common in molecular surveys and are detected in both CRS and non-CRS samples (Hoggard, Mackenzie, et al., 2017). Despite many attempts at using these high-resolution techniques to compare CRS to non-CRS microbiota, no strong patterns have emerged. When 16S genes are quantitated, there is no significant difference in gene copy number between CRS and non-CRS subjects, suggesting that increased bacterial load cannot explain pathogenesis completely in CRS. Several studies have shown that sinus

bacterial communities demonstrate a spectrum of diversity with CRS microbiota generally considered to be less diverse than non-CRS, however the significance of this comparison varies (Abreu et al., 2012; Biswas et al., 2015; Feazel et al., 2012; Ramakrishnan et al., 2015). In two separate studies, Ramakrishnan et al. found lower diversity communities to be associated with comorbidities asthma and purulent sinus secretions, while cigarette smoking was associated with lower diversity in both non-CRS and CRS subjects. Furthermore, patients whose samples exhibited higher bacterial diversity had better outcomes after surgery (Ramakrishnan et al., 2015; Ramakrishnan and Frank, 2015). Currently, the description of bacterial diversity has had limited value in differentiating the bacterial communities of CRS from non-CRS. These data indicate, however, that use of patient clinical parameters, coupled with longitudinal sampling and larger cohorts are promising ways of stratifying CRS disease for more informative diversity comparisons.

Molecular surveys have also been used to identify associations of individual organisms with CRS. Abreu et al. used the 16S-based PhyloChip approach to show increased relative abundance of *Corynebacterium tuberculostearicum* in CRS. Importantly, this is the only study of CRS microbiota to corroborate their findings *in vivo*. In a murine model of CRS, *C. tuberculostearicum* inoculation in animals with antibiotic-depleted sinus microbiota exhibited goblet cell hyperplasia - a common indicator of sinus pathology (Abreu et al., 2012). In contrast, another study found *C. tuberculostearicum* to be associated with better FESS outcomes and milder disease compared to *S. aureus* (Ramakrishnan et al., 2015). In a study by Cope et al., samples clustered into subgroups based on the dominance of either *Streptococcaceae, Pseudomonadaceae,*

Corynebacteriaceae, or *Staphylococcaceae,* with non-CRS subjects only appearing in clusters dominated by *Streptococcaceae* and *Corynebacteriaceae* (Cope et al., 2017). Interestingly, several studies have now demonstrated a reciprocal relationship between *S. aureus* and *Corynebacterium* spp. abundance, and antagonistic interactions *in vitro* (Lina et al., 2003; Mackenzie et al., 2017; Ramsey et al., 2016; Yan et al., 2013). Pathogenic mechanisms may not be revealed through bacterial identification alone.

Given the results of both culture-dependent and independent surveys, it is apparent that the contribution of sinus microbiota to chronic disease is complicated. The high variability seen in CRS necessitates stratification of the disease in clinically meaningful ways. To this end, Chapters 1 and 2 contribute much needed molecular surveys of sinus and lung microbiota in CF-specific CRS. Conclusions made from recent studies discussed in this section are (a) the mere detection of a suspected pathogenic bacterium in the sinuses is not necessarily associated with disease, and (b) high interpatient variability in both health and disease. These conclusions serve to point research objectives in a new direction that explores ecological parameters of the CRS microenvironment. These include bacterial community facilitated functions that may loosely be related to taxonomy but have a large impact on disease.

New hypotheses: Mucin-microbe interactions in CRS

Mucus is a viscous secreted gel matrix that coats many epithelial surfaces in the body. In the healthy human respiratory tract, mucus sits on top of a periciliary fluid layer and is in constant motion across the pseudostratified epithelium, propelled by coordinated ciliary beat function. Mucus serves several roles for maintaining homeostasis including maintaining hydration and carrying out innate immune barrier functions. Despite its major role in protecting the epithelium, respiratory mucus is also the site of dense microbial life. Mucus-mediated mechanisms involved in microbial pathogenesis have been investigated for decades, yet our understanding of this dynamic relationship is still evolving.

There are at least three mucus-related processes that occur in CRS. First is goblet cell hyperplasia, or increased development of mucus secreting cells in the sinus epithelium (Majima et al., 1997; Petruson, 1994; Tos and Mogensen, 1984). Second is increased mucus production observed both in expression-based studies, and patient symptom presentation (Ding and Zheng, 2007; Kim et al., 2004). Third is the slowing of mucus clearance, mediated by reduced ciliary beat and inflammatory swelling (Stevens et al., 2015). Based on these mechanisms, static mucus becomes a dominant component of the CRS microenvironment.

The major components of mucus are mucins - glycoproteins that are heavily decorated with *O*-linked glycans attached to tandem repeating elements rich in proline, serine and/or threonine residues. N- and C- termini are cysteine-rich regions important for its multimeric gel-forming properties (Wagner et al., 2018). By weight, glycans make up 80% of the mass of these molecules (Bansil and Turner, 2006). The complex and diverse

glycan structures scaffolded on protein backbones are composed primarily of five monosaccharides (galactose, N-acetylglucosamine (GlcNAc), N-acetylgalactosamine (GalNAc), fucose, sialic acid) (Bansil and Turner, 2006). Mucin glycoproteins produced in the respiratory tract include MUC5B, MUC5AC, MUC1, MUC4, and MUC16 (Zanin et al., 2016).

Mucins have several functions with implications for microbial ecology and virulence potential. The immense diversity of glycan structures on mucins have been appreciated as cues for microbial metabolism, virulence, interbacterial interaction, and aggregation (Wagner et al., 2018). The oligomerization of mucins results in a physical matrix that creates nutrient and oxygen gradients which are hypothesized to be important for spatial niche partitioning and stable assembly of multi-species in the gastrointestinal tract (Wagner et al., 2018). Finally, mucins can act as a nutrient source to those microorganisms with specialized enzymes to degrade them (Bradshaw et al., 1994; Derrien and Passel, 2010; Hoeven and Camp, 1991; Wickström et al., 2009). Most microorganisms do not have the enzymatic repertoire to completely degrade a mucin glycoprotein, therefore, mucin as a nutrient source is thought to promote metabolically stable communities with diverse enzymatic functions that act to competitively exclude less well adapted organisms. The ecological function of competitive exclusion is often seen as a positive outcome of stability of mucin-utilizing communities in the gut and oral cavity (Bergstrom and Xia, 2013; Buffie and Pamer, 2013; Hibbing et al., 2010; Malago, 2015). Alternatively, this stability may contribute to chronic infection in the sinuses by reducing therapeutic effectiveness and producing metabolites and chemical signals that may

potentiate virulence in commensal microorganisms. In Chapter 4, we predict the presence of anaerobic mucin-degrading communities in CRS sinus mucus, show their presence in *in vitro* enrichment experiments, and demonstrate their ability to alter *S. aureus* growth and transcription.

Taken together, mucin glycoproteins likely influence many aspects of microbial behavior seen in the sinuses. This thesis presents a novel investigation into bacterial mucin degradation with respect to CRS pathogenesis.

Chapter 2: 16S rRNA gene sequencing reveals site-specific signatures of the upper and lower airways of cystic fibrosis patients†

---

† Reprinted from *Journal of Cystic Fibrosis*. Sarah K. Lucas, Robert Yang, Jordan M. Dunitz, Holly C. Boyer, and Ryan C. Hunter. "16S rRNA gene sequencing reveals site-specific signatures of the upper and lower airways of cystic fibrosis patients." ©
European Cystic Fibrosis Society. Originally published by Elsevier B.V. in *Journal of Cystic Fibrosis* 17 (2018) 204-212. DOI: https://doi.org/10.1016/j.jcf.2017.08.007

Summary

Metastasis of sinus microbiota in cystic fibrosis (CF) patients may have significant implications in the development of chronic lung disease. Here, we compare bacterial communities of matched sinus and lung mucus samples from CF subjects undergoing endoscopic surgery for treatment of chronic sinusitis. Mucus was isolated from the sinuses and lungs of twelve patients. 16S rRNA gene sequencing was then performed to compare the structure and function of CF airway microbiota. Bacterial richness was comparable between airway sites, though the sinuses harbored a higher prevalence of dominant microorganisms. Ordination analyses revealed that samples clustered more consistently by airway niche rather than by individual. Finally, predicted metagenomes suggested that anaerobiosis was enriched in the lung environment. Our findings indicate that while the paranasal sinuses and lungs may comprise a unified airway in which the lungs are seeded by individual sinus pathogens, discrete airway microenvironments harbor distinct bacterial communities.

Introduction

Defective CFTR ion transport at the sinus epithelium leads to decreased mucociliary clearance and obstruction of sinus ostia (Robertson et al., 2008). Secondary events such as the impairment of host defenses render this niche susceptible to bacterial colonization and chronic rhinosinusitis (CRS) (Becker, 2010; Robertson et al., 2008). Notably, there is a striking incidence of CRS in the CF population relative to non-CF subjects (~16% (Babinski and Trawinska-Bartnicka, 2008)). This is particularly evident in CF patients with classical mutations (class I-III), who, based on radiological evidence, have a CRS incidence rate of nearly 100% (Robertson et al., 2008).

Culture-based studies have revealed that CF-associated CRS (CF-CRS) patients harbor distinct microbiota, including *Staphylococcus aureus* and *Haemophilus influenzae* in pediatric patients, followed by *Pseudomonas aeruginosa* and other pathogens as patients age (Roby et al., 2008). This dynamic generally follows the same succession of CF lung microbiota (Cox et al., 2010) and several groups have demonstrated similarities in upper and lower airway bacteriology in CF subjects (Bonestroo et al., 2010; Fischer et al., 2014). In fact, evidence has implicated the sinuses as infection foci for lung pathogens, where they first adapt to the host before descending into the lungs (Ciofu et al., 2013; Hansen et al., 2012; Johansen et al., 2012; Mainz et al., 2009, 2012; Rudkjøbing et al., 2014; Syed et al., 2016). Genotypic analyses suggest a direct exchange between sites; *P. aeruginosa* isolates cultured simultaneously from the sinuses and lungs were genetically identical in 38 of 40 subjects (Johansen et al., 2012). These data are supported by studies of CF lung transplants, where recipient allografts were re-colonized by the same *P. aeruginosa* clones found prior

to transplantation (Ciofu et al., 2013; Syed et al., 2016). Altogether, these observations support the notion of a sinus pathogen reservoir and a unified airway, in which the treatment of CRS could have profound benefits for CF lung disease management.

While *P. aeruginosa* and *S. aureus* are commonly isolated from the CF sinuses (Mainz et al., 2009), culture-independent studies also suggest colonization by anaerobes (e.g. *Cutibacterium*) and other non-canonical pathogens (Rudkjøbing et al., 2014). These data are consistent with microbiome profiles of CF lung disease, which is recognized to have a polymicrobial etiology (Coburn et al., 2015; Cox et al., 2010). Recent sequencing studies have evaluated relationships between oral, nasal and lung microbiota in adult CF patients (Boutin et al., 2015; Caldas and Boisramé, 2015), but to our knowledge, molecular approaches have not been used to assess relationships between sinuses and lungs at a microbial community level. From a clinical perspective, these data could be of considerable therapeutic benefit; sinus culture can be invasive and time consuming, and to date, sputum culture-guided therapies for CRS have been largely ineffective, with many subjects ultimately requiring surgical intervention (Lavin et al., 2013; Osborn et al., 2011). Therefore, a deeper understanding of microbiological relationships between the sinuses and lungs may not only improve upon CF-CRS management, but may also motivate the use of less-invasive sinonasal sampling to help inform patient therapy (Fischer et al., 2014; Mainz et al., 2009; Mainz and Koitschev, 2012).

Materials and Methods

Patient cohort and specimen collection

Twelve participants with CF undergoing functional endoscopic sinus surgery (FESS) were recruited at the University of Minnesota Department of Otolaryngology. Informed consent was obtained from all subjects. Prior to FESS, each patient spit to discard saliva, followed by sputum expectoration into a collection tube. All samples were assessed macroscopically for salivary contamination, and none were rejected. Sinus secretions were obtained from a single maxillary sinus (middle meatal region) under endoscopic visualization by suction into mucus traps (Cardinal Health, Dublin, OH). Clinical data were also obtained (Table S1, Appendix A), including CFTR genotype, FESS procedures, clinical cultures, spirometry (FEV1%) and sinonasal outcome test (SNOT-22) scores. The UMN Institutional Review Board approved these studies (#1403M49021).

Quantitative PCR

Bacterial burden was estimated by quantifying 16S copy number from DNA extracted from clinical specimens using quantitative PCR. Reactions were prepared in triplicate using QuantiTect SYBR Green (Qiagen) and Universal 16S rRNA qPCR primers (Abreu et al., 2012). Details can be found in the supplemental data (Appendix A).

DNA sequencing and analysis

Genomic DNA was extracted from 300 μL of mucus using Powersoil Kits (MoBio, Carlsbad, CA) and was submitted to the UMN Genomics Center (UMGC) for 16S library

preparation using a two-step PCR protocol (Gohl et al., 2016). The V4 region was amplified and sequenced using Illumina MiSeq TruSeq 2 × 300 paired-end technology. Water and reagent control samples were also submitted but were below detection thresholds. Raw sequence files were deposited in the NCBI Sequence Read Archive (accession #PRJNA374847). Data were analyzed using a pipeline developed by the UMN Informatics Institute in collaboration with UMGC. Details are provided in the supplemental data (Appendix A).

Metagenomic prediction

Metagenomes were inferred from 16S rRNA data using Phylogenetic Investigation of Communities by Reconstruction of Unobserved States (PICRUSt) (Langille et al., 2013). PICRUSt uses marker gene survey data to predict metagenome content through ancestral state reconstruction of quality-filtered 16S sequence data. We also used BugBase (Ward et al., 2017) to summarize predicted metagenomes by bacterial phenotype. BugBase scripts were run with default settings using filtered sequence data used in PICRUSt. Details are provided in the supplemental data (Appendix A).

Statistical analyses

Analyses were performed in GraphPad Prism 6.0 unless stated otherwise. Significance was assessed at the $\alpha = 0.05$ level. Hypothesis testing was conducted assuming a paired sample study design. Student's t-tests were used where data passed the Kolmogorov-Smirnov test

for normality. Statistics implemented in beta diversity and BugBase analyses are documented in the supplemental data (Appendix A).

Results

Patient Cohort

Twelve CF adults with CRS undergoing functional endoscopic sinus surgery (FESS) each provided an expectorated sputum sample. Sinus mucus was collected at the beginning of FESS. These samples are herein referred to as "sinus" and "lung" samples, denoting their anatomical origin. Clinical data, including CF genotype, microbiology cultures, prior FESS procedures, spirometry and sino-nasal outcome test (SNOT-22) scores were also collected (Table S1, Appendix A). Six patients were homozygous ΔF508, five were heterozygous ΔF508, and two had heterozygous non-ΔF508 mutations. Sinus culture data were available for 11 of 12 sinus samples. Of these, 6 were positive for *P. aeruginosa*, and 5 were positive for *S. aureus*. Predominant lung pathogens detected by sputum culture were also recorded (Table S2, Appendix A).

Bacterial load in sinus and lung samples

qPCR of 16S ribosomal RNA (rRNA) gene copy number was used to estimate bacterial load (Figure 2.1). On average, sinus specimens contained 2.72 × 103 (IQR = 2.69 × 102 − 1.72 × 103) 16S gene copies per ng genomic DNA, while lung sputum harbored 5.33 × 104 (IQR = 6.18 × 102 − 5.02 × 104). These data suggest a modest difference in 16S gene abundance between sample types (Figure 2.1A, $P = 0.0637$). Interestingly, patient age was positively associated with 16S gene abundance in sinus samples, but this relationship was not observed for the lung (Figure 2.1B). We also assessed the relationship between bacterial load and two clinical metrics, FEV1% and SNOT-22, neither of which

significantly correlated with 16S copy number in either sample group (Figure 2.1B). Taken together, these data suggest that the specific composition of each bacterial community rather than bacterial abundance contributes to disease states in both sinus and lung niches.

Bacterial community membership varies with location

Bacterial composition was profiled using 16S rRNA gene sequencing. After filtering for quality and subsampling to an even depth, 51 genera were identified across samples (Figure 2.2). To investigate genera that accounted for the majority of sequences, we adopted the definition of a dominant genus (the most abundant genus with over twice the abundance of the second most abundant genus) (Coburn et al., 2015). A dominant genus was present in 100% of sinus samples but only 33% of lung samples. *Pseudomonas* and *Staphylococcus* were dominant genera in five sinus samples each (42%), while *Streptococcus* and *Burkholderia* were each dominant in a single sample (Figure 2). As expected, only *P. aeruginosa* and *S. aureus* were dominant lung pathogens. Species-level identification for abundant pathogens was determined by culture data, when available (Table S2, Appendix A). The median relative abundance of the predominant genus was 0.88 (IQR = 0.75–0.99) in each sinus sample, and 0.42 (IQR = 0.34–0.78) for lung samples. The most abundant sinus OTUs were assigned to *Pseudomonas*, *Staphylococcus*, and *Streptococcus*. By contrast, lung samples harbored an abundance of *Pseudomonas*, *Veillonella*, and *Prevotella*, consistent with previous studies (Coburn et al., 2015; Cox et al., 2010). Interestingly, although many taxa were shared between sample pairs, the absence of a pathogen (e.g. *Pseudomonas*, *Achromobacter*) in one sample was not

predictive of its absence in its paired sample sequence data. For example, subjects 5 and 12 harbored *Achromobacter* in their upper airways, despite being undetectable in sputum. This was also true of *Staphylococcus* in subject 6. Conversely, subjects 1 and 11 harbored an abundance of known CF pathogens (*Pseudomonas* and *Haemophilus*, respectively) in the lung that were not associated with upper airway infection. These examples demonstrate that infections at either site can be perpetuated by different pathogen within an individual, and that sputum cultures and 16S rRNA sequence data are not always representative of upper airway infection.

Based on these examples, we then determined the extent to which genera were shared between sites. Spearman correlations between genera in matched pairs revealed that within-patient similarities allowed for significant positive correlation between sites in ten of twelve sample pairs (average Spearman $\rho = 0.45$) (Table S3, Appendix A). However, a group-wise comparison of paired samples showed a weaker correlation (Spearman $\rho = 0.32$, $P = 0.001$). These results highlight the potential for bacterial communities of the upper and lower airways to be similar within a given patient, yet the group correlation underlines the general dissimilarity in microbiota between sinus and lung microenvironment.

Bacterial diversity varies between upper and lower airways

As described above, few taxa dominated most sequences in each sample. To investigate this further, two alpha diversity metrics, observed operational taxonomic units (OTUs) and Shannon diversity, were used as measures of richness (biodiversity) and

evenness (equitability) (Hill, 1973). Observed OTUs in lung samples were greater than in sinuses, indicating greater richness, though the difference was not significant (Figure 2.3A). Using the Shannon diversity index, sinuses were characterized by greater unevenness relative to lung samples, consistent with the high prevalence of dominant sinus genera (Figure 2.3B). When ordered by rank, an average of 10 and 20 genera accounted for 99% of sequences in sinus and lung samples, respectively (Figure 2.3C). These data indicate that the lung bacterial community is greater in both richness and evenness relative to the sinuses.

Spearman correlations were then calculated to assess relationships between bacterial load, alpha diversity and patient clinical data (Figure 2.3D). These data revealed a significant inverse correlation between Shannon diversity in the sinus and lung ($\rho = -0.664$, $P = 0.022$). Because the data show a similar richness between sites, and both sinus and lung Shannon diversity revealed positive relationships with observed OTUs (sinus $\rho = 0.881$, $P = 3.35 \times 10{-}4$; lung, $\rho = 0.774$, $P = 0.007$), we infer that diversity differences are driven by evenness in these niches. Lung Shannon diversity was also positively correlated with lung 16S rRNA copy number ($\rho = 0.678$, $P = 0.019$), and these data reiterate the positive correlation between sinus 16S rRNA gene copy number and patient age ($\rho = 0.624$, $P = 0.033$; Figure 2.1B). There was no correlation found between alpha diversity metrics, or relative abundance of *Staphylococcus*/*Pseudomonas* and antibiotics prescribed three days prior to surgery for both sample types (Table S4, Appendix A). Altogether, these results demonstrate that bacterial diversity differs between sinus and lung niches, and that a decrease in diversity at either site is associated with the decrease in even distribution of

bacterial taxa.

Airway location as a descriptor of phylogenetic variance.

Beta diversity of airway microbiota was then visualized using ordination. Of interest was whether bacterial communities would cluster more closely by patient or sampling site. Previous studies characterizing upper and lower airway microbiota revealed shared taxa between sites, but also inter-individual variation (Boutin et al., 2015; Charlson et al., 2011; Fischer et al., 2014). Evidence also suggests that bacterial metastasis between the sinuses and lung is commonplace (Mainz et al., 2009). Based on these previous studies, we hypothesized that samples would cluster more closely by patient, rather than by sampling site. To address this hypothesis, we compared samples utilizing weighted Unifrac, an abundance-sensitive, phylogenetically relevant diversity metric (Lozupone and Knight, 2005). This metric was calculated to determine phylogenetic pairwise distances between each sample, then plotted using principal coordinates analysis (PCoA). Contrary to our hypothesis, within-patient sample pairs did not cluster together nearly as strongly as they did by sampling site (Figure 2.4A), which rejected the null hypothesis the groupings (sinuses and lungs) had the same centroid (PERMANOVA, $P = 0.019$). Lung samples also demonstrated considerable phylogenetic variation when compared to sinus samples (Figure 2.4A). When relative abundances from dominant taxa (*Pseudomonas* and *Staphylococcus*) were overlaid, there was a strong association with the PCoA sample distribution (Figure 2.4B). These analyses demonstrate that overall community structure is largely driven by dominant genera, and that upper and lower airways select for unique bacterial community structures, despite sharing individual taxa.

Predicted metagenomes show phenotypic conservation between sites

To gain insight into bacterial community function, PICRUSt (Langille et al., 2013) was implemented to infer bacterial metagenomes based on 16S rRNA gene content. Sequences derived from each sample had a low Nearest Sequenced Taxon Index average of 0.017, indicating a high relatedness between bacteria found in the samples to sequenced genomes, and a high prediction accuracy for the dataset. Twenty unique KEGG pathways were represented among inferred metagenomes and showed striking similarity between sinus and lung samples (Figure S1, Appendix). This suggests that the functional capacity of lung and sinus bacterial communities is relatively similar, despite taxonomic differences.

To further summarize PICRUSt output, we utilized BugBase, a bioinformatics tool that infers community-wide phenotypes from predicted metagenomes (Ward et al., 2017). BugBase identified that gene functions associated with anaerobiosis were enriched in lung samples (P = 0.01), and could be attributed to three genera: *Veillonella*, *Prevotella*, and *Porphyromonas* (Figure 5A). Gram-negative ultrastructure and biofilm formation are two bacterial phenotypes often associated with airway pathogenicity, however, our analysis showed that these phenotypes did not differ significantly between sites. Gram-negative genera contributing to this phenotype were more varied in lung samples and included *Veillonella*, *Prevotella*, *Neisseria*, *Stenotrophomonas*, supporting the increased richness observed in these samples. Biofilm-forming bacteria were observed in both sinus and lung predicted metagenomes. This phenotype was influenced by the presence of *Pseudomonas* in both airway sites, but *Burkholderia* and *Achromobacter* both differentiated sinus from lung samples, while Neisseria and Stenotrophomonas were more highly represented in lung

samples. Altogether, these data point towards the lung environment being a more anaerobic niche, but that other phenotypes classically linked to bacterial pathogenicity, such as biofilm formation, are similar between sites.

Discussion

It is poorly understood how complex bacterial communities promote the development of sinus disease. It is also not known how upper airway microbiota contributes to lower airway infections that are a primary cause of CF patient morbidity. The sinuses have been proposed as a reservoir in which individual pathogens adapt to the host prior to lung colonization, but it is unclear whether polymicrobial community composition of the CF lung can be a reasonable surrogate for upper airway microbiota and treatment of CF-CRS. We therefore took an ecological approach towards exploring bacterial diversity throughout the airways.

Our cohort showed striking variability in bacterial community membership between subjects. Despite this variability, we found that lung samples harbored an increased diversity (evenness) relative to sinuses which were dominated by either *Staphylococcus* or *Pseudomonas*. The abundances of these two canonical pathogens are commonly revealed by sinus culture (Mainz et al., 2009), though many other taxa identified in our study are not. For example, when compared to summarized culture data comparing the upper and lower CF airways (Fischer et al., 2014), the most striking difference between analyses was the identification of obligate anaerobes. These differences highlight the utility of molecular-based methods in detecting fastidious and anaerobic bacterial taxa. Given the emerging evidence of anaerobes being causative agents of pulmonary disease (Flynn et al., 2016), increased use of culture-independent diagnostics to detect these bacteria throughout the airways is warranted.

Our most intriguing data were that several sinus samples harbored canonical CF pathogens, yet these bacteria were absent in the paired lung samples. Conversely, the lungs of several subjects were colonized by a dominant pathogen that went undetected in the upper airways. This study outcome has significant clinical implications; respiratory cultures and sequence data from the two sites are not necessarily interchangeable for the determination of antibiotic therapy. These findings are consistent with those of Muhlebach (Muhlebach et al., 2006) who showed that bronchoalveolar lavage and oropharyngeal cultures are poor predictors (40–50% accuracy) of sinus bacteriology in children. Together, these observations may partially explain why patient response to therapy is poor, and suggest that the expanded use of non-invasive, sequence-based sinonasal sampling measures could be beneficial in steering patient therapies.

Often in microbiome surveys, bacterial membership may differ dramatically between samples, but functional capabilities remain conserved (Huttenhower et al., 2012). Here, we highlight this relationship in the airways. Contrasting differences in bacterial diversity and community composition between sinuses and lungs, we found that the predicted functional capacity in both niches was similar. In the context of bacterial contribution to CF disease, it is plausible that there are many similarities in the microenvironments of the upper and lower airways that may contribute, or even result from these conserved functions.

This exploratory study reveals many opportunities for future research. Notably, this work focuses on a small adult cohort with lung function lower than 70% predicted (mean). While the inter-individual variability reported is not unfounded, it highlights the need for

increased enrollment for assessing clinical and sequencing variables. Moreover, future work should extend to both pediatric and adult subjects across the spectrum of disease severity, as our conclusions may not be generalizable to all subjects. For example, it is possible that in patients where lung-adapted strains differ in prominence, the influence of bacterial trafficking from the upper airways on bacterial structure also varies. Likewise, longitudinal studies are warranted to investigate microbiota trafficking dynamics over time as patients age. Our work also does not account for airway microenvironments harboring distinct microbiomes. For example, a single maxillary sinus may not capture an infectious agent present in another sinus, whereas sputum may reflect multiple lower airway niches. Prior studies have shown that the middle meatus is a valid representation of the sinus cavity (Ramakrishnan et al., 2016), though multiple samples that define the biogeography of the upper airways will be informative for infection management. Finally, a common concern in sputum-based studies is the potential for salivary contamination. Though we cannot rule out the contribution of oral flora to our analyses, samples from lung explants and bronchoalveolar lavage have clearly demonstrated the presence of oral-associated anaerobes in the lung (Blainey et al., 2012; Hogan et al., 2016). Moreover, others suggest that contamination of sputum is limited during transit through the oral cavity (Blainey et al., 2012; Charlson et al., 2011). Moving forward, oropharyngeal swabs should be included in analyses to help define the site of sequence origin, particularly for diagnostic purposes.

Despite these limitations, our data shed important light on microbial community relationships throughout the CF airways. Though airway niche spaces differ in diversity, shared taxa between the sample pairs reflects the interconnectedness of the airway and does

not discount the sinuses as a source of lower airway colonization. However, the distinct bacterial community structures suggest sinus and lung microenvironments play a critical role in governing the prevalence and abundance of canonical CF pathogens. These data can be translated to the clinic by informing caregivers to utilize respiratory specimens originating from the site of infection. In the context of our findings, we advocate for the use of 16S rRNA gene sequences in the clinical setting to supplement culture data in the assessment and informed therapeutic approach towards the management of CF-associated CRS infections.

Acknowledgements

This work was supported by a Pathway to Independence Award from the National Heart Lung and Blood Institute to RCH (R00HL114862); an Investigator-Sponsored Research Grant from Gilead Sciences to RCH, JD, and HCB; a Lions 5M International award to RY; a National Institutes of Health T32 Fellowship (#T90 DE 0227232) awarded through the National Institute of Dental and Craniofacial Research to SKL; and the University of Minnesota Medical School. We acknowledge the Minnesota Supercomputing Institute (MSI), Daryl Gohl and John Garbe at the UMN Genomics Center for sequencing assistance. We thank Abayo Itabiyi, Ali Stockness and Rebecca Dove of the Department of Otolaryngology, and the members of BioNet at the University of Minnesota for facilitating sample collection. Our thanks go out to Tonya Ward, Dan Knights, and the Knights Lab at UMN for their assistance with the BugBase analysis.

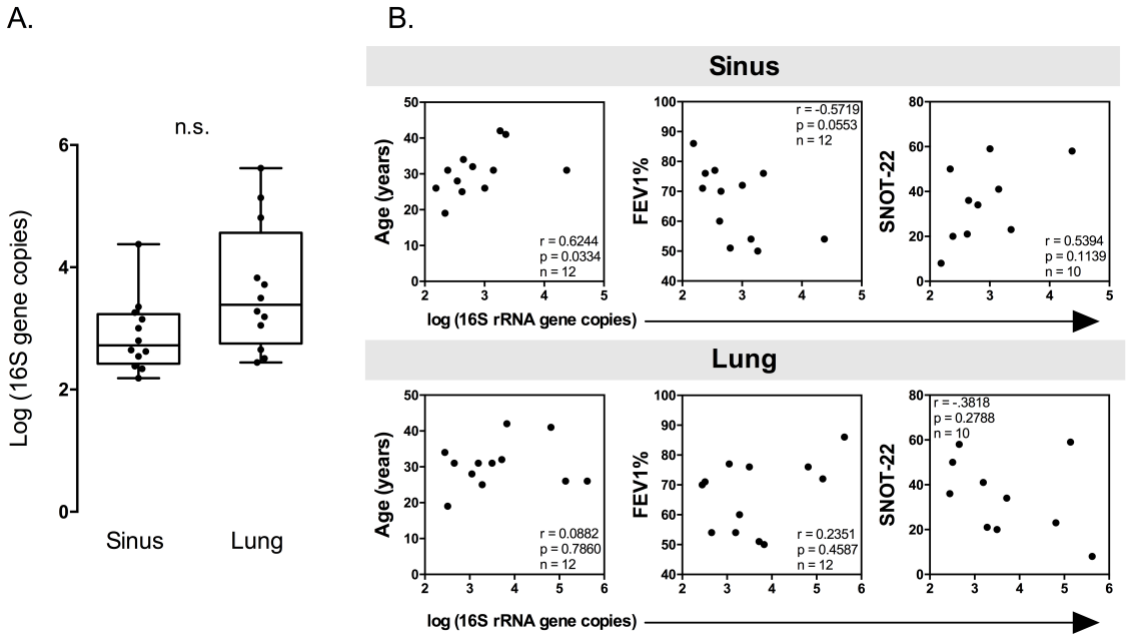

Figure 2.1 Bacterial Load in Sinus and Lung Samples. 16S gene copies are greater in CF lung sputum compared to sinus samples, and correlate with patient age. Quantitative PCR was used to enumerate 16S rRNA gene copies ng of genomic DNA isolated from sinus and lung samples. A. Comparison of 16S rRNA gene copies in sinus and lung sample pairs by qPCR. (Paired Student's t-test $P = 0.0637$). B. Spearman correlations with 16S rRNA gene copies and patient clinical data. In sinus samples, 16S copies are positively and significantly correlated with patient age.

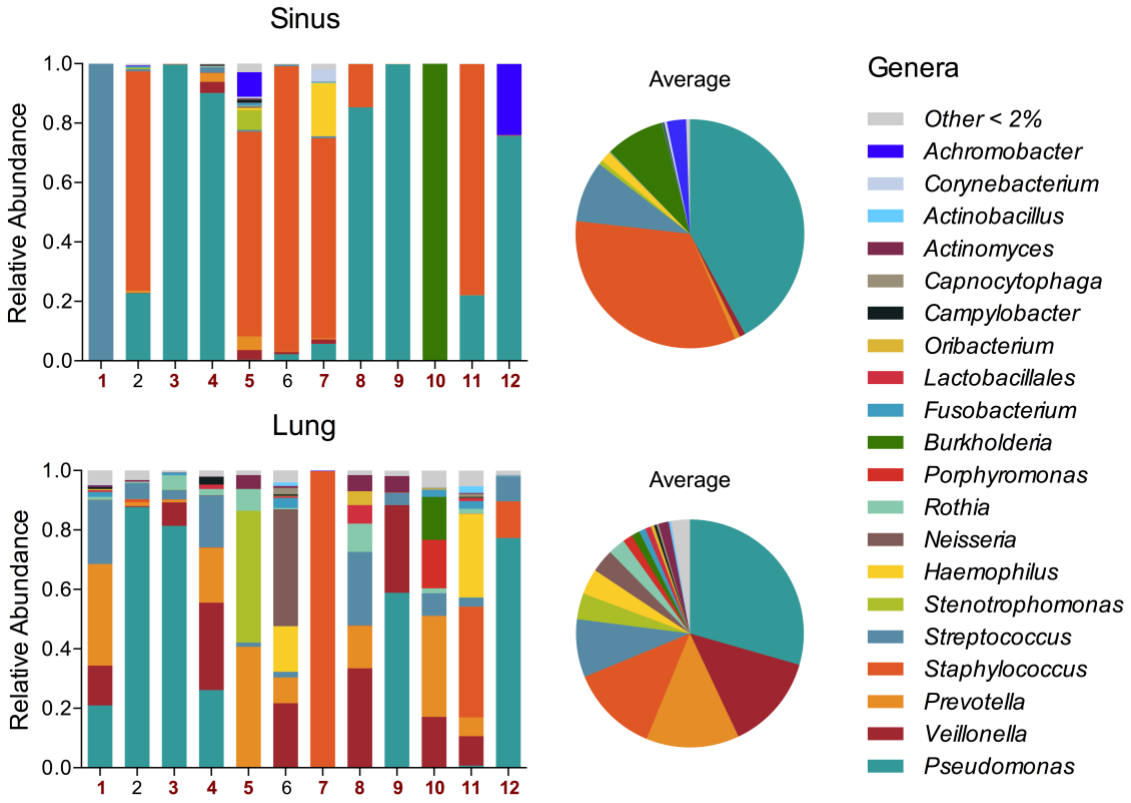

Figure 2.2 Bacterial community composition of the upper and lower airways. Stacked bar plots of relative abundances of genera in paired sinus and lung samples demonstrate dominance of *Pseudomonas*, *Staphylococcus*, and *Streptococcus* genera. Red patient numbers indicate samples where bacterial membership was significantly correlated within pairs. Data for these relationships is presented in Table S2. Pie charts show the average abundance of genera for each sample type across the patient cohort.

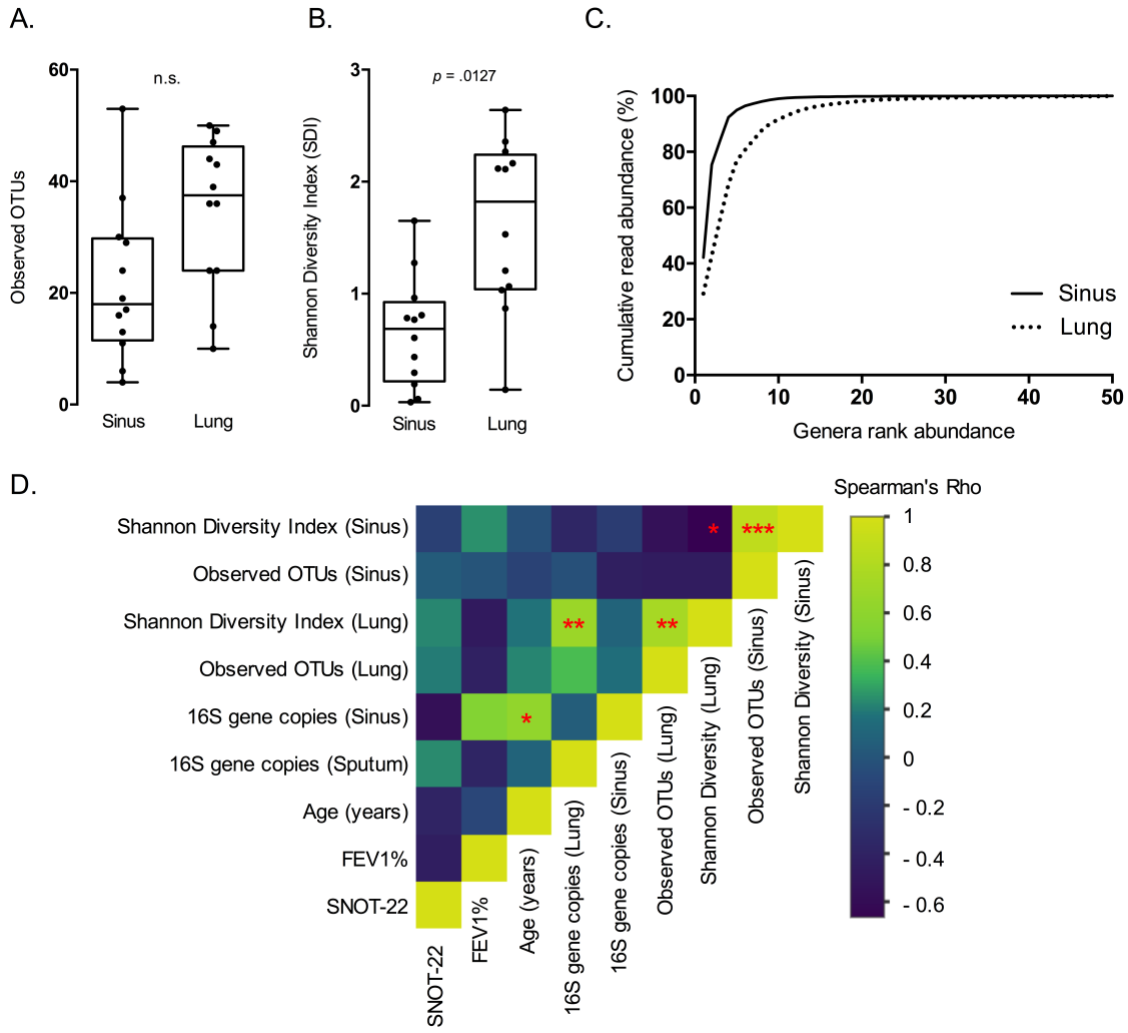

Figure 2.3 Alpha diversity of CF maxillary sinuses differs from CF lung sputum. A. Observed OTUs are modestly greater in lung samples compared to the sinuses. Lung samples display significantly greater evenness in OTU distribution relative to sinus samples (paired Student's t-test, $P = 0.0127$). B. Rank abundance curves reveal that both sinus and lung bacterial communities are dominated by a few organisms. 10 and 20 genera represent 99% of the sequences for sinus and lung samples, respectively. C. Spearman correlation heat map shows association of bacterial diversity (observed OTUs, Shannon), bacterial 16S gene abundance, and clinical factors. (*P ≤ 0.05, **P ≤ 0.01, ***P ≤ 0.001).

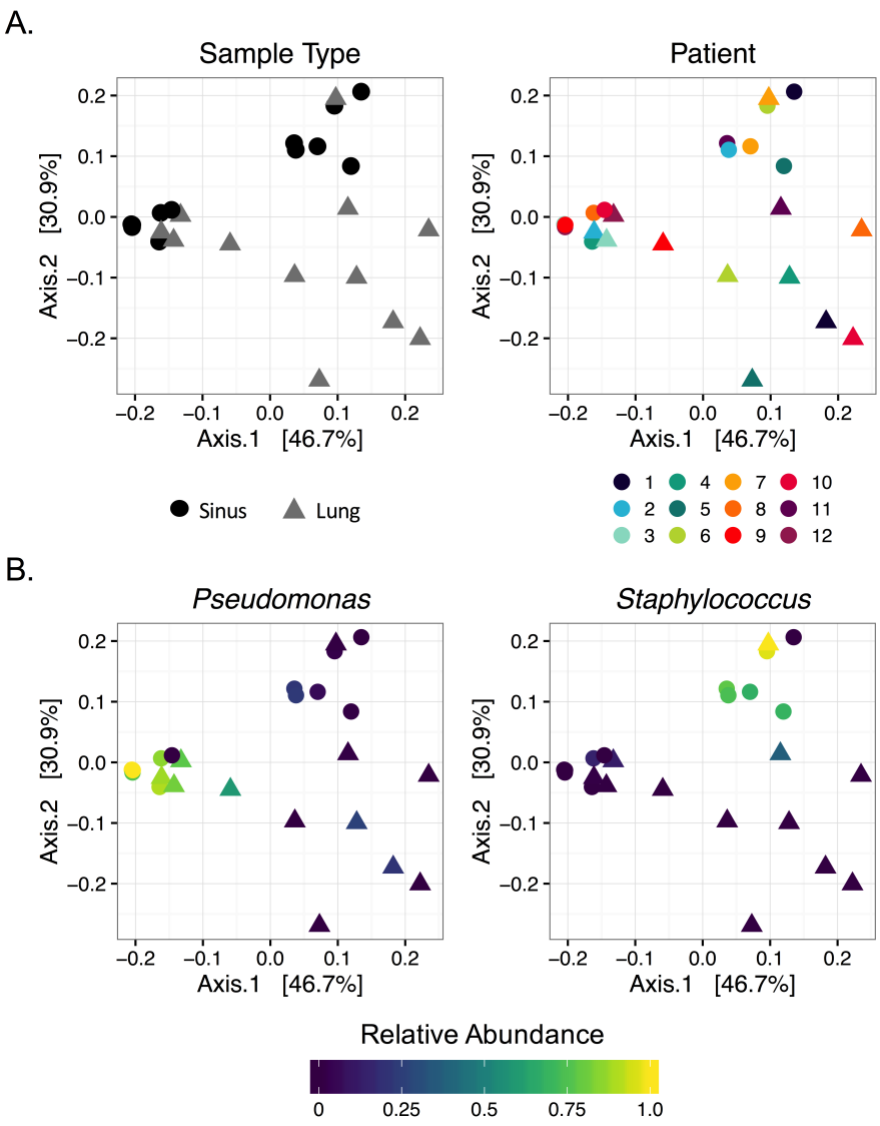

Figure 2.4 Ordination of weighted Unifrac distances. Principal Coordinate Analysis shows clustering by sample type and dominant organism. A. Samples show more similarity by sample type rather than sampled individual (PERMANOVA, $P = 0.019$). Color and shape denote patient and sample type, respectively. Sinus and lung samples do not cluster by patient, but do show clustering by sample type. B. PCoA colored by relative abundance of dominant organisms (defined in text), shows sinus sample grouping is highly dependent on relative abundance of *Pseudomonas* and *Staphylococcus*.

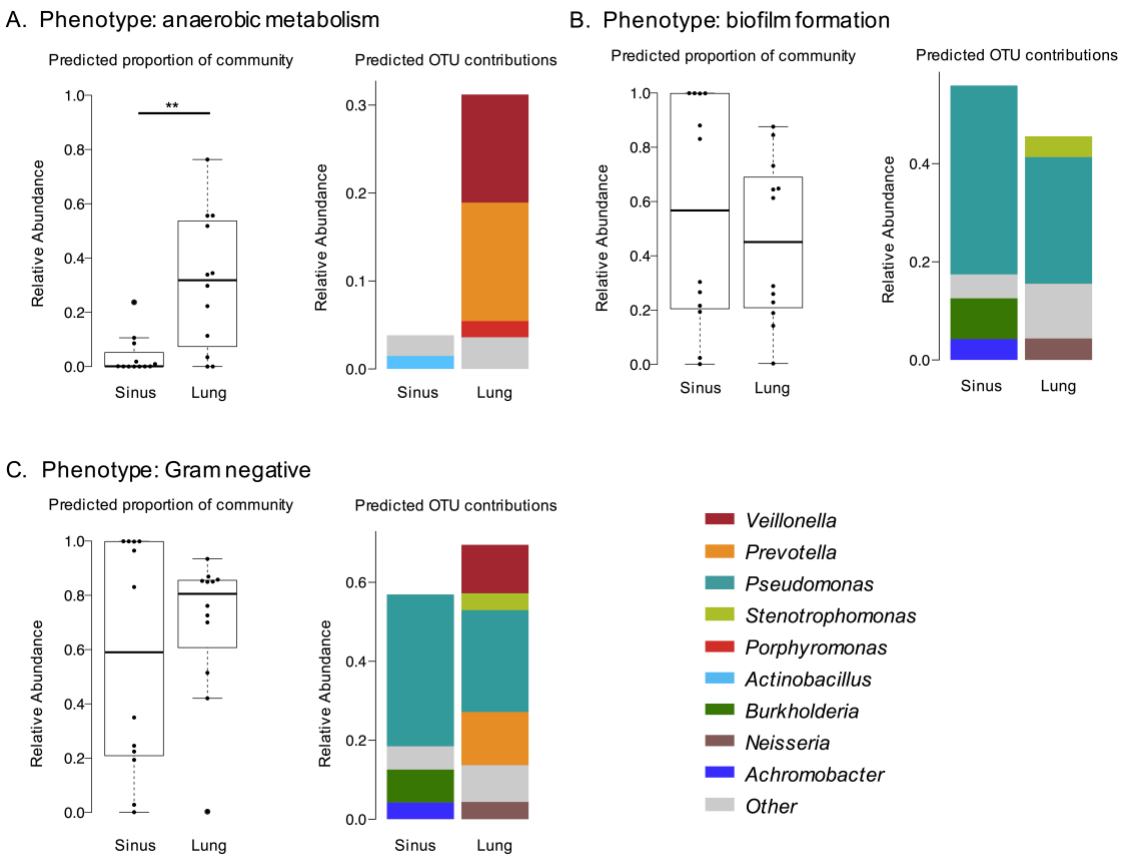

Figure 2.5 BugBase analysis of PICRUSt-predicted metagenomes. BugBase was used to summarize PICRUSt analysis results into categories based on bacterial phenotype. A. Anaerobic metabolism is significantly enriched in lung samples (Wilcoxon signed-rank test, $P = 0.01$). B. Biofilm formation does not differ significantly with sample type (Wilcoxon signed-rank test, $P = 0.57$). C. Gram-negative phenotype is driven by presence of *Veillonella*, *Prevotella* and *Pseudomonas* in lung samples (Wilcoxon signed-rank test, $P = 0.47$). (*P ≤ 0.05, **P ≤ 0.01, ***P ≤ 0.001).

Chapter 3: The microbiome of chronic rhinosinusitis in a cystic fibrosis patient cohort at University of Minnesota

Summary

Chronic rhinosinusitis (CRS) affects nearly all individuals with cystic fibrosis (CF) and is thought to serve as a reservoir for pathogens that subsequently colonize the lung. To better understand the microbial ecology of CRS, we generated a 16S rRNA gene sequencing profile of sinus mucus from CF-CRS patients. We show that CF-CRS sinuses harbor bacterial diversity not entirely captured by clinical culture. Culture data consistently identified the dominant organism in most patients, though lower abundance bacteria were not always identified. We also demonstrate that bacterial communities dominated by *Staphylococcus* spp. were significantly more diverse compared to those dominated by *Pseudomonas* spp. Diversity was not significantly associated with clinical factors or patient age, however, younger subjects yielded a much wider range of bacterial diversity. These data mirror bacterial community dynamics in the lung and provide additional insight into the role of sinus microbiota in chronic airway disease progression.

Introduction

Chronic rhinosinusitis (CRS) reaches a strikingly high prevalence among CF adults (>99%) (Chaaban et al., 2013). While there are several proposed causes of CF-associated CRS (CF-CRS), including abnormal sinus anatomy and aberrant immune responses (Benninger et al., 2003), bacterial infection remains widely implicated (Hoggard, Mackenzie, et al., 2017; Vickery et al., 2019). The "unified airway" model, whereby bacterial pathogens adapt to the upper airways before migration to the lungs has become a major impetus for studying CF-CRS microbiology (Godoy et al., 2011; Illing and Woodworth, 2014).

16S rRNA gene sequencing has significantly improved our understanding of CF microbial ecology. Cross-sectional and longitudinal studies of sputum have established that bacterial diversity decreases into adulthood, concomitant with lung function decline (Cox et al., 2010; Zhao et al., 2012). Fewer studies have investigated these dynamics in the upper airways, however, CF sinuses harbor significantly lower bacterial diversity compared to non-CF-CRS and non-CRS patients (Cope et al., 2017). Clinical culture has shown that *Staphylococcus aureus* and *Pseudomonas aeruginosa* are both prevalent and abundant in CF-CRS (L. Sobin et al., 2017), while their genotypes show within-individual concordance between upper and lower airways (Johansen et al., 2012). This relationship is particularly striking in lung transplant recipients (K. J. Choi et al., 2018; Ciofu et al., 2013; Mainz et al., 2009; Syed et al., 2016), supporting the notion that sinuses serve as a reservoir for CF lung pathogens.

To better understand microbial community ecology in CF-CRS and its role in CF disease progression, we performed 16S rRNA gene sequencing on sinus mucus derived from patients undergoing endoscopic sinus surgery (ESS). We explored bacterial diversity with respect to dominance of canonical CF pathogens, patient demographics, and clinical parameters. We discuss these data in the context of interspecies interactions as determinants of CF pathogenesis.

Materials and Methods

Study design

The UMN Institutional Review Board (approval number #1403M49021) approved this study. Informed consent was obtained from all participants. Adult patients with CF (n=25) undergoing endoscopic sinus surgery for the treatment of CRS were enrolled at the University of Minnesota Department of Otolaryngology. Samples from 3 patients did not yield sequencing depth that exceeded 2000 reads and were excluded from analysis. Twenty-two patients were included in further analysis (Table 3.1).

Sample collection DNA extraction

Sinus secretions were obtained from a single maxillary sinus (middle meatal region) under endoscopic visualization by suction into Argyle Mucus Traps (Cardinal Health, Dublin, OH) which were frozen at -80°C. Demographic data, recent clinical history, recent antibiotic and medication use (less than 3 months prior procedure date), and comorbidities such as presence of polyps, diagnosed asthma or allergies, GERD, were collected at time of surgery.

Genomic DNA was extracted from 300 µL of sinus mucus using DNeasy Powersoil kits (Qiagen, Carlsbad, CA) and submitted to the UMN Genomics Center (UMGC) for 16S rRNA gene library preparation[1]. The V4 region was amplified and sequenced using Illumina MiSeq TruSeq 2x300 paired-end technology. Reagent control samples were also sequenced. The samples were run as part of larger sample groups across four different sequencing runs.

16S rRNA gene sequencing and analysis

Sequence analyses, statistical analysis, and data visualizations were performed in R (v.4.0.0). Cutadapt (v.2.6) (Martin, 2011) was used to remove primer sequences, with size filtering set to 215bp (minimum) and 285bp (maximum). DADA2 (v.1.17.0) (Callahan et al., 2016) was used to trim sequences and filter for quality. DADA2 inferred a parametric error model used to identify and correct sequencing errors. Reads were de-replicated, paired ends merged, and chimeric reads removed using default options. Genus-level taxonomy was assigned using the Ribosomal Database Project (RDP) Bayesian classifier (Q. Wang et al., 2007) and SILVA-132 taxonomy training set (Quast et al., 2013). Species-level taxonomy was assigned only if an amplicon sequence variant (ASV) unambiguously matched a sequence in SILVA-132 or *e*HOMD databases (Escapa et al., 2018). A phylogenetic tree was approximated by first performing a multiple-alignment using DECIPHER (v.2.14.0) (Wright, 2016). Phangorn (v.2.5.5) was used to construct a phylogenetic tree (Schliep, 2011).

Functions from the Phyloseq (v.1.33.0) (McMurdie and Holmes, 2013) and ampvis2 (v.2.6.0) (Andersen et al., 2018) R packages were used for abundance-related filtering of ASVs from the dataset, and diversity analyses. First, the resulting ASV table was rarified without replacement to 2000 sequences. Phyla with ambiguous taxonomic assignments, total feature prevalence less than 10, or mean feature prevalence of 1 were removed, as were ASVs with a mean relative abundance below 1x10-4. Ordination using double principal coordinate analysis (DPCoA) was carried out using the rarified ASV data transformed to proportions. Permutational multivariate analysis was carried out using

adonis in the vegan (v. 2.5-6) R package (Oksanen et al., 2013) and was used to test for differences in beta diversity centroids across patient data. The Shannon diversity metric was calculated for each sample individually using the rarified dataset.

Data availability

Code for all analyses in this section has been made available at:
https://github.com/hunterlabumn/CF-CRS-Microbiome

Results

Using 16S rRNA gene sequencing, we profiled bacterial community membership of CF-CRS mucus. Double principal coordinate analysis (DPCoA) was used to assess sample similarity with respect to taxonomic identity, phylogenetic relationships, and relative abundance (Figure 3.1A,B). Samples clustered into three groups defined by Firmicutes and Proteobacteria, with 52.3% of variation described on the first axis. Multivariate analysis showed no association between clinical parameters or comorbidities (polyps, GERD, asthma, allergies, prior sinus surgery, CFTR genotype) and the DPCoA (Figure 3.2A-F).

Hierarchical clustering and heatmapping were used to visualize relative abundances of bacterial genera (Figure 3.1C). Indeed, samples were differentiated by Firmicutes (*Streptococcus, Staphylococcus*) or Proteobacteria (*Pseudomonas)*. Other Proteobacteria (*Haemophilus, Achromobacter, and Burkholderia*) were abundant, but at lower prevalence, and accounted for second axis variation. Several amplicon sequence variants (ASVs) were assigned specific epithets (i.e. 100% sequence identity without multiple database matches) (Table 3.2), allowing for comparisons to culture-based data (Figure 31D). With exceptions, the dominant genus identified by sequencing was also identified by culture, though the second most abundant genus was often not. Notably, *Streptococcus* was third most abundant and comprised primarily of ASVs assigned to *S. intermedius*. However, *S. intermedius* is not generally recovered clinically, underscoring the utility of molecular methods for bacterial identification.

Many taxa identified by sequencing, particularly those with fastidious growth requirements (e.g. anaerobiosis) are not reported by clinical culture. This was particularly apparent in *Staphylococcus*-dominated samples, which tended to have greater bacterial diversity overall. Notwithstanding their lower abundance, we note that fastidious organisms (e.g. *Prevotella, Veillonella*) may also play a role in CRS, either through their own pathogenic potential or by affecting pathogen biology via interspecies interactions.

In most cases (21 of 22 samples), communities were structured by a taxon that was more than twice as abundant as the next highest-ranking taxon (Figure 3.3A). The top two dominant genera were *Pseudomonas* (9 samples, 41%) and *Staphylococcus* (7 samples, 32%). *Achromobacter*, *Burkholderia*, *Haemophilus*, *Streptococcus*, and *Veillonella* were dominant in one sample each. *Veillonella* was noteworthy as it is not commonly considered pathogenic. We then compared alpha diversity (richness and evenness) between samples. *Staphylococcus*-dominated communities were significantly more diverse than those dominated by *Pseudomonas* (Wilcoxon, p=0.012) (Figure 3.3B). *S. aureus* is a known early colonizer of the CF lung, but as patients age, colonization with *P. aeruginosa* becomes more prevalent and coincides with a reduction in bacterial diversity (Coburn et al., 2015). Here, a significant relationship between age and Shannon diversity was not observed (Figure 3.3C), though diversity in samples from younger patients (16-25 years old) varied greatly compared to older age groups. Additionally, samples dominated by *Staphylococcus* in this group (50%) were greater than any other age. These data are consistent with the temporal acquisition of *S. aureus* and *P. aeruginosa* in the CF lung.

Finally, colonization of the lung by either *S. aureus* or *P. aeruginosa* has been associated with pulmonary function decline (Ahlgren et al., 2015; Coburn et al., 2015). Given the "unified airway" hypothesis, we asked whether pathogen dominance in the sinuses fits this association (Figure 3.3D). While we found no statistically significant relationship, almost all patients with moderate to severe lung disease (FEV1%<70) yielded sinus mucus dominated by *Pseudomonas*. These data suggest that sinus microbiology may reflect lung function among a larger patient cohort.

Discussion

CRS studies commonly use CF as an exclusionary criterion, limiting both culture-based and molecular surveys of CF-CRS microbiota. However, the importance of sinus microbial ecology is underscored by the concordance of bacterial genotypes between upper and lower CF airways (Johansen et al., 2012). Data presented here support the notion that CF sinuses serve as a site for pathogen adaptation prior to chronic lung infection.

Bacterial diversity in CF sputum negatively correlates with age and pulmonary function decline (Cox et al., 2010; Klepac-Ceraj et al., 2010). Similarly, lung infections by the two most prevalent CF pathogens, *S. aureus* and *P. aeruginosa,* correlate with age; *S. aureus* is generally isolated from young CF patients and *P. aeruginosa* becomes the primary pathogen in adulthood (Salsgiver et al., 2016). Co-colonization also occurs and is associated with poor clinical outcomes (Limoli et al., 2016). Interestingly, many of these trends were observed in our CF-CRS cohort; (i) nearly all sinus mucus was dominated by either *Pseudomonas* or *Staphylococcus* (ii) 13 of 22 (59%) were co-colonized, (iii) community diversity and *Staphylococcus*-dominated samples were highest among younger subjects and declined with increasing age, and (iv) most sinus samples from patients exhibiting moderate to severe lung function were dominated by *Pseudomonas*. Collectively, these data suggest that CRS microbial dynamics may reflect, or even prognosticate, trajectories of CF lung infections.

By using amplicon sequence variants (ASVs), we improved upon the resolution by which microbiota associated with CF-CRS are surveyed (Table 3.2). We showed an increased diversity of bacterial species in *Staphylococcus*-dominated communities,

including those from *Veillonella* (*V. dispar, V. parvula*), *Megasphaera* (*M. micronuciformis*), *Prevotella* (*P. melaninogenica, P. salivae*), *Corynebacterium* (*C. tuberculostearicum*), several *Streptococcus* spp., and others. While contributions of these less prevalent and less abundant species to overall community stability and pathogenesis is currently unknown, their presence raises the question of whether interbacterial interactions are determinants of canonical CF pathogen dominance and/or virulence potential. Expanding *in vitro* investigations of interbacterial interactions will be critical to identify the contributions of community ecology to CF-CRS.

Sinusitis and its contributions to CF pathogenesis are poorly understood. Once thought to be sterile, sinuses are now known to harbor diverse polymicrobial communities that influence chronic bacterial colonization of the lung. Data presented here add to our emerging understanding of this important airway niche and its role in CF morbidity.

Acknowledgements

We would like to acknowledge the UMN Genomics Center for sequencing assistance. We give our thanks to Abayo Itabiyi and Erin Feddema, who were research associates in the UMN Department of Otolaryngology, Head & Neck Surgery and helped with FESS sample collection. Thank you to Holly Boyer, who was the surgeon on all FESS cases for sample collection.

Table 3.1 CF-CRS patient clinical information

Subject ID	Age	Gender	CFTR Mutation 1	CFTR Mutation 2	Homozygous dF508	Polyps	GERD	Asthma	Allergies	Prior FESS	# Prior FESS	FEV1(%)
4	25	M	dF508	R553X	-	+	+	-	+	-	0	66
9	22	F	dF508	dF508	+	-	+	-	+	+	> 4	76
36	31	F	dF508	1717-1G>A	-	+	+	-	-	+	> 4	117
38	22	M	dF508	dF508	+	+	+	-	+	+	> 4	110
51	33	M	dF508	dF508	+	-	+	-	-	+	2	69
11	28	M	dF508	dF508	+	+	+	-	-	-	0	74
18	22	F	N1303K	A1087P	-	+	+	-	-	+	NA	85
21	42	M	dF508	dF508Polyp T	+	+	+	-	+	+	> 4	55
47	16	M	dF508	dF508	+	+	+	-	-	+	> 4	122
61	31	M	dF508	dF508	+	+	-	-	+	+	2	NA
85	26	M	G551D	2789+5G>A	-	+	-	-	+	+	NA	105
87	19	F	NA	NA	NA	-	-	-	-	+	> 4	NA
94	26	F	dF508	1717-1G>A	-	-	-	-	-	+	1	98
102	32	F	dF508	dF508	+	+	-	+	+	+	1	31
112	36	M	dF508	L558S	-	-	-	+	+	-	0	26
115	48	M	dF508	W1282X	-	-	-	+	-	+	1	76
130	22	F	dF508	394delTT	-	-	-	-	-	+	2	101
131	41	M	1717-1G-7A	3849+10kbc-T1	-	+	-	-	-	+	1	72
133	18	F	dF508	dF508	+	-	-	-	-	-	0	105
158	36	F	dF508	dF508	+	-	-	-	-	+	1	61
169	21	M	dF508	dF508	+	+	-	-	-	+	> 4	94
171	31	M	dF508	394delTT	-	+	-	-	-	+	3	57

Table 3.2 Prevalence and abundance of ASVs of top 20 genera in CF-CRS samples

Taxonomic Feature	Prevalence in Samples	Average Relative Abundance (%)
Burkholderia	**1**	**99.70**
Burkholderia	1	99.70
Streptococcus	11	67.43
Streptococcus	7	1.48
Streptococcus intermedius	2	51.20
Streptococcus pneumoniae	1	14.30
Streptococcus sanguinis	1	0.45
Pseudomonas	**22**	**46.75**
Pseudomonas	2	0.10
Pseudomonas aeruginosa	20	46.65
Haemophilus	**5**	**41.28**
Haemophilus	3	38.35
Haemophilus parainfluenzae	2	2.93
Veillonella	**19**	**36.22**
Veillonella	7	7.12
Veillonella atypica	1	25.95
Veillonella denticariosi	1	1.10
Veillonella dispar	4	0.56
Veillonella parvula	4	0.79
Veillonella rogosae	2	0.70
Achromobacter	**5**	**34.08**
Achromobacter	1	9.00
Achromobacter xylosoxidans	4	25.08
Staphylococcus	**19**	**30.23**
Staphylococcus	19	30.23
Prevotella	**21**	**9.26**
Prevotella	4	1.61
Prevotella conceptionensis	1	0.15
Prevotella histicola	2	2.23
Prevotella melaninogenica	4	2.45
Prevotella nanceiensis	1	0.15
Prevotella nigrescens	2	0.10
Prevotella oulorum	1	0.15

Prevotella pallens	2	1.20
Prevotella salivae	4	1.23
Stenotrophomonas	**2**	**6.85**
Stenotrophomonas	1	6.70
Stenotrophomonas maltophilia	1	0.15
Klebsiella	**3**	**6.43**
Klebsiella	3	6.43
Capnocytophaga	**5**	**4.20**
Capnocytophaga gingivalis	2	0.23
Capnocytophaga leadbetteri	2	3.73
Capnocytophaga sputigena	1	0.25
Megasphaera	**3**	**4.13**
Megasphaera micronuciformis	3	4.13
Peptoniphilus	**1**	**3.90**
Peptoniphilus	1	3.90
Enterobacter	**1**	**3.65**
Enterobacter	1	3.65
Actinobacillus	**2**	**3.38**
Actinobacillus	2	3.38
Campylobacter	**6**	**3.22**
Campylobacter	1	2.50
Campylobacter concisus	5	0.72
Neisseria	**2**	**2.35**
Neisseria	2	2.35
Corynebacterium	**6**	**1.67**
Corynebacterium	1	0.15
Corynebacterium tuberculostearicum	5	1.52
Moraxella	**3**	**1.50**
Moraxella	3	1.50
Cutibacterium	7	0.49
Cutibacterium acnes	7	0.49

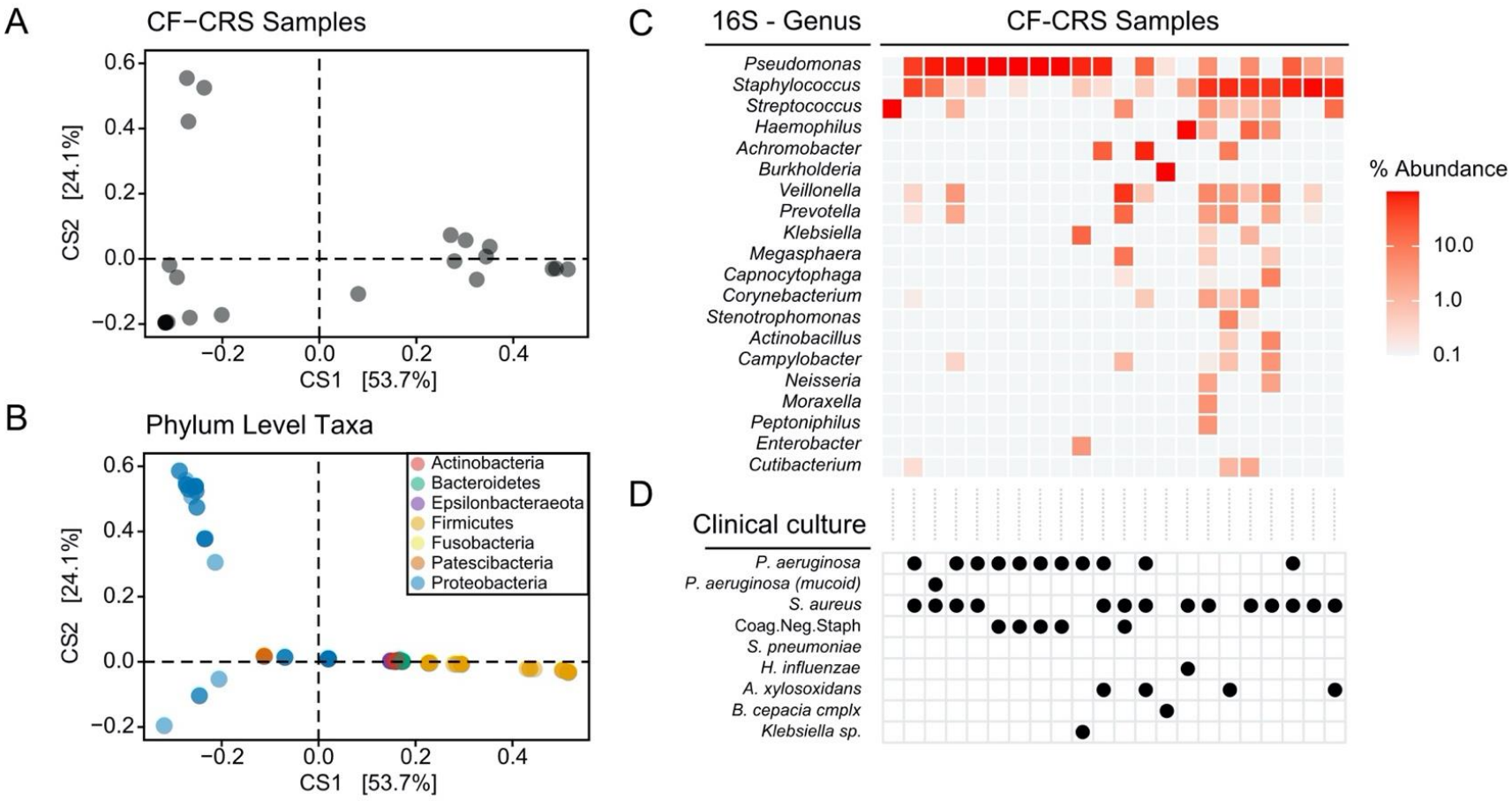
A
CF−CRS Samples
CS2 [24.1%]
CS1 [53.7%]
B
Phylum Level Taxa
Actinobacteria
Bacteroidetes
Epsilonbacteraeota
Firmicutes
Fusobacteria
Patescibacteria
Proteobacteria
C
16S - Genus
CF-CRS Samples
Pseudomonas
Staphylococcus
Streptococcus
Haemophilus
Achromobacter
Burkholderia
Veillonella
Prevotella
Klebsiella
Megasphaera
Capnocytophaga
Corynebacterium
Stenotrophomonas
Actinobacillus
Campylobacter
Neisseria
Moraxella
Peptoniphilus
Enterobacter
Cutibacterium
% Abundance
10.0
1.0
0.1
D
Clinical culture
P. aeruginosa
P. aeruginosa (mucoid)
S. aureus
Coag.Neg.Staph
S. pneumoniae
H. influenzae
A. xylosoxidans
B. cepacia cmplx
Klebsiella sp.

Figure 3.1 CF-CRS sinus communities differentiate by Proteobacteria or Firmicutes. (A-B) Double principal coordinates analysis (DPCoA) of CF-CRS sinus bacterial communities. In (A) each point represents a single sample/community (n=22) (B) Shows corresponding ASVs, colored by Phylum. (C) Hierarchical clustered heatmap of CF-CRS samples with the top 20 genera by mean relative abundance. (D) Clinical culture results corresponding to each of the samples in the order of the heatmap in (C).

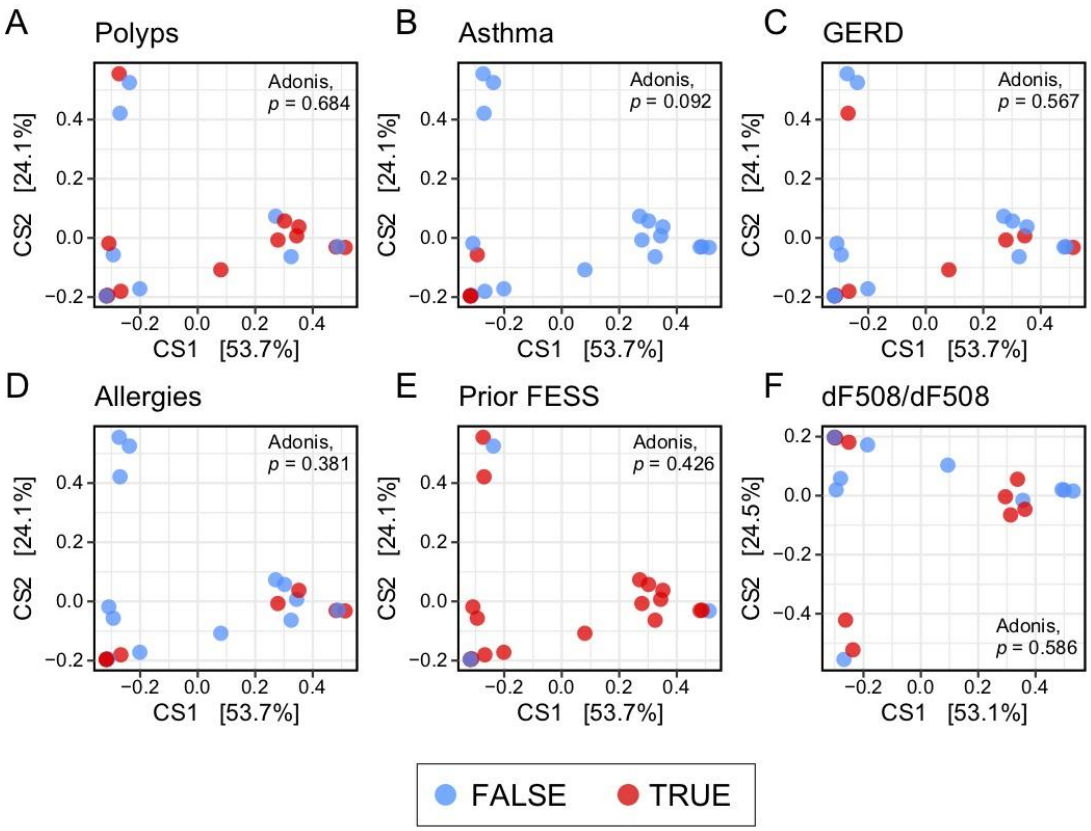

Figure 3.2 DPCoA of bacterial community composition with clinical factors. Double principal coordinate analysis (DPCoA) of CF-CRS bacterial communities (n=22) colored by (A) polyps, (B) asthma, (C) gastroesophageal reflux disease (GERD), (D) allergies, (E) prior FESS, and (F) homozygous ΔF508 genotype. Adonis ('vegan' R package) was used to test whether each clinical parameter explains a significant amount of DPCoA distances between communities.

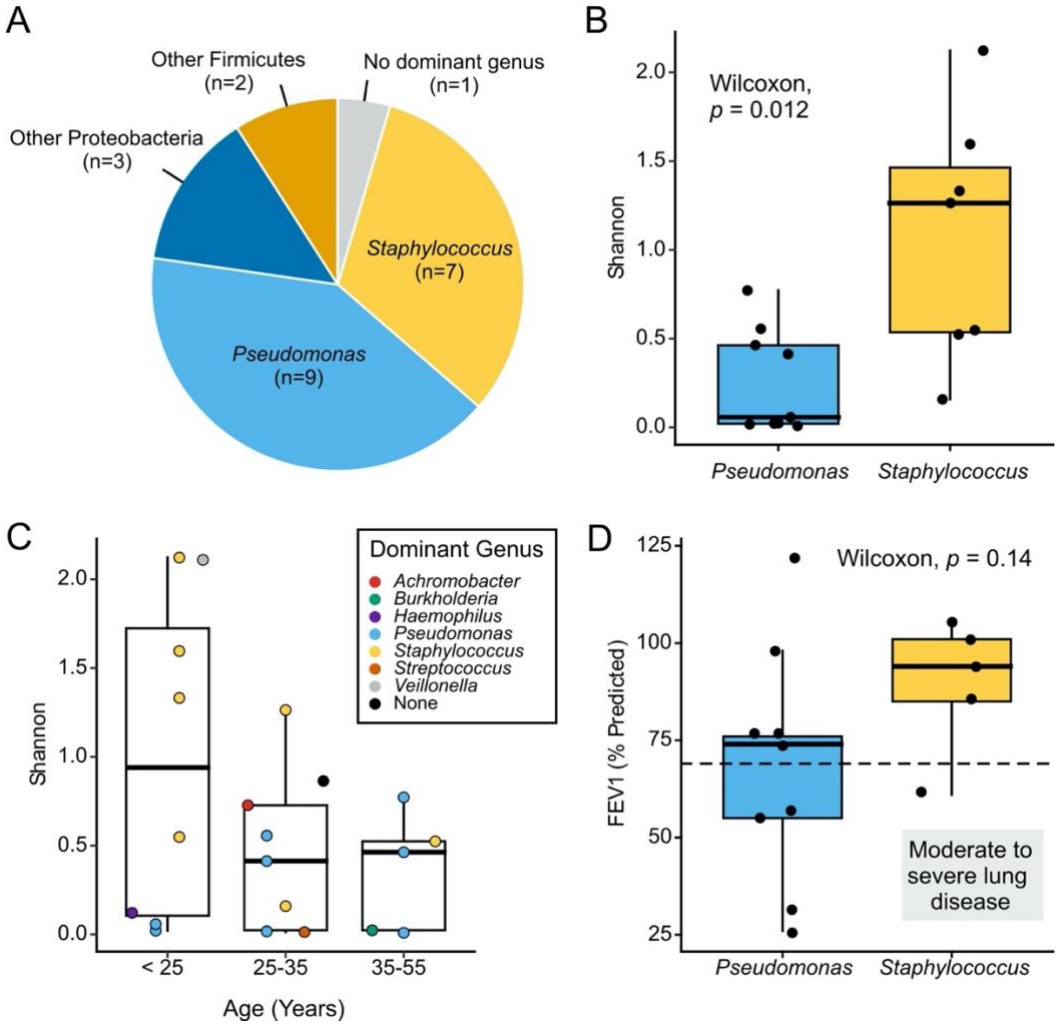

Figure 3.3. Shannon diversity and dominant *Pseudomonas* or *Staphylococcus*. (A) Number and proportion of samples with a dominant genus present (n = 22). (B) Shannon diversity compared between *Pseudomonas* or *Staphylococcus* dominance (Wilcoxon test, p = 0.012). (C) Shannon diversity compared to CF patient age (Kruskal-Wallis, p = 0.3). Points are colored by dominant genus. (D) Lung function measured by FEV1% compared between dominant genera (Wilcoxon test, p = 0.14). Dashed line denotes level below which lung function is considered to be moderate to severe.

Chapter 4: Anaerobic mucin degrading bacterial communities differentiate the microbiome in chronic rhinosinusitis and can impact physiology of nasal pathobiont *Staphylococcus aureus*

Summary

Chronic rhinosinusitis (CRS) describes a group of inflammatory disorders characterized by chronic sinonasal inflammation for which the etiology is incompletely understood. Culture-based and genomic methods have provided support for the presence of similar bacterial taxa in the CRS and non-CRS sinuses, confounding the role of bacteria in pathogenesis. The presence of anaerobic bacterial taxa has been associated with CRS cases that are recalcitrant to treatment, suggesting they may play a role in pathogenesis either directly or through community-level interactions. 16S rRNA gene sequencing data presented in this chapter demonstrates the increased relative abundance of anaerobic bacterial genera belonging to *Streptococcus, Prevotella,* and *Fusobacterium* in CRS sinus mucus, in contrast with the higher relative abundance of Actinobacteria in non-CRS sinus mucus. From these data, we hypothesized that bacterial consortia associated with CRS would have an anaerobic mucin-degrading phenotype, and that anaerobic mucin degradation could augment CRS pathogen *S. aureus* growth *in vitro*. Functional predictions made from the amplicon sequence variants were compared to the carbohydrate active enzyme database (CAZy) and suggest increased genetic potential for mucin degradation in CRS-associated communities. Anaerobic enrichments of CRS sinus mucus in minimal medium with mucin (MMM) as the sole nutrient source yielded communities that degraded high-molecular weight mucins and were characterized by genera *Streptococcus*, *Prevotella,* and *Fusobacterium*. We demonstrated that *in vitro* aerobic growth of *S. aureus* on cell-free supernatants (CFS) derived from CRS-enrichment cultures is enhanced

compared to MMM alone. Finally, transcriptional profiles of *S. aureus* grown on CFS revealed that mucin degradation and fermentation products can alter metabolism- and virulence-associated gene expression. From these experiments we conclude that there is an anaerobic mucin-degrading phenotype associated with bacterial communities found in the CRS sinonasal cavity. Furthermore, cooperative mucin-degradation by these communities can affect *S. aureus* physiology and virulence potential *in vitro.* This research provides novel insight into the metabolic activities and interbacterial interactions of CRS communities that may influence chronic infection by *S. aureus* in the sinonasal niche.

Introduction

Chronic sinusitis (CRS) is a heterogeneous inflammatory disease of the upper airways that affects 2-13% of the US population (Bhattacharyya and Gilani, 2018). Despite its prevalence, the complex pathogenesis of CRS is poorly understood. The disease has been linked to anatomic variation, immune dysfunction, host genetics, impaired mucus clearance, and microbial dysbiosis[2], but the importance of these factors and the order in which they occur remains controversial (Hoggard, Mackenzie, et al., 2017; Ooi et al., 2008). General consensus is that bacterial infection is integral to CRS pathogenesis. Thus, antibiotic therapy remains standard-of-care (Hoggard, Mackenzie, et al., 2017). However, given the low efficacy of conventional treatment regimens and rising concerns about multidrug resistance (Essack and Pignatari, 2013; Kennedy and Borish, 2013; Manarey et al., 2004), there remains a critical need to understand the precise role(s) of upper airway microbiota in CRS.

S. aureus is recognized as a primary pathogen of CRS and is the most common bacterium isolated from both inpatient and outpatient cultures (Busaba et al., 2004; Feazel et al., 2012; Ramakrishnan et al., 2013). Paradoxically, *S. aureus* also resides, persistently or intermittently, in the nasal cavity of up to 50% of adults without complications (Bassis et al., 2014; Gorwitz et al., 2008; Wertheim et al., 2005). Individuals colonized by *S. aureus* tend to retain the same strain over time, and *S. aureus* infections tend to be caused by the carried strain (Bode et al., 2010; Pugliese and Favero, 2001; H. F. L. Wertheim et al., 2004). Interestingly, total bacterial load is not significantly different between CRS and non-CRS

subjects colonized by *S. aureus* (Abreu et al., 2012; Ramakrishnan et al., 2013). This observation suggests that extrinsic host and environmental variables, not bacterial overgrowth, are determinants of the commensal versus pathogenic lifestyle of *S. aureus* within the upper airways.

S. aureus pathogenesis can be attributed to its vast repertoire of virulence factors whose expression is dependent on complex regulatory networks, growth phase, and diverse environmental stimuli (Balasubramanian et al., 2017; Jenul and Horswill, 2018). Interactions with co-colonizing microbiota can also affect *S. aureus* pathogenicity, particularly in the sinonasal cavity, where *S. aureus* thrives as part of a complex microbial community. For example, it has been suggested that *Cutibacterium* spp. can inhibit *S. aureus* growth through propionic acid production, and decrease virulence via extracellular porphyrins (Y. Wang et al., 2014; Wollenberg et al., 2014). Similarly, *Corynebacterium* spp. restrict *S. aureus* pathogenesis through bactericidal activity (Hardy et al., 2019) or by suppressing the expression of virulence factors (Ramsey et al., 2016). Early culture-based studies found facultative and obligate anaerobic bacteria to be associated with CRS (I Brook et al., 1994; Erkan et al., 1994, 2009), significantly so in comparison to non-CRS subjects (Klossek et al., 1998). A longitudinal study also implicated colonization by facultative and obligately anaerobic bacteria as a significant risk factor in CRS development (I Brook et al., 1996). However, mechanistic contributions of anaerobes to CRS pathogenesis, either directly or through interactions with *S. aureus*, have not yet been identified.

We recently demonstrated that commensal microbiota potentiate the growth and virulence of airway pathogens through the degradation of mucin glycoproteins (Flynn et al., 2020). Specifically, fermentation of *O*-linked oligosaccharides by oral-associated anaerobes generates amino acids and mixed-acid fermentation metabolites that *P. aeruginosa* can then use as nutrient sources. Building on our prior work and reports of hypoxia and increased mucin expression (MUC5B, MUC5AC) in CRS (Ding and Zheng, 2007; Kim et al., 2004), here we tested the hypothesis that CRS microbiota are characterized by anaerobic mucin-degrading activity. Using 16S rRNA gene sequencing we found that, as expected, *S. aureus* abundance did not differ between CRS mucus and non-CRS controls. However, a significant decrease in the relative abundance of Actinobacteria (*Corynebacterium*, *Cutibacterium*) in CRS was observed that inversely correlated with an increase in Bacteroidetes (*Prevotella*) and Fusobacteria. We then hypothesized that an increase of these known mucin-degrading taxa would alter the nutritional landscape of the sinuses and drive a shift in *S. aureus* physiology from commensalism to pathogenesis. Indeed, we discovered that by degrading and fermenting mucins into bioavailable substrates, *S. aureus* growth was supported. Finally, RNAseq analysis demonstrated that mucin-degrading bacterial consortia differentially modulate gene expression in *S. aureus*, including several genes associated with central metabolism and virulence. This work reveals a mechanism whereby bacterial metabolic functions and interactions have critical implications for the onset, progression, and treatment of chronic sinus disease.

Materials and Methods

FESS Sample Collection

69 participants with a positive diagnosis of CRS undergoing functional endoscopic sinus surgery (FESS) and 19 participants with no history of CRS, but undergoing unrelated sinonasal surgery, were recruited at the University of Minnesota Department of Otolaryngology. Exclusion criteria were diagnosis of cystic fibrosis, granulomatous polyangiitis, sarcoidosis, or Churg-Strauss syndrome. Informed consent was obtained from all subjects. Prior to surgery, each patient completed a sino-nasal outcomes test (SNOT-22) (Kennedy et al., 2013). Sinus secretions were obtained from a single maxillary sinus (middle meatal region) under endoscopic visualization by suction into Argyle Mucus Traps (Cardinal Health, Dublin, OH) which were frozen at -80°C. Clinical data were also obtained for each subject (Table 4.1). The UMN Institutional Review Board approved these studies (#1403M49021).

DNA extraction, 16S rRNA gene sequencing, and analysis

Genomic DNA was extracted from 300 µL of mucus using DNeasy Powersoil kits (Qiagen, Carlsbad, CA) and submitted to the UMN Genomics Center (UMGC) for 16S rRNA gene library preparation (Gohl et al., 2016). The V4 region was amplified and sequenced using Illumina MiSeq TruSeq 2x300 paired-end technology. Reagent control samples were also submitted and were below detection thresholds.

Sequence analyses, statistical analysis, and data visualizations were performed in R. Cutadapt/2.6 (Martin, 2011) was used to remove primer sequences, with size filtering set to 215bp (minimum) and 285bp (maximum). DADA2/1.14 (Callahan et al., 2016) was used to trim sequences and filter for quality. DADA2 inferred a parametric error model used to identify and correct sequencing errors. Reads were de-replicated, paired ends merged, and chimeric reads removed using default options. Genus-level taxonomy was assigned using the RDP bayesian classifier (Q. Wang et al., 2007) and SILVA-132 taxonomy training set (Quast et al., 2013). Species-level taxonomy was assigned only if an amplicon sequence variant (ASV) unambiguously matched a sequence in SILVA-132 or *e*HOMD databases (Escapa et al., 2018). A phylogenetic tree was approximated by first performing a multiple-alignment using DECIPHER/2.14.0 (Wright, 2016). Phangorn/2.5.5 (Schliep, 2011) was used to construct a phylogenetic tree. Resulting data were filtered to include samples with greater than 2000 reads. Phyla with ambiguous taxonomic assignments, total feature prevalence less than 10, or mean feature prevalence of 1 were removed, as were ASVs with a mean relative abundance below $1x10^{-4}$.

PICRUSt2 (Douglas et al., 2020) was used to perform hidden-state prediction of metagenomic content, summarized into enzyme classes (ECs). Carbohydrate active ECs were identified through comparison to the Carbohydrate Active Enzyme Database (CAZy) (Lombard et al., 2014), downloaded from the dbCAN2 meta server (Zhang et al., 2018). EC count abundances were normalized to relative abundances of the top ten contributing ASVs in each subject group (CRS/non-CRS).

Bacterial strains and culture conditions.

Enrichments of mucin-degrading microbial communities were obtained through inoculation of a defined minimal mucin medium (MMM) (Flynn et al., 2016) with 100 uL of FESS-derived mucus. Cultures were incubated at 37°C under anaerobic conditions (5%H_2, 5%$CO_2$90% N_2) in a Coy anaerobic chamber (Coy Lab Products, Grass Lake, MI) without mixing for 48 hours, sub-cultured 1:100 into fresh MMM, and incubated for another 48 hours. Aliquots for 16S rRNA gene sequencing and 20% glycerol stocks were retrieved from each enrichment culture and stored at -80°C. Cell-free supernatants (CFS) were generated through inoculation of MMM from glycerol stocks and incubated for 48 hours at 37°C under anaerobic conditions. Each culture was then sub-cultured 1:100 in MMM and incubated for 48 hours. Cells were removed by centrifugation at 7000 x g for 10 min, followed by filtration through a 0.2 um polyethersulfone (PES) membrane filter. Filtrates were stored at -80°C until use.

S. aureus strain USA300 LAC (Diep et al., 2006) was maintained on tryptic soy agar (TSA). Prior to all growth experiments, overnight cultures were grown in tryptic soy broth shaking at 220 RPM at 37°C. Cells were washed three times with phosphate buffered saline (PBS) and diluted to an optical density (OD_{600}) of 0.02 in MMM or CFS. Amendments to MMM included 0.25% glucose (MMMG), 0.5% lactate (0.5%) (MMML), casamino acids (0.5%) (MMMC), or lactate (0.5%) and casamino acids (0.5%) (MMMLC). Respiratory conditions were induced in anaerobic cultures by addition of 3mM sodium nitrate. OD_{600} measurements were obtained using a Synergy H1 plate reader (BioTek, Winooski, VT) with continuous orbital shaking (282 cycles

per minute) at 37°C. Growth experiments were performed in triplicate using three biological replicates.

FPLC/HPLC analysis of CFS

Fast protein liquid chromatography (FPLC) was used to evaluate the integrity of high molecular weight mucins. Using an Äkta Pure FPLC (GE Healthcare Bio-Sciences, Marlborough, MA) at 4C, 500 uL of MMM or CFS was injected and subject to an isocratic run at a flow rate of 0.4 mL/min for 1.5 CV with 50 mM phosphate buffer (pH 7.2) and 150 mM NaCl on a 15mL column volume (CV) 10/200mm Tricorn column packed with Sepharose 2B-CL beads. Data were collected using Unicorn 7 software (GE Healthcare Bio-Sciences AB, Uppsala, SE) and analyzed using a custom R script.

High-performance liquid chromatography (HPLC) was used to measure concentrations of acetate, butyrate, propionate, lactate, succinate, and pyruvate using pure standards ranging from 0.1 mM to 10 mM. To remove high molecular weight glycoproteins, CFS were filtered using regenerated cellulose protein concentrators (3000 MWCO; Amicon, MilliporeSigma). Eluent was analyzed using a Dionex UltiMate 3000 UHPLC (Thermo Fisher) system equipped with an Acclaim Organic Acid Column (5um, 120A, 4.0x250mm). A 32-minute isocratic instrument method was used for analysis consisting of an 8-minute equilibration period followed by a 24-minute sample run at 1.0ml/min at 30°C. Sodium sulfate (100mM, pH 2.6) was the mobile phase. All samples were analyzed at a wavelength of 210nm. Chromeleon 7 software (Dionex, Sunnyvale, CA, USA) was used to visualize and process data, and Cobra Wizard was used to identify and automatically gate chromatogram peaks of interest.

RNA Isolation, RNA-Seq, and data analysis

Total RNA was extracted from 5 mL cultures grown to early stationary phase in CFS, or MMMG following a previously described method (Carroll et al., 2014) with modifications. Briefly, cells were pelleted by centrifugation for 5 minutes at 7000 x *g* and snap frozen in liquid nitrogen before storage at -80°C overnight. RNA was extracted from cell pellets using an RNeasy Mini kit (Qiagen). DNaseI treatment was carried out as part of the RNA Clean and Concentrator kit (Zymo, Irvine CA). RNA quality (RIN ≥ 9.8) and quantity were assessed using an Agilent Bioanalyzer. Paired-end 75bp libraries were prepared by UMGC using Illumina TruSeq Stranded RNA workflow with bacterial ribosomal reduction using Ribo-Zero (Illumina, San Diego, CA). Libraries were sequenced using the Illumina NextSeq platform.

Raw fastq files were checked for quality and adapter sequences using FastQC. Sequences were then aligned to the USA300_FPR3757 genome (NCBI RefSeq NC_007793.1) (Diep et al., 2006) using the Subread aligner, implemented using RSubread (Liao et al., 2013, 2019). Gene counting for each sample was performed using '*featureCounts'*, also using RSubread. Sample ordination was carried out on regularized-log transformed counts using '*rlog'* and *'pcomp'* functions within DESeq2/3.9 (Love et al., 2014). The *'deseq'* function was used to estimate size factors, carry out variance-stabilizing transformation and statistical testing via the Wald Test. Genes with a log2 fold-change greater than 1 (set using the lfcThreshold parameter) with two-tailed Benjamini-Hochberg adjusted $p<0.05$ were considered significant.

Data availability

Code for all analyses in this section has been made available at: https://github.com/hunterlabumn/CRS-mucin-degradation

Results

CRS is associated with an anaerobic mucin-degrading bacterial phenotype

To first test our hypothesis that CRS sinuses harbor an increased prevalence of anaerobic microbiota, we obtained sinus mucus from CRS (n=61) and non-CRS (n=19) subjects. Community composition was described using taxonomy derived from amplicon sequence variants (ASVs) generated from 16S rRNA gene sequence analysis. Demographic and clinical data associated with each subject were also obtained (Table 4.1). A comparison of bacterial communities using double principal coordinate analysis (DPCoA) revealed considerable within-group variation among CRS microbiota (Figure 4.1A). With exceptions, non-CRS samples clustered more closely compared to CRS samples. The split plot demonstrated 53.5% variation represented along the first axis which suggests that CRS samples deviate from non-CRS based on the presence/absence of Actinobacteria, Bacteroidetes, and Fusobacteria. Indeed, a greater relative abundance of Actinobacteria was significantly associated with non-CRS samples (Wilcoxon, $P < 0.001$) (Figure 4.1B). A greater relative abundance of Actinobacteria was also significantly associated with samples from patients with no prior history of FESS (Wilcoxon, $P = 0.015$) (Figure 4.1C), suggesting an association with earlier stages of disease. Actinobacteria also exhibited an inverse relationship with the relative abundance of both Bacteroidetes and Fusobacteria (Wilcoxon, $P < 0.001$, Figure 4.1D). Second axis variance in the DPCoA (11%, Figure 4.1A) was primarily driven by Proteobacteria. Relative abundances of phyla across all samples are shown in Figure 4.2. These analyses demonstrate that while CRS

and non-CRS samples share many of the same bacterial taxa, differences between groups occur at the phylum level.

Where identification of obligate anaerobes in CRS has been previously hindered by cultivability, sampling, or database representation, we leveraged the increased resolution of ASVs over conventional use of molecular operational taxonomic units (OTUs) to provide a detailed characterization of bacterial diversity in the sinus cavity (Table 2). At the genus level (Figure 4.1E), relative abundances of *Staphylococcus* spp. did not appreciably differ between CRS (11%) and non-CRS (15%), as expected. These data support previous culture-based and culture-independent studies demonstrating similar prevalence and abundance of *S. aureus* between patient groups (Abreu et al., 2012; Ramakrishnan et al., 2013). In agreement with the DPCoA (Figure 4.1A), non-CRS samples were distinguished by Actinobacteria – *Corynebacterium* (14% vs 6%), *Cutibacterium* (3.6% vs 1.1%), and *Actinomyces* (1.1% vs 0.2%) – consistent with their roles as commensal inhabitants of the upper airways while attenuating *S. aureus* pathogenicity (Hardy et al., 2019; Ramsey et al., 2016; Y. Wang et al., 2014; Wollenberg et al., 2014). ASVs belonging to *Pseudomonas* and *Staphylococcus* were second and third most abundant in CRS, respectively, consistent with their role as airway pathogens. Most notable, however, was that *Streptococcus* was highly abundant in CRS at an average relative abundance of 17.2% compared to 6.8% in non-CRS subjects. *Prevotella* and *Fusobacterium,* both obligate anaerobes, were also more abundant in CRS. Together, these

data suggest that the CRS sinus bacterial communities exhibit a loss of commensal taxa, and favors (and/or is driven by) growth of facultative and obligate anaerobes.

Given the association of *Streptococcus, Prevotella, and Fusobacterium* with oral- and gut-associated bacterial communities known for metabolizing host-derived mucin glycoproteins (Argüeso et al., 1998; Beighton and Whiley, 1990; Bradshaw et al., 1994; Byers et al., 2000; Homer et al., 1996; Kiyohara et al., 2010; Mondal et al., 2014; Rho et al., 2005; Sanders et al., 2007; Tailford et al., 2015; Terra et al., 2010; Wickström et al., 2009; D. P. Wright et al., 2000), we then hypothesized that CRS microbiota would exhibit the functional capacity to degrade mucins, which are increased in expression in CRS (Ding and Zheng, 2007; Kim et al., 2004). To test this hypothesis, we used PICRUSt2 (Douglas et al., 2020) to predict metagenomic content based on 16S rRNA sequencing data, which was then summarized into enzyme categories (ECs) and compared to the Carbohydrate Active Enzyme (CAZy) database (Lombard et al., 2014). Selection of the top CAZy EC classes by relative functional abundance revealed that glycoside hydrolases and polysaccharide lyases were more prevalent in CRS predicted metagenomes (Figure 4.3A), including many with previously defined roles in mucin degradation (β-glucuronidase, β-galactosidase, hyaluronate lyase, exo-α-sialidase, and chitinase). By contrast, metagenomes predicted from non-CRS samples were characterized by the presence of ECs with glycotransferase (GT) and carbohydrate esterase (CE) functions (Figure 4.3B). These *in silico* analyses are predictive of CRS microbiota having increased capacity for cleavage of glycosidic bonds and degradation of mucin oligosaccharides.

To validate our metagenome predictions, and to demonstrate that CRS microbiota retain their mucin degradation capacity in vivo, we used an anaerobic enrichment scheme (Flynn et al., 2016) in which sinus mucus was serially passaged in a defined growth medium containing 15g L^{-1} purified MUC5AC as the carbon source (minimal mucin medium, MMM). After two passages of 48h, bacterial composition pre- and post-enrichment was profiled. Similar to our initial sequencing data (Figure 4.1), CRS subjects harbored diverse bacterial communities, often dominated by a single recognized pathogen (Figure 4.4A). Post-enrichment mean relative abundances of *Prevotella* (19.4%), *Veillonella* (19.7%), *Fusobacterium* (13.3%) and *Streptococcus* (15.3%) all increased across samples (Figure 4.4B). Enrichment cultures were similar between patients, even when original community membership differed (Figure 4.4C), suggesting a core mucin-degrading consortium. FPLC was also used to assess integrity of high-molecular weight mucins included in the enrichment medium. As predicted, chromatograms (Figure 4.4D) show that the peak area derived from each bacterial community was markedly decreased, reflecting reduced mucin integrity as a result of enrichment. Together, these data support our hypothesis that anaerobic microbiota alter the CRS microenvironment via degradation of mucin glycoproteins.

S. aureus *growth on mucin is inefficient and respiration dependent.*

When *Staphylococcus* ASVs were present in the original sample (subjects B-F, H), they were notably absent from the enrichment (Figure 4.4A). This suggests that

Staphylococcus spp. are either (i) inhibited by enrichment communities, (ii) unable to efficiently use mucins or degradation byproducts as nutrients, or (iii) unable to do so under oxygen limitation, despite fermentative capacity. To test these possibilities, *S. aureus* strain USA300 LAC was first grown aerobically in MMM. Growth was limited on MMM alone, suggesting that metabolic requirements are not met by intact high-molecular weight mucins. However, growth rate and yield were significantly increased when supplemented with casamino acids, lactate, and glucose, which mimic metabolites generated via mucin degradation and fermentation (Figure 4.5A). Growth on these supplements was restricted under anaerobic (fermentative) conditions but was partially restored with the addition of 3mM sodium nitrate as an electron acceptor (Figure 4.5B). From these results it can be concluded that *S. aureus* does not efficiently use mucins as a nutrient source. As expected, the *in vitro* conditions support growth when additional nutrients are supplied, particularly under respiratory conditions.

Secondary metabolites from mucin degradation support* S. aureus *growth.

To test whether degradation and fermentation by other bacteria could provide nutrients to *S. aureus*, and to ensure that *S. aureus* was not inhibited by co-colonizing microbiota, LAC was cultured on cell-free supernatants (CFS) derived from enrichment samples (A-H in Figure 4.4) under aerobic and anaerobic (respiratory and non-respiratory) conditions. Under aerobic conditions, LAC exhibited equal or improved growth in all CFS, despite having less total carbon in the growth medium (i.e. it was removed by anaerobes

during enrichment) (Figure 4.6A). Interestingly, communities A, E, and G which generated CFS supporting low *S. aureus* growth yields were enriched from samples in which *Staphylococcus* ASVs were absent or at very low abundance (see Figure 4.4A).

Anaerobic growth yields after 24h showed a similar pattern, signifying the presence of fermentable metabolites (e.g. glucose, galactose) as a result of mucin degradation (Figure 4.6B). Establishment of respiratory conditions with the addition of sodium nitrate (3mM) resulted in increased growth yields in all conditions. We conclude that aerobic and anaerobic growth of *S. aureus* can be supported by metabolites liberated or produced by CRS-derived mucin-degrading bacteria.

Byproducts of fermentation by mucin degrading communities constitute one source of metabolites that can alter *S. aureus* physiology. We used high performance liquid chromatography (HPLC) to measure fermentation byproducts acetate, propionate, butyrate, and lactate in the CFS (n = 1 replicate for each). We found these metabolites to be present in the millimolar range, and highly variable across supernatants. CFS-A with very low levels of SCFA, Succinate/Pyruvate, and CFS-E, with high levels of Acetate and Propionate, were also associated with the lowest growth rate and yield under aerobic conditions (Figure 4.6A). The two CFS-F and -H resulted in the greatest growth rates and yields, and also had higher levels of lactate, however, high lactate could not explain growth patterns seen in the other supernatants. There are likely many more other metabolites resulting from mucin-degradation not measured here that influence *S. aureus* growth in our *in vitro* conditions.

Mucin degradation supernatants influence S. aureus *transcription*

Increased *S. aureus* growth on CFS also raised the question of how metabolism, virulence, or other cell processes were modified at the transcriptional level. To gain insight into pathways that were differentially expressed in response to anaerobic mucin degradation, we used RNAseq to profile *S. aureus* gene expression during growth on cell-free supernatants (CFS) relative to growth on MMM supplemented with glucose (MMMG), a preferred carbon source of *S. aureus* during infection (Vitko et al., 2016). CFS samples D, F, and H were selected for their consistent ability to support *S. aureus* growth under both aerobic and anaerobic conditions.

Differential gene expression in all three supernatants relative to MMMG is shown in Figure 4.7A. Across samples, 93 genes (79 upregulated, 14 downregulated) were differentially expressed (2-fold or greater, $P < 0.05$). Common to all supernatants was increased expression of genes in the *nan* locus involved in transport and catabolism of sialic acid (*N*-acetylneuraminic acid [Neu5Ac]) (Olson et al., 2013) (Figure 4.7 A, B). PTS-dependent glucose and ManNAc transporter *glcC* (Vitko et al., 2016), was also differentially expressed.

Interestingly, there was increased expression of NAD-dependent formate dehydrogenase (*fdh*) and formyltetrahydrofolate synthetase (*fhs*), implying formate catabolism. However, these genes were not accompanied by increases in pyruvate formate lyase (*pflA, pflB*) expression, whose gene products supply formate to FDH and pyruvate for substrate-level phosphorylation (Leibig et al., 2010). The gene involved in the

conversion of acetate to acetyl-CoA (*acsA)* was also significantly increased (Figure 4.7C), but not the reverse process (*pta, ackA*). Altogether, these data suggest that mixed-acid fermentation metabolites such as formate and acetate are provided exogenously to *S. aureus* by CRS anaerobes.

An increase in expression of genes associated with glutamate import (*gltS*) and synthesis via catabolism of arginine (*rocF, rocD, rocA*) and proline (*putA, rocA*) was observed in the supernatant conditions (Figure 4.7A,C) (Halsey et al., 2017). Increased expression of *gudB* signifies glutamate conversion to 2-oxoglutarate for entry into the TCA cycle. Additionally, expression of genes associated with the left side of the TCA cycle and gluconeogenesis (*sucA, sucC, sdhA, fumC, mqo1, pckA*) were all significantly increased, indicating that amino acids may be fueling gluconeogenesis under the conditions tested. Other functional categories of genes consistently expressed across supernatants include peptidoglycan recycling (*murQ*) (Borisova et al., 2016), fatty acid metabolism (*fadA, fadB, fadD, fadE, fadX*) (Kenny et al., 2009), biotin biosynthesis (*bioA, bioB, bioD, bioF, bioW, bioY*) (Satiaputra et al., 2018), and virulence (*spa* and a gene encoding a putative immunoglobulin-blocking virulence protein, RS09510) (Balasubramanian et al., 2017). The differential transcription of these genes indicates that *S. aureus* metabolism is significantly altered in comparison to growth on glucose.

Several transcripts were differentially expressed between supernatants conditions. Hierarchical clustering revealed that the *S. aureus* transcriptome from CFS-H was distinct from CFS-D and CFS-F (Figure 4.7D). Transcripts associated with amino acid transport

and biosynthesis were more abundant in CFS-D/F. Of note was expression of the *ilv-leu* operon involved in branched-chain amino acid (BCAA) synthesis, accompanied by increased expression of genes encoding α-acetolactate decarboxylase (*budA)* and α-acetolactate synthase (*budB*) (Kaiser and Heinrichs, 2018). Genes required for galactose import (*lacCDEF*) (Rosey et al., 1991) were also upregulated in CFS-D/F, suggestive of its availability in these supernatants. Genes involved in cysteine-sulfur-methionine homeostasis (*ssuABC, metICFH-mdf operons*) (Schoenfelder et al., 2013) and peptide transport (*opp3DAF*) (Lehman et al., 2019) were also seen at higher levels in CFS-D/F.

Virulence-related gene transcription also differentiated supernatant growth conditions. Notably, transcription of the *agr* operon and RNAIII (*hld)* were higher in CFS-H. Protease transcripts staphopain B (*sspB*), aureolysin (*aur*), and immunodominant antigen B (*isaB*) were also more abundant in this condition. Supernatants CFS-D/F yielded transcriptomes that exhibited more of a biofilm-like phenotype, with increased prevalence of transcripts for holin protein (*cidA*) and exopolysaccharide (*icaABC)* (Cramton et al., 1999; Rice et al., 2007). Taken together, these data demonstrate that, in addition to supporting *S. aureus* growth, expression of genes associated with metabolism, virulence, and other cellular processes is highly dependent on the specific composition of their co-colonizing microbiota and the metabolites they exchange.

Discussion

S. aureus is consistently associated with the development of CRS, and the inefficacy of clinical therapies (Bhattacharyya and Kepnes, 1999; Ramakrishnan et al., 2015). However, *S. aureus* is also present in the nasal passages of ~50% of healthy individuals (Bassis et al., 2014; Gorwitz et al., 2008; H. F. Wertheim et al., 2005), suggesting that the sinus microenvironment and bacterial activities within, may tip the balance between commensalism and pathogenesis of *S. aureus in vivo*. Here we demonstrate differences in CRS and non-CRS bacterial communities and implicate mucin as a nutrient source supporting anaerobic bacterial diversity in the sinuses. Moreover, we show that the degradation of mucins by CRS-derived communities impacts *S. aureus* growth and alters its transcriptional profile.

Research spanning several decades has described the microbiology of CRS, both by culture and molecular methods (Hoggard, Mackenzie, et al., 2017). There is general agreement in the prevalence of potential pathogenic bacteria implicated in disease, including *S. aureus*. However, surveying bacterial diversity in this niche is subject to bias in the observation of low abundance or fastidious organisms based on sampling methods, cultivability, and representation in databases for taxonomic assignment (Hoggard, Mackenzie, et al., 2017). Observation of anaerobes in CRS has therefore varied across studies (Itzhak Brook, 2011). Here, we leverage the use of ASVs for taxonomic assignment, resulting in high-resolution observations that both confirm species-level identification of anaerobes in culture-based studies (e.g. *P. melaninogenica, F. nucleatum*),

and contribute previously unreported bacterial species (e.g. *F. periodonticum, Dialister invisus, Porphyromonas pasteri*) (Table 2). Although this resolution is useful for generating hypotheses about potential interbacterial interactions, differences in bacterial consortia in CRS and non-CRS can also be seen at the phylum level. Actinobacteria relative abundance differentiates CRS subjects from non-CRS subjects, and within CRS subjects, is negatively correlated with the number of therapeutic surgical interventions (FESS). Interestingly, *Corynebacterium* (Actinobacteria) presence in the sinuses prior to FESS has been linked with better patient outcomes (Ramakrishnan et al., 2015), suggesting it is a member in a less inflammatory community. Furthermore, the relative abundance of Actinobacteria have an inverse relationship with both Bacteroidetes and Fusobacteria, suggesting that the presence of anaerobes may represent a distinct dysbiotic stage in CRS disease progression.

Hypersecretion of mucus is a hallmark of CRS disease (Ding and Zheng, 2007; Kim et al., 2004). Due to their complex structure, mucins, the main component of mucus, paradoxically provide both mucosal barrier protection and a rich source of nutrients for organisms that can degrade them (Wagner et al., 2018). In better characterized ecosystems such as the gut and oral cavity, mucins act as important mediators of microbial community assembly, requiring a diversity of glycolytic and proteolytic enzymatic functions for degradation (Wagner et al., 2018). Metagenomic prediction showing increased carbohydrate active enzyme abundances from CRS associated bacterial communities led us to hypothesize that mucins support anaerobic bacterial taxa in this niche. We found

mucins support the major anaerobic taxa observed in our original analysis, recovering communities dominated by *Streptococcus, Veillonella, Prevotella,* and *Fusobacteria.* The similarity across enrichment communities despite dissimilar original samples was striking. Interestingly, diverse metabolic phenotypes are represented within and between the top genera. Several species of *Streptococcus* and *Prevotella* have been noted for their saccharolytic capabilities necessary to break down mucin glycans (Bradshaw et al., 1994; Derrien and Passel, 2010; Wickström et al., 2009; D. P. Wright et al., 2000). By contrast, characterization of *F. nucleatum* indicates it is only minimally saccharolytic, and instead relies on amino acid catabolism and peptide assimilation (Bradshaw et al., 1994; Loesche and Gibbons, 1968). Carbohydrate fermentation has not been described for *Veillonella spp.* which instead rely on fermentation byproducts such as lactate for growth (Ng and Hamilton, 1971). These results indicate that under anaerobic conditions, mucin degradation alone can support diverse bacterial metabolisms within a community.

A critical component of *S. aureus'* capacity for colonization and virulence potential is its ability to adopt metabolic states given a range of nutrient sources and respiratory conditions (Carvalho et al., 2017; Halsey et al., 2017; Krismer et al., 2014; Spahich et al., 2016), However, *S. aureus* use of mucins as a nutrient source has not been described, and our results demonstrate that intact, high molecular weight mucins do not support robust growth. Lactate, amino acids, and glycolytic substrates have all been indicated as important metabolites in models of *S. aureus* survival and pathogenicity (Spahich et al., 2016; Vitko et al., 2016), and their addition to MMM demonstrates that these metabolites support

growth under our experimental conditions. Proposed sources of these metabolites are host and *S. aureus* activities such as collagen degradation and carbohydrate fermentation (Halsey et al., 2017; Lehman et al., 2019). We hypothesized that co-colonizing bacteria in CRS can also provide these and other metabolites through mucin degradation and cross-feed *S. aureus*. Counter to this prediction was the observation that the genus *Staphylococcus* was not recovered in any of our enrichment cultures, suggesting that antagonistic bacterial interactions, competition, or lack of oxygen or other nutrients was inhibiting Staphylococcal survival. However, when we used cell-free supernatants from CRS mucin-degrading communities, we showed that *S. aureus* grew to higher densities compared to mucin alone. Our results suggest that mucin degradation can supply nutrients to support *S. aureus* growth. Interbacterial interactions governing *S. aureus* co-existence with mucin-degrading communities, and the metabolic parameters that shape these relationships, are the subject of ongoing investigation.

The mechanisms whereby the microenvironment influences *S. aureus* ability to colonize mucosal surfaces, subvert the immune system, and initiate infection continue to be an active area of research. Respiratory microbiota have been shown to impact the microenvironment at the respiratory mucosa in non-trivial ways. For example, cleavage of sialic acids from host proteins is a well-documented characteristic of various members of the Streptococci seen in our study (Blanchette et al., 2016; Bradshaw et al., 1994). Our transcriptome analysis of *S. aureus* growth on three different supernatants from CRS-derived mucin-degrading communities revealed upregulation of sialic acid transport and

catabolism genes from the *nan* locus, indicating a response to this carbon and nitrogen source. Current models of *S. aureus* metabolic adaptation under changing respiration and nutrient levels support a strong link between the metabolite pool, metabolic state, and virulence (Jenul and Horswill, 2018). Expression profiles revealed upregulation of many of the same pathways deemed important for *S. aureus* survival and virulence potential in these models, such as glutamate synthesis via arginine and proline (Halsey et al., 2017). Separately, the supernatants impacted virulence-related gene transcription in different ways. Genes of the *agr locus*, a master regulatory system controlling the expression of virulence factors including extracellular proteases (Jenul and Horswill, 2018), were upregulated only when *S. aureus* was grown in CFS-H. The transcriptional profiles of *S. aureus* grown in CFS-D/F exhibited gene expression associated with nitrosative stress tolerance, clumping, adhesion, and biofilm formation (Carvalho et al., 2017; Cramton et al., 1999; Rice et al., 2007). *S. aureus* exacerbation of CRS disease is complex, likely involving both inflammation-inducing virulence factor expression, and aggregation and biofilm formation known to reduce efficacy of antibiotic therapies (Archer et al., 2011). Altogether, our data show that mucin-degradation contributes to the microenvironment in significant ways, altering *S. aureus* growth and transcription.

The scope of our results is limited in that our observations only include bacteria. We acknowledge that fungi may be present in our samples as well, and mucin-fungal interactions have been reported previously. Additionally, we did not look further into the impact of community-derived proteins and small molecules in the supernatants that may

directly impact *S. aureus* growth and gene expression phenotypes, though there is precedence for these interactions. For example, *Corynebacterium* spp. quench *S. aureus* quorum sensing via small molecule interference (Ramsey et al., 2016). Finally, our observations of *S. aureus* growth and transcription were all conducted in monoculture, which excludes spatial and contact-dependent polymicrobial interactions, such as the recently demonstrated aggregate formation with *Fusobacterium nucleatum* (Lima et al., 2019). Observations of increased virulence through protease expression, or biofilm formation will need to be tested *in vivo* to better understand the contribution of these interactions to the development and persistence of CRS.

Overall, our results suggest that a reduction in the relative abundance of Actinobacteria, including *Corynebacterium*, and increase in Bacteroides and Fusobacteria may represent a dysbiotic state in CRS. Members of Bacteroidetes, Fusobacteria and anaerobic Firmicutes are common members of mucin degrading communities, which can be isolated from CRS sinus mucus, and whose collective metabolic activities can support *S. aureus* growth and alter gene transcription. Our findings provide a basis for further characterization of anaerobe-*S. aureus* interactions and determination of their importance *in vivo.*

Acknowledgements

We would like to acknowledge the UMN Genomics Center for sequencing assistance. Alex Villarreal in the Hunter Lab generated the HPLC data for this study. My thanks to Abayo

Itabiyi and Erin Feddema, who were research associates in the UMN Department of Otolaryngology, Head & Neck Surgery and helped with FESS sample collection. Thank you to Holly Boyer, who was the surgeon on all FESS cases for sample collection.

Table 4.1 Demographic and clinical data for FESS patients

CRS Diagnosis	CRS (*n* = 61)	Non-CRS (n = 19)
Age (mean ± S.D.)	49.5 ±13.8	43.1 ±14.4
SNOT22 (mean ± S.D.)	1.9 ± 1.0	0.93 ± 0.8
Sex (% Female)	52.5	42.1
Polyps (%)	42.6	0
GERD (%)	23.0	15.8
Asthma (%)	50.8	5.3
Allergies (%)	36.1	21.1

Table 4.2 Prevalence and average relative abundance of anaerobe features in CRS and non-CRS samples †

Taxonomic Feature	Prevalence in Samples		Average Relative Abundance (%)		Species Assignment Database (SILVA/HOMD)
	(CRS)	(Non-CRS)	(CRS)	(Non-CRS)	
Actinomyces					
Actinomyces	9	4	0.03	0.59	
Actinomyces graevenitzii	7	3	0.04	0.03	SILVA/HOMD
Actinomyces odontolyticus	17	9	0.16	0.59	SILVA
Total	**33**	**16**	**0.23**	**1.22**	
Akkermansia					
Akkermansia muciniphila	2	0	0.13	0.00	SILVA
Total	**2**	**0**	**0.13**	**0.00**	
Anaerococcus					
Anaerococcus	7	6	0.57	0.22	
Anaerococcus nagyae	2	1	0.01	0.01	SILVA
Anaerococcus octavius	6	8	0.19	0.37	SILVA/HOMD
Anaerococcus provenciensis	1	3	0.00	0.27	SILVA
Total	**16**	**18**	**0.77**	**0.87**	
Atopobium					
Atopobium parvulum	6	2	0.03	0.02	SILVA/HOMD
Atopobium rimae	1	1	0.02	0.03	SILVA/HOMD
Total	**7**	**3**	**0.05**	**0.05**	
Bacteroides					
Bacteroides	3	1	1.25	0.17	
Bacteroides acidifaciens	2	1	0.20	0.19	SILVA
Total	**5**	**2**	**1.46**	**0.36**	
Campylobacter					
Campylobacter	6	4	0.07	0.36	
Campylobacter concisus	15	3	0.15	0.48	SILVA
Campylobacter gracilis	5	0	0.28	0.00	SILVA/HOMD
Campylobacter ureolyticus	1	2	0.00	0.07	SILVA/HOMD
Total	**27**	**9**	**0.50**	**0.91**	
Capnocytophaga					
Capnocytophaga gingivalis	2	1	0.01	0.01	SILVA/HOMD
Capnocytophaga leadbetteri	7	2	0.06	0.06	SILVA/HOMD
Capnocytophaga ochracea	1	0	0.03	0.00	SILVA
Total	**10**	**3**	**0.09**	**0.07**	
Cutibacterium					
Cutibacterium acnes	36	13	0.96	3.43	SILVA/HOMD

Cutibacterium granulosum	9	8	0.13	0.20	HOMD
Total	**45**	**21**	**1.08**	**3.62**	SILVA/HOMD
Dialister					SILVA
Dialister invisus	7	2	0.05	0.07	
Dialister micraerophilus	0	1	0.00	0.09	
Dialister pneumosintes	8	3	0.33	0.06	
Dialister propionicifaciens	2	3	0.04	0.06	SILVA/HOMD
Total	**17**	**9**	**0.42**	**0.28**	
Eikenella					
Eikenella	1	0	0.02	0.00	SILVA/HOMD
Eikenella corrodens	4	0	0.05	0.00	
Total	**5**	**0**	**0.07**	**0.00**	
Finegoldia					
Finegoldia magna	11	9	1.16	0.50	SILVA/HOMD
Total	**11**	**9**	**1.16**	**0.50**	SILVA/HOMD
Fusobacterium					SILVA/HOMD
Fusobacterium	16	2	1.53	0.08	
Fusobacterium necrophorum	1	0	0.02	0.00	
Fusobacterium nucleatum	18	5	3.39	2.94	
Fusobacterium periodonticum	14	4	0.45	0.43	
Total	**49**	**11**	**5.39**	**3.46**	
Gemella					HOMD
Gemella	14	8	0.15	0.24	SILVA/HOMD
Total	**14**	**8**	**0.15**	**0.24**	
Granulicatella					
Granulicatella adiacens	14	8	0.12	1.72	
Granulicatella elegans	6	2	0.04	0.03	
Total	**20**	**10**	**0.16**	**1.74**	
Oribacterium					SILVA/HOMD
Oribacterium	2	0	0.02	0.00	
Total	**2**	**0**	**0.02**	**0.00**	
Parvimonas					
Parvimonas micra	15	1	0.36	0.02	SILVA
Total	**15**	**1**	**0.36**	**0.02**	SILVA/HOMD
Peptoniphilus					
Peptoniphilus	7	8	0.05	0.83	
Peptoniphilus duerdenii	1	0	0.03	0.00	SILVA/HOMD
Peptoniphilus lacrimalis	1	0	0.04	0.00	
Total	**9**	**8**	**0.13**	**0.83**	
Peptostreptococcus					
Peptostreptococcus stomatis	8	2	0.11	0.02	SILVA
Total	**8**	**2**	**0.11**	**0.02**	SILVA
Porphyromonas					SILVA
Porphyromonas	3	1	0.06	0.27	
Porphyromonas endodontalis	9	3	0.54	0.34	

Porphyromonas gingivalis	1	0	0.01	0.00	
Porphyromonas pasteri	8	3	0.23	0.14	SILVA/HOMD
Total	**21**	**7**	**0.84**	**0.76**	SILVA
Prevotella					SILVA/HOMD
Prevotella	19	7	2.18	0.76	SILVA/HOMD
Prevotella baroniae	3	0	0.04	0.00	SILVA
Prevotella conceptionensis	2	0	0.06	0.00	SILVA/HOMD
Prevotella dentalis	3	0	0.05	0.00	SILVA/HOMD
Prevotella denticola	2	1	0.00	0.06	SILVA/HOMD
Prevotella disiens	1	0	0.03	0.00	SILVA/HOMD
Prevotella histicola	7	4	0.37	0.51	SILVA/HOMD
Prevotella intermedia	2	1	0.19	0.54	SILVA/HOMD
Prevotella loescheii	3	0	0.02	0.00	SILVA/HOMD
Prevotella melaninogenica	16	5	0.42	0.71	SILVA/HOMD
Prevotella nanceiensis	6	3	0.07	0.07	SILVA/HOMD
Prevotella nigrescens	9	3	0.70	0.15	SILVA/HOMD
Prevotella oris	14	2	0.90	0.04	SILVA/HOMD
Prevotella pallens	7	5	0.13	0.17	
Prevotella salivae	9	6	0.29	0.62	
Prevotella shahii	1	1	0.00	0.11	
Prevotella veroralis	0	1	0.00	0.07	SILVA/HOMD
Total	**104**	**39**	**5.45**	**3.81**	SILVA/HOMD
Rothia					
Rothia	5	5	0.02	1.22	
Rothia dentocariosa	12	6	0.06	1.12	
Rothia mucilaginosa	10	5	0.10	0.55	SILVA
Total	**27**	**16**	**0.19**	**2.88**	SILVA
Selenomonas					SILVA/HOMD
Selenomonas	12	4	0.13	0.28	SILVA
Selenomonas artemidis	2	1	0.02	0.00	
Selenomonas infelix	2	0	0.02	0.00	
Selenomonas noxia	4	0	0.17	0.00	SILVA/HOMD
Selenomonas sputigena	7	2	0.03	0.05	
Total	**27**	**7**	**0.38**	**0.33**	
Solobacterium					
Solobacterium moorei	3	2	0.01	0.04	HOMD
Total	**3**	**2**	**0.01**	**0.04**	HOMD
Streptococcus					HOMD
Streptococcus	31	16	5.60	6.00	SILVA
Streptococcus anginosus	3	1	0.02	0.00	HOMD
Streptococcus constellatus	2	1	0.02	0.25	HOMD
Streptococcus intermedius	8	1	2.80	0.01	
Streptococcus oralis	3	0	0.04	0.00	
Streptococcus pneumoniae	15	2	8.76	0.12	SILVA/HOMD
Streptococcus sanguinis	10	2	0.04	0.27	

Total	**72**	**23**	**17.29**	**6.65**	
Tannerella					
Tannerella forsythia	7	1	0.12	0.02	HOMD
Total	**7**	**1**	**0.12**	**0.02**	SILVA
Treponema					SILVA
Treponema	3	0	0.06	0.00	SILVA/HOMD
Treponema denticola	3	1	0.07	0.01	SILVA/HOMD
Treponema lecithinolyticum	1	1	0.00	0.03	SILVA
Treponema medium	2	2	0.03	0.19	
Treponema putidum	3	0	0.07	0.00	
Treponema socranskii	3	2	0.02	0.01	
Treponema vincentii	1	2	0.01	0.07	HOMD
Total	**16**	**8**	**0.27**	**0.31**	HOMD
Veillonella					HOMD
Veillonella	23	10	1.86	2.87	
Veillonella dispar	15	5	0.12	1.09	
Veillonella parvula	14	8	0.30	0.65	HOMD
Veillonella rogosae	10	3	0.13	0.28	SILVA/HOMD
Total	**62**	**26**	**2.41**	**4.89**	

† Taxonomic features are ASVs aggregated at the lowest level of classification available (genus or species) and belonging to select anaerobic and facultative anaerobic bacterial taxa.

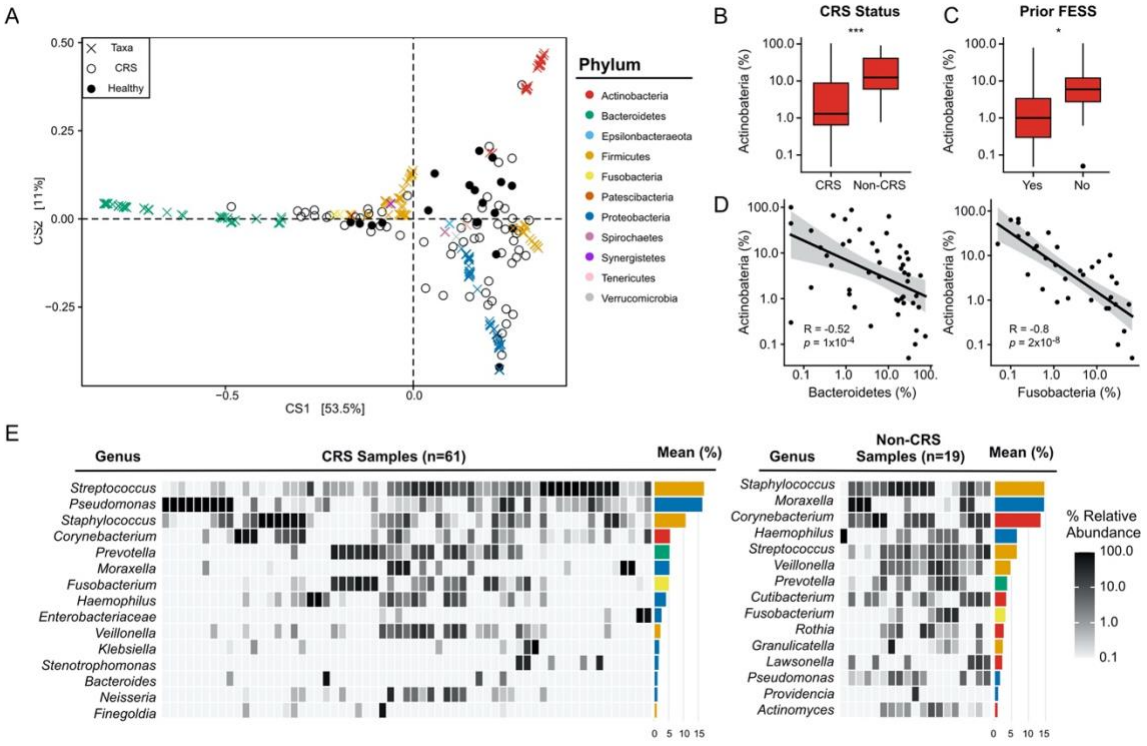

Figure 4.1 Bacterial diversity differs between CRS and non-CRS samples. (A) DPCoA ordination biplot shows dissimilarity in presence and abundance of bacteria in CRS and non-CRS samples. (B) Percent abundance of Actinobacteria is associated with non-CRS status (Wilcoxon, p<.0001). (C) Among CRS samples, percent abundance of Actinobacteria is associated with no prior FESS treatment (Wilcoxon, p<.05). (D) Percent abundance of Actinobacteria is negatively correlated with percent abundance of both Bacteroidetes and Fusobacteria. (E) Heat map representation of the top 15 genera in each sample group (CRS, Non-CRS).

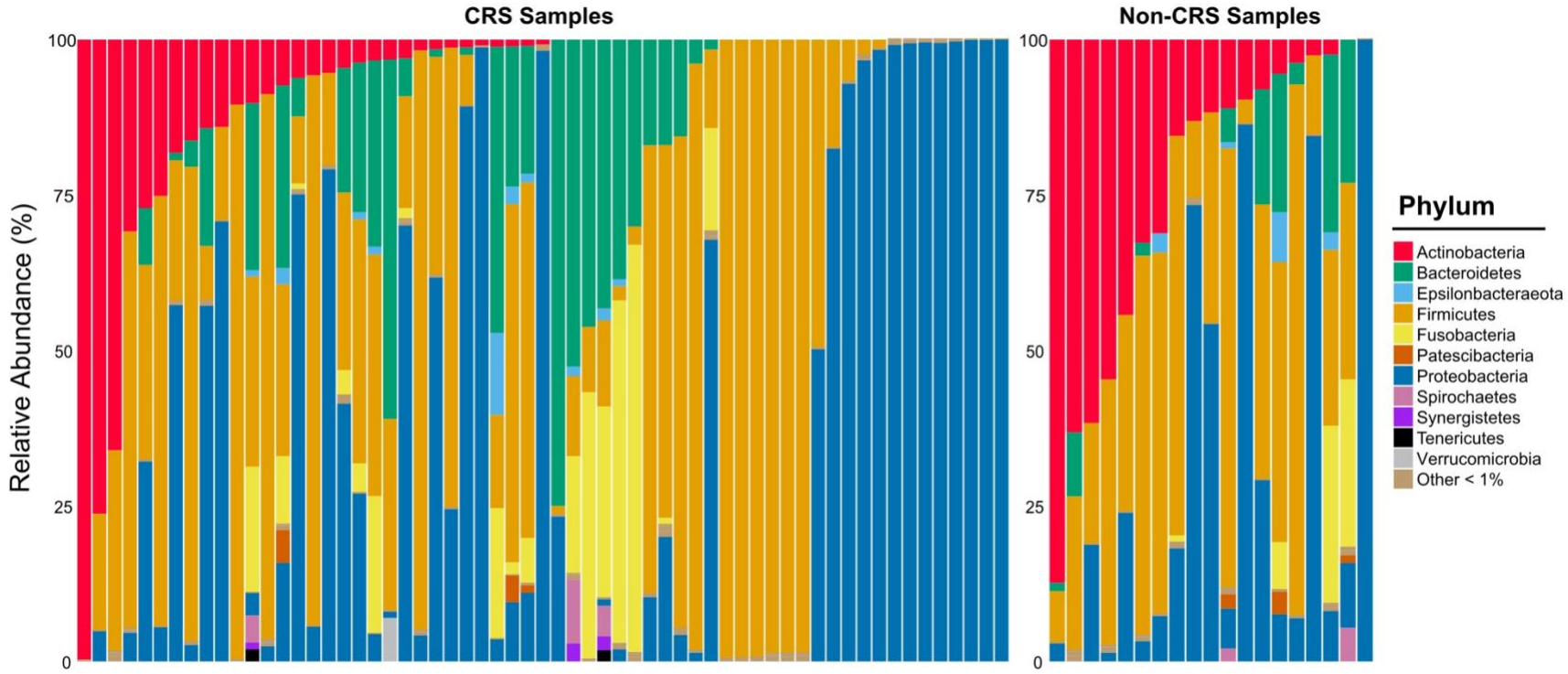

Figure 4.2 Relative abundance of Bacterial phyla in CRS and non-CRS samples. The relative abundance of ASVs grouped by phylum are shown for each sample.

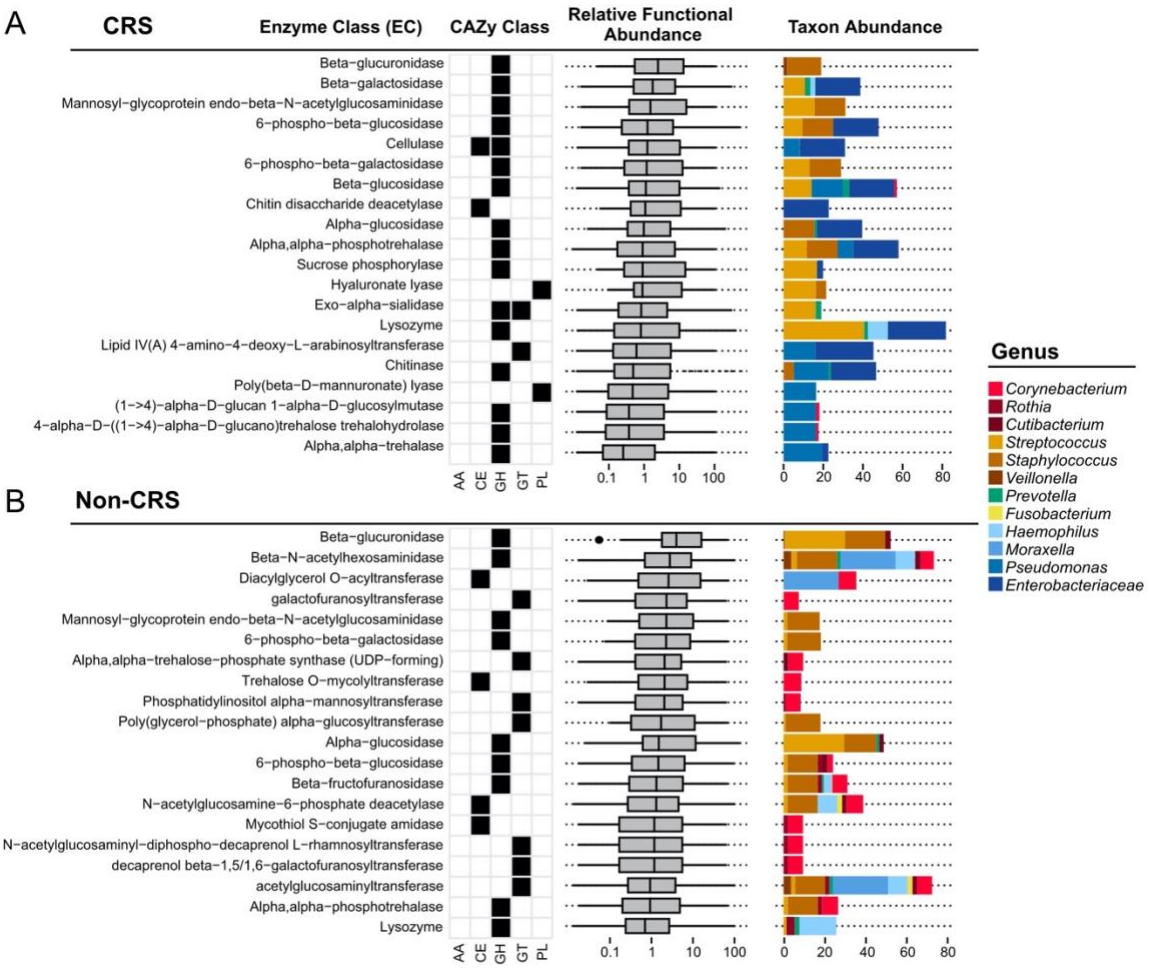

Figure 4.3 Carbohydrate active enzyme classes in PICRUSt2-predicted metagenomes from CRS and non-CRS 16S sequences. Average relative functional abundances of each enzyme class (EC) represented in the CAZy database for the top ten taxa by relative abundance in (A) CRS and (B) non-CRS samples. CAZy classes: Auxiliary Activity (AA), Carbohydrate Esterase (CE), Glycoside Hydrolase (GH), Glycoside Transferase (GT), and Polysaccharide Lyase (PL).

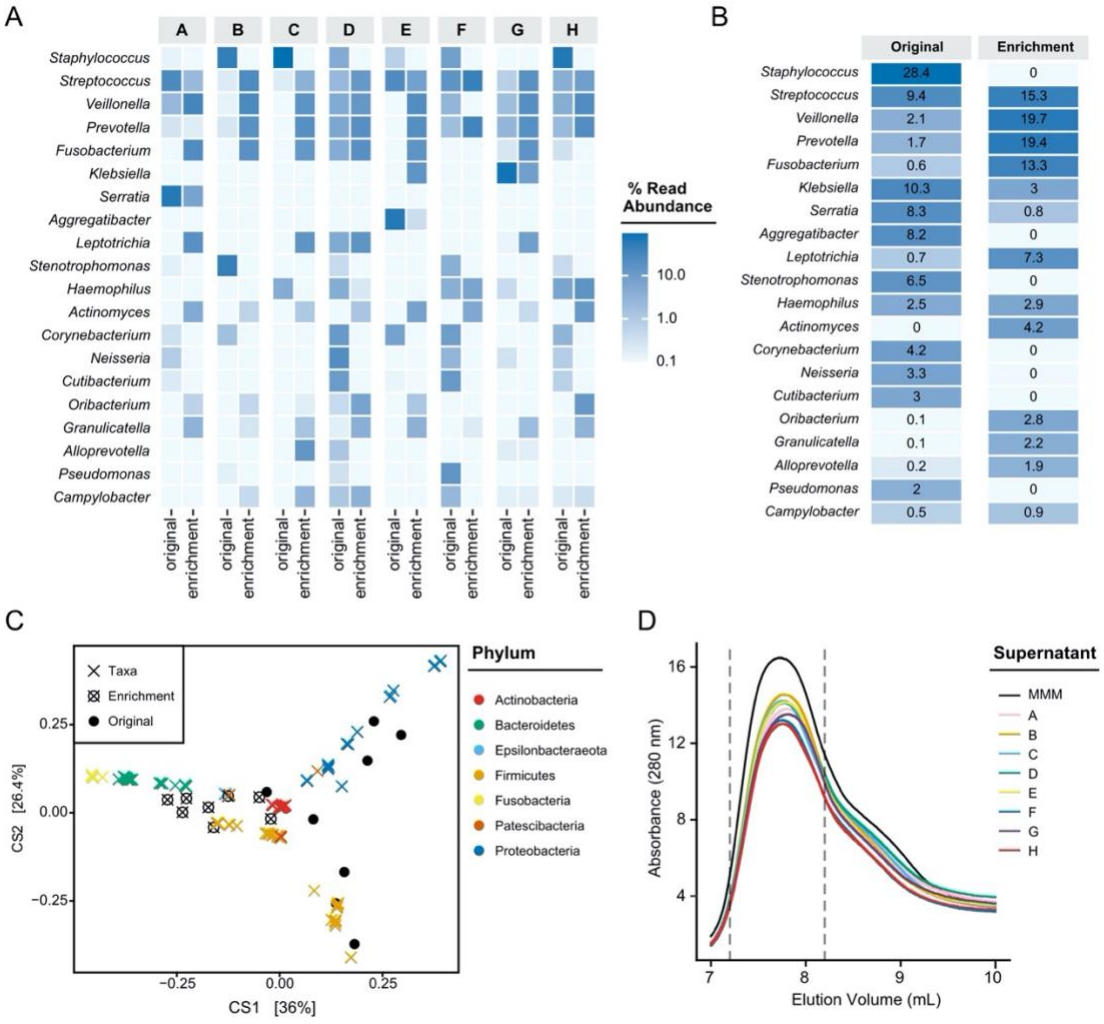

Figure 4.4 Anaerobic mucin enrichment cultures of CRS sinus mucus. (A) Heatmap showing relative abundance of ASVs grouped at the genus level for each original sample and enrichment culture. (B) Mean relative abundances for the top 20 genera in original sample and enrichment culture. (C) DPCoA biplot comparing proportional data from original samples and enrichment cultures with associated phyla. (D) FPLC chromatogram of high molecular weight mucin proteins in MMM and CFS from 48 hour CRS mucin enrichment cultures.

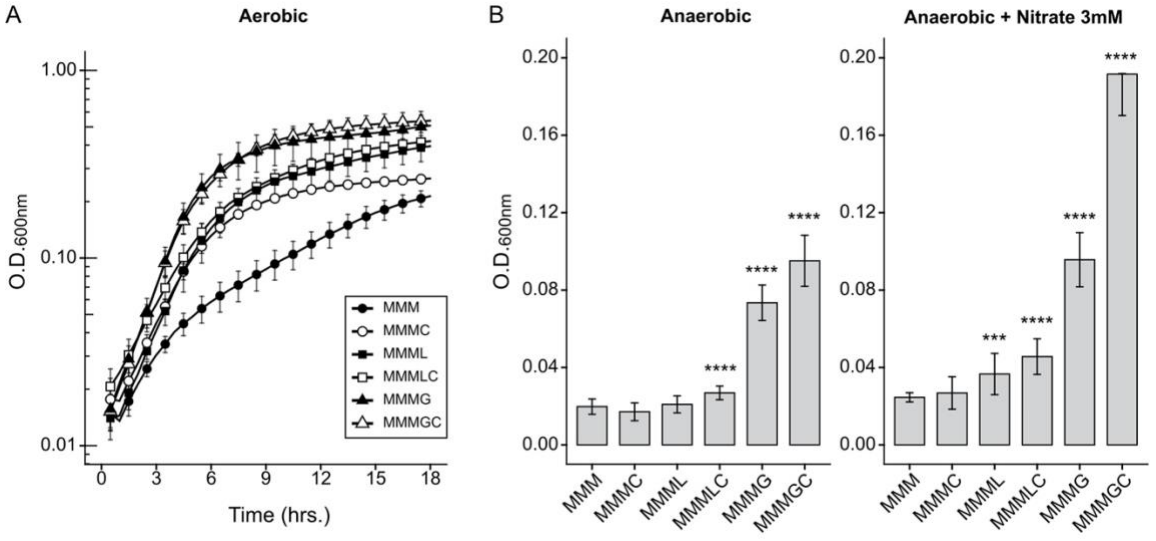

Figure 4.5 *S. aureus* growth on mucin under aerobic and anaerobic conditions. *S. aureus* LAC grown in minimal mucin medium (MMM), supplemented with 0.5% casamino acids (MMMC), 0.5% lactate (MMML), 0.25% glucose (MMMG), or a combination of these (MMMLC, MMMGC). (A) growth curves measured under aerobic conditions, points represent the mean and standard deviation; n=3. (B) Growth measured at O.D.600nm after 24 hours of growth under anaerobic conditions with and without the addition of 3mM nitrate; Data shown are the mean of n = 6 (MMM, MMMC, MMML, MMMLC), n=3 (MMMG, MMGC) biological replicates; Error bars are s.d.; significance determined by t-test with Holm-Bonferroni adjustment.

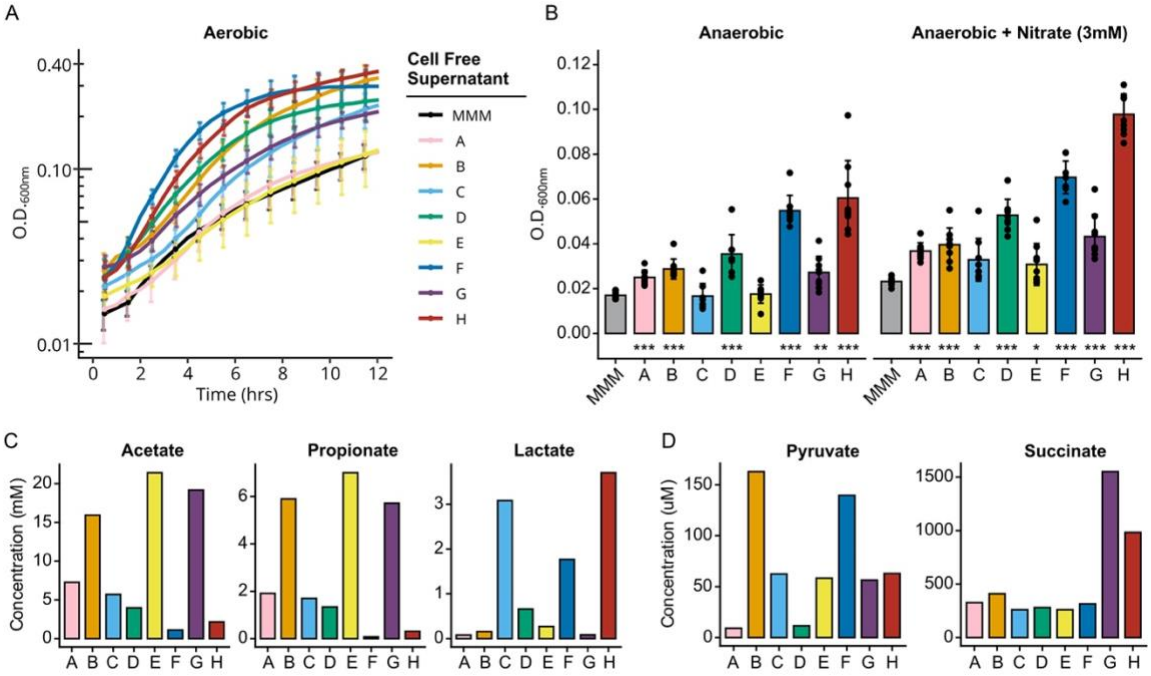

Figure 4.6. *S. aureus* growth on CFS from CRS mucin-degrading communities. (A) *S. aureus* LAC aerobic growth curves on CFS from CRS derived mucin-degrading communities. (B) *S. aureus* anaerobic growth after 24 hours in CFS from CRS derived mucin-degrading communities A-H with and without sodium nitrate (3 mM). Error bars are s.d.; significance determined by t-test with Holm-Bonferroni adjustment. (C) HPLC measurement of fermentation metabolites Acetate, Propionate, and Lactate in CFS A-H. (D) HPLC measurements of metabolites pyruvate and succinate in CFS A-H.

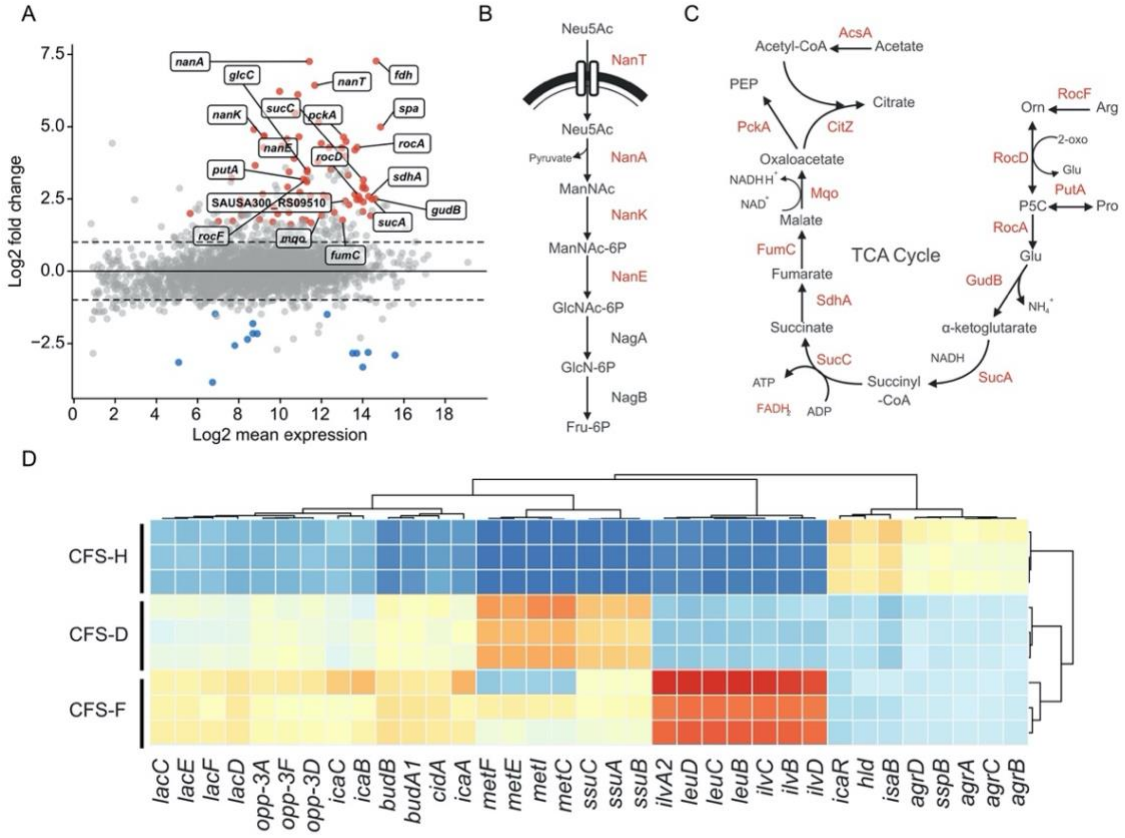
A
Log2 fold change
Log2 mean expression
nanA
glcC
nanT
fdh
sucC
pckA
spa
nanK
nanE
rocD
rocA
putA
sdhA
SAUSA300_RS09510
gudB
rocF
mqo
sucA
fumC
B
Neu5Ac
NanT
Neu5Ac
Pyruvate
NanA
ManNAc
NanK
ManNAc-6P
NanE
GlcNAc-6P
NagA
GlcN-6P
NagB
Fru-6P
C
AcsA
Acetyl-CoA
Acetate
PEP
Citrate
PckA
CitZ
Oxaloacetate
NADH H+
NAD+
Mqo
Malate
FumC
TCA Cycle
Fumarate
SdhA
Succinate
SucC
ATP
FADH2
ADP
Succinyl
-CoA
NADH
SucA
α-ketoglutarate
GudB
NH4+
RocA
Glu
RocD
2-oxo
Glu
PutA
P5C
Pro
RocF
Orn
Arg
D
CFS-H
CFS-D
CFS-F
lacC
lacE
lacF
lacD
opp-3A
opp-3F
opp-3D
icaC
icaB
budB
budA1
cidA
icaA
metF
metE
metI
metC
ssuC
ssuA
ssuB
ilvA2
leuD
leuC
leuB
ilvC
ilvB
ilvD
icaR
hld
isaB
agrD
sspB
agrA
agrC
agrB

Figure 4.7. RNA-seq reveals impact of mucin degradation and fermentation on *S. aureus* transcription. (A) Differential expression of genes (79 up, 14 down) in cell-free supernatant conditions from communities D, F, and H compared to MMMG controls. Wald test was used to assign significance for genes with |FC| > 2, and FDR adjusted p-value < 0.05. (B, C) Transcripts involved in sialic acid degradation and central metabolism were differentially increased in expression in supernatant conditions compared to glucose. (D) Select genes with significant differences between each CFS condition. Significance was determined using the likelihood-ratio test, keeping only genes with a |LFC| >2 and FDR adjusted p-value < $1x10^{-10}$. Data presented are differences from the mean for each gene calculated from regularized log-transformed counts. All data are representative of three biological replicates per condition.

Chapter 5: Conclusion

Summary of research

This thesis addresses the microbial ecology of bacteria associated with chronic rhinosinusitis (CRS). The heterogeneity of this disease complicates our understanding of bacterial contributions to pathogenesis. Genomic, bioinformatic, and classical microbiology techniques were used in this work to describe bacterial diversity in the sinuses, then make novel inferences into the functions carried out by microbiota in the CRS niche.

The first section of this thesis focused on CRS in the cystic fibrosis (CF) population, where it is seen at a prevalence close to 100%. Chronic sinus colonization has been implicated as a source of pulmonary infections that are associated with loss of lung function, and the primary cause of morbidity and mortality in this population. In Chapter 2, we explored the relationship of bacterial diversity in paired sinus and lung samples from CF patients. We demonstrated that there is high interindividual variability between bacterial communities across CF patients, and interestingly, many taxa are shared between the upper and lower airways. We also demonstrate that obligate anaerobes are prevalent in the CF lung.

Since publishing this study in 2017, the topic of anaerobes in CF sputum has been the subject of a larger debate in the field (Caverly and LiPuma, 2018).The question of whether anaerobes identified in sputum are members of polymicrobial communities in the lungs of CF patients, or simply a byproduct of oral contamination during sputum collection remains controversial. A later study comparing bacterial communities of the sinuses and

lungs of CF patients instead used endoscopically obtained bronchial brushings, comparing their work to ours (Pletcher et al., 2019). The study did not confirm our results showing significant differences in diversity between grouped sinus and lung samples. However, the similarity in bacterial membership between the two sites within patients was again demonstrated. Moreover, bronchial brushings of recent lung transplants (LTx) showed increased diversity including the presence of anaerobic taxa. At 4.5 months post-transplant, one bronchial brushing showed little resemblance to a paired sinus sample, however the other sample pair, collected 9 months after LTx already showed presence of the dominant genus in the sinuses (*Pseudomonas*). Moving forward, sequential sampling of the upper and lower airways of CF patients will provide better insight into the relationship between the bacterial communities in each niche. Furthermore, the increased resolution in bacterial genomics afforded from metagenomic sequencing will enable strain-level tracking of bacteria within the airways, and how they are trafficked between sites.

Further investigation of CF-CRS bacterial communities is presented in Chapter 3. Similar to Chapter 2, dominance of either *Pseudomonas* or *Staphylococcus* in each sample is apparent. Research into virulence mechanisms of these canonical pathogens have revealed a great deal about their physiology *in vitro*. Comparatively less attention has been paid to the polymicrobial context of the upper and lower airways in CF. We found an interesting result when comparing communities dominated by *Pseudomonas*, and communities dominated by *Staphylococcus*: *Staphylococcus*-dominated communities were more diverse. The prevalence of *S. aureus* and *P. aeruginosa* in the CF airways has been

associated with patient age, with *S. aureus* colonization occurring early in life, and *P. aeruginosa* becoming more prominent in adulthood (Cystic Fibrosis Foundation Patient Registry, 2019). Mechanisms that govern this transition are not well understood. Patterns in the data suggest there is an age-related relationship with diversity and *Staphylococcus* dominance, however a larger cohort will be needed to test this. Apart from the association with age, these data introduce the idea that interbacterial interactions of a more diverse community may influence *S. aureus* physiology and pathogenic potential, and community dominance in the chronically colonized sinuses. While not addressed in this thesis, the question has been posed by our group before (Flynn et al., 2016) that anaerobic organisms present in *S. aureus*-associated communities may also play a role in conditioning the airway niche for *P. aeruginosa* colonization of the upper airways – a process that is thought to precede pulmonary infection (Folkesson et al., 2012; Hansen et al., 2012).

The final study presented in this thesis investigates how host-derived mucin glycoproteins support bacterial diversity in CRS. 16S rRNA sequencing, metagenomic prediction, and bioinformatic analysis led to the observation that there may be a mucin-degrading bacterial phenotype in CRS. Using classical enrichment experiments to maintain metabolic dependencies, this study became the first to isolate mucin-degrading bacterial communities from CRS patient sinus mucus. Growth assays were paired with RNA-seq to demonstrate that the metabolic activities of mucin-utilizing communities influence *S. aureus* growth and gene transcription. Previous research investigating interbacterial interactions of *S. aureus* focused on pairs of co-abundant organisms such as *P. aeruginosa*,

Haemophilus influenzae, or *Corynebacterium* spp. (Filkins et al., 2015; Margolis et al., 2010; Ramsey et al., 2016; Yan et al., 2013). Rarely is the physiology of *S. aureus* considered in response to the metabolic activities of bacterial consortia. This chapter reveals that the transcription of several genes involved in staphylococcal metabolism and virulence are differentially expressed in response to metabolites liberated from mucin degradation. These results form the basis for future experiments explicitly testing the effect of mucin degradation by anaerobic bacteria on *S. aureus* virulence.

Future Directions

Brooke et al. demonstrated the association of anaerobes with the progression of acute rhinosinusitis to CRS, yet this study has not been replicated either by culture or molecular methods (I Brook et al., 1996). Results presented in this thesis reiterate a need for longitudinal sampling of a large cohort of patients to overcome the heterogeneity seen in CRS and gain a better understanding of bacterial diversity changes over time. Additionally, a limitation of our work is that the methods only consider the bacterial component of microbial communities in the sinuses, although some research has shown that viral and fungal community members are associated with pulmonary exacerbations in CF (Kiedrowski and Bomberger, 2018; Soret et al., 2020). To date, there are no published metagenomic analyses of sinonasal microbiota. Future metagenomic analysis would allow for inclusion of fungal, viral, and archaeal detection providing a more comprehensive picture of CRS associated communities.

Our results demonstrate that mucin-degradation byproducts are able to improve *S. aureus* growth and alter gene transcription, however, it is unclear whether these happen in more physiologically relevant settings, and an impact on *S. aureus* virulence has not been explicitly tested. A first step would be to use a multi-omics approach to describe the taxonomic identities and transcriptional profiles of bacterial communities from CRS patients who are culture-positive for *S. aureus*. Metagenomic profiling of CRS sinus mucus will provide taxonomic identities that can be used to build a reference database. This database can then be used for metatranscriptomic comparison to test the hypothesis that mucinase gene expression is occurring *in vivo*. Furthermore, *S. aureus* genes identified in Chapter 4 as differentially abundant during growth on mucin degradation products can be verified *in vivo*.

Our lab recently developed a respiratory anaerobic co-culture (RACC) system that can be used to study anaerobic bacteria at the epithelial cell surface (unpublished data). Using this model, we can test a variety of host-microbe co-culture scenarios that impact respiratory epithelial cells. First, while our research focused on how mucin-degradation by anaerobic bacteria impacts the physiology of *S. aureus*, it is important to test whether the metabolic byproducts of mucin degradation and fermentation are inflammatory to the host on their own. Mirkovic et al. reported a dose-dependent expression of pro-inflammatory cytokine IL-8 in response to short chain fatty acids in conventional bronchial epithelial cell culture (Mirković et al., 2015). Using the RACC experimental model, anaerobic mucin-degrading communities isolated from CRS sinuses can be applied to the anoxic apical

surface of the cells, and mucin integrity, epithelial cell tight junction integrity, cell viability and inflammatory signaling can be measured using methods established in our lab.

These proposed experiments will produce baseline knowledge for how polarized, differentiated respiratory cells react to mucin degradation. Building upon this knowledge, we can use the RACC experimental system again, but include a *S. aureus* challenge following growth of mucin-degrading consortia. In addition to the variables of epithelial cell layer integrity listed above, RNA-seq can be used to measure both host cell inflammation and *S. aureus* virulence gene transcription. Altogether, these experiments will contribute an *in vivo* perspective to complement the research presented in this thesis, and provide mechanistic detail to the pathogenic contribution of anaerobic bacteria to CRS.

Concluding Remarks

Work presented here combines molecular based surveys, bioinformatics, and classical microbiology techniques to better understand the biology of understudied members of CRS-associated microbiota. This research stresses the need for future research to incorporate systems biology approaches to understanding bacterial pathogenesis in chronic infections.

Importantly, studying how CRS-associated anaerobes impact the pathogenic potential of *S. aureus* has implications for other types of chronic infections where it is also the dominant organism. For example, an analysis of 2,963 chronic non-healing wound patients established that, compared to *P. aeruginosa*, when *S. aureus* was the dominant organism it was accompanied by increased diversity of bacteria in the polymicrobial

biofilm, including many of the same anaerobe genera seen in CRS (Wolcott et al., 2016). Corollaries like this suggest that there are likely important interactions between *S. aureus* and anerobic bacteria that promote chronic infection in varied sites of infection. Further investigation of the intriguing relationships between *S. aureus* and comparatively less well studied anaerobic bacteria are needed.

Where our understanding of the pathogenic potential of organisms like *S. aureus* and *P. aeruginosa* are increasingly well understood, the physiology of many anaerobic bacteria is comparatively less well studied. The requisite laboratory cultivation that enabled such great strides in understanding the biology of these aerobic pathogens inherently disrupts microbial metabolic relationships that may be essential to understanding the biology of polymicrobial communities with anaerobe constituents. However challenging, further study of these organisms is warranted by their involvement in chronic infections in CRS and elsewhere. Just as the classical "Staph Streak" procedure enables *Haemophilus* isolation, microbiological methods such as enrichment and co-culture may be essential to reveal novel and medically important bacterial interactions and reveal unrealized biological diversity. To this end, the inclusion of complex glycoproteins such as mucins, which support diverse and discrete microbial metabolic niches should be considered in media preparation when studying members of the airway microbiome in isolation or in communities. Additionally, recently developed high resolution imaging techniques incorporating multiplexed fluorescent staining (e.g. CLASI-FISH) can provide great

insight into spatial organization of polymicrobial communities (Valm et al., 2011). These imaging methods have not yet been applied to study microbiota in CRS.

Finally, it is tempting to extend what has been learned here to propose antibiotic therapies for CRS, and indeed other chronic infections, that target anaerobes. However, it is becoming increasingly clear that a loss in microbial diversity and pathogen dominance is associated with increased disease burden in CRS. Moreover, antibiotic resistance is already seen widely in anaerobic bacteria(Hecht, 2004). With the known efficacy of FESS, sinus drainage, and debridement, and the microbiology associated with its failure of these treatments, other regimens should be explored that combine destabilization the low-oxygen infection site, while re-establishing microbial diversity associated with health. Use of probiotic therapies to treat CRS and other airway infections such as asthma and COPD is an active area of investigation.

CRS is a complex disease. If we are to understand the nature of the microbial contribution to CRS pathogenesis, we must build upon decades of reductionist microbiological research to make meaningful mechanistic hypotheses that don't exclude bacterial interactions with each other and the surrounding infection microenvironment. With this approach, new treatment methods can be established, and new biology uncovered.

Bibliography

Abreu, N., Nagalingam, N., Song, Y., Roediger, F., Pletcher, S., Goldberg, A., and Lynch, S. (2012). Sinus Microbiome Diversity Depletion and Corynebacterium tuberculostearicum Enrichment Mediates Rhinosinusitis. *Science Translational Medicine*, *4*(151), 151ra124-151ra124. https://doi.org/10.1126/scitranslmed.3003783

Ahlgren, H. G., Benedetti, A., Landry, J. S., Bernier, J., Matouk, E., Radzioch, D., Lands, L. C., Rousseau, S., and Nguyen, D. (2015). Clinical outcomes associated with Staphylococcus aureus and Pseudomonas aeruginosa airway infections in adult cystic fibrosis patients. *BMC Pulmonary Medicine*, *15*(1), 67. https://doi.org/10.1186/s12890-015-0062-7

Andersen, K. S. S., Kirkegaard, R. H., Karst, S. M., and Albertsen, M. (2018). ampvis2: an R package to analyse and visualise 16S rRNA amplicon data. *BioRxiv*, 299537. https://doi.org/10.1101/299537

Archer, N. K., Mazaitis, M. J., Costerton, J. W., Leid, J. G., Powers, M. E., and Shirtliff, M. E. (2011). Staphylococcus aureus biofilms: properties, regulation, and roles in human disease. *Virulence*, *2*(5), 445–459. https://doi.org/10.4161/viru.2.5.17724

Argüeso, P., Herreras, J. M., Calonge, M., Citores, L., Pastor, J. C., and Girbés, T. (1998). Analysis of Human Ocular Mucus: Effects of Neuraminidase and Chitinase Enzymes. *Cornea*, *17*(2), 200–207. https://doi.org/10.1097/00003226-199803000-00015

Babinski, D., and Trawinska-Bartnicka, M. (2008). Rhinosinusitis in cystic fibrosis: Not a simple story. *International Journal of Pediatric Otorhinolaryngology*, *72*(5), 619–624. https://doi.org/10.1016/j.ijporl.2008.01.010

Balasubramanian, D., Harper, L., Shopsin, B., and Torres, V. J. (2017). Staphylococcus aureus pathogenesis in diverse host environments. *Pathog. Dis.*, *75*(1). https://doi.org/10.1093/femspd/ftx005

Bansil, R., and Turner, B. S. (2006). Mucin structure, aggregation, physiological functions and biomedical applications. *Current Opinion in Colloid & Interface Science*, *11*(2–3), 164–170. https://doi.org/10.1016/j.cocis.2005.11.001

Bassiouni, A., Cleland, E., Psaltis, A., Vreugde, S., and Wormald, P.-J. (2015). Sinonasal Microbiome Sampling: A Comparison of Techniques. *PLOS ONE*, *10*(4), e0123216. https://doi.org/10.1371/journal.pone.0123216

Bassis, C. M., Tang, A. L., Young, V. B., and Pynnonen, M. A. (2014). The nasal cavity microbiota of healthy adults. *Microbiome*, *2*, 27. https://doi.org/10.1186/2049-2618-2-27

Becker, K. (2010). The Role of Sphingolipids and Ceramide in Pulmonary Inflammation in Cystic Fibrosis. *The Open Respiratory Medicine Journal*, *4*(1), 39–47. https://doi.org/10.2174/1874306401004010039

Beighton, D., and Whiley, R. A. (1990). Sialidase activity of the "Streptococcus milleri group" and other viridans group streptococci. *Journal of Clinical Microbiology*, *28*(6), 1431–1433.

Benninger, M. S., Ferguson, B. J., Hadley, J. A., Hamilos, D. L., Jacobs, M., Kennedy, D. W., Lanza, D. C., Marple, B. F., Osguthorpe, J. D., Stankiewicz, J. A., Anon, J., Denneny, J., Emanuel, I., and Levine, H. (2003). Adult chronic rhinosinusitis: definitions, diagnosis, epidemiology, and pathophysiology. *Otolaryngol. Head Neck Surg.*, *129*(3 Suppl), S1-32. https://doi.org/10.1016/s0194-5998(03)01397-4

Bergstrom, K. S. B., and Xia, L. (2013). Mucin-type O-glycans and their roles in intestinal homeostasis. *Glycobiology*, *23*(9), 1026–1037. https://doi.org/10.1093/glycob/cwt045

Bhattacharyya, N. (2011). Incremental Health Care Utilization and Expenditures for Chronic Rhinosinusitis in the United States. *Annals of Otology, Rhinology & Laryngology*, *120*(7), 423–427. https://doi.org/10.1177/000348941112000701

Bhattacharyya, N., and Gilani, S. (2018). Prevalence of Potential Adult Chronic Rhinosinusitis Symptoms in the United States. *Otolaryngol. Head Neck Surg.*, *159*(3), 522–525. https://doi.org/10.1177/0194599818774006

Bhattacharyya, N., and Kepnes, L. J. (1999). *The Microbiology of Recurrent Rhinosinusitis After Endoscopic Sinus Surgery*. *125*, 1117–1120. https://doi.org/doi:10.1001/archotol.125.10.1117

Biswas, K., Hoggard, M., Jain, R., Taylor, M. W., and Douglas, R. G. (2015). The nasal microbiota in health and disease: variation within and between subjects. *Frontiers in Microbiology*, *9*, 134. https://doi.org/10.3389/fmicb.2015.00134

Blainey, P. C., Milla, C. E., Cornfield, D. N., and Quake, S. R. (2012). Quantitative Analysis of the Human Airway Microbial Ecology Reveals a Pervasive Signature for Cystic Fibrosis. *Science Translational Medicine*, *4*(153), 153ra130-153ra130. https://doi.org/10.1126/scitranslmed.3004458

Blanchette, K. A., Shenoy, A. T., Milner, J., Gilley, R. P., McClure, E., Hinojosa, C. A., Kumar, N., Daugherty, S. C., Tallon, L. J., Ott, S., King, S. J., Ferreira, D. M., Gordon, S. B., Tettelin, H., and Orihuela, C. J. (2016). Neuraminidase A-Exposed Galactose Promotes Streptococcus pneumoniae Biofilm Formation during Colonization. *Infection and Immunity*, *84*(10), 2922–2932. https://doi.org/10.1128/iai.00277-16

Bode, L. G., Kluytmans, J. A., Wertheim, H. F., Bogaers, D., Vandenbroucke-Grauls, C. M., Roosendaal, R., Troelstra, A., Box, A. T., Voss, A., Tweel, I. van der, Belkum, A. van, Verbrugh, H. A., and Vos, M. C. (2010). Preventing surgical-site infections in nasal carriers of Staphylococcus aureus. *N. Engl. J. Med.*, *362*(1), 9–17. https://doi.org/10.1056/nejmoa0808939

Bonestroo, H. J. C., Groot, K. M. de W., Ent, C. K. van der, and Arets, H. G. M. (2010). Upper and lower airway cultures in children with cystic fibrosis: Do not neglect the upper airways. *Journal of Cystic Fibrosis*, *9*(2), 130–134. https://doi.org/10.1016/j.jcf.2010.01.001

Borisova, M., Gaupp, R., Duckworth, A., Schneider, A., Dalügge, D., Mühleck, M., Deubel, D., Unsleber, S., Yu, W., Muth, G., Bischoff, M., Götz, F., and Mayer, C. (2016). Peptidoglycan Recycling in Gram-Positive Bacteria Is Crucial for Survival in Stationary Phase. *MBio*, *7*(5), e00923-16. https://doi.org/10.1128/mbio.00923-16

Boutin, S., Graeber, S. Y., Weitnauer, M., Panitz, J., Stahl, M., Clausznitzer, D., Kaderali, L., Einarsson, G., Tunney, M. M., Elborn, J. S., Mall, M. A., and Dalpke, A. H. (2015). Comparison of microbiomes from different niches of upper and lower airways in children and adolescents with cystic fibrosis. *PloS One*, *10*(1), e0116029. https://doi.org/10.1371/journal.pone.0116029

Bradshaw, D. J., Homer, K. A., Marsh, P. D., and Beighton, D. (1994). Metabolic cooperation in oral microbial communities during growth on mucin. *Microbiology*, *140 (Pt 12)*, 3407–3412. https://doi.org/10.1099/13500872-140-12-3407

Brook, I, Frazier, H. E., and Foote, P. A. (1996). Microbiology of the transition from acute to chronic maxillary sinusitis. *Journal of Medical Microbiology*, *45*(5), 372–375. https://doi.org/10.1099/00222615-45-5-372

Brook, I, Thompson, D. H., and Frazier, E. H. (1994). Microbiology and Management of Chronic Maxillary Sinusitis. *Archives of Otolaryngology - Head and Neck Surgery*, *120*(12), 1317–1320. https://doi.org/10.1001/archotol.1994.01880360015003

Brook, Itzhak. (2011). Microbiology of sinusitis. *Proceedings of the American Thoracic Society*, *8*(1), 90–100. https://doi.org/10.1513/pats.201006-038RN

Brook, Itzhak, and Frazier, E. H. (2001). Correlation between Microbiology and Previous Sinus Surgery in Patients with Chronic Maxillary Sinusitis. *Annals of Otology, Rhinology & Laryngology*, *110*(2), 148–151. https://doi.org/10.1177/000348940111000210

Brown, C. A., Paisner, H. M., Biel, M. A., Levinson, R. M., Sigel, M. E., Garvis, G. E., and Tedford, T. M. (1998). Evaluation of the Microbiology of Chronic Maxillary Sinusitis. *Annals of Otology, Rhinology & Laryngology*, *107*(11), 942–945. https://doi.org/10.1177/000348949810701107

Buffie, C. G., and Pamer, E. G. (2013). Microbiota-mediated colonization resistance against intestinal pathogens. *Nature Reviews Immunology*, *13*(11), 790–801. https://doi.org/10.1038/nri3535

Busaba, N. Y., Siegel, N. S., and Salman, S. D. (2004). Microbiology of chronic ethmoid sinusitis: is this a bacterial disease? *Am. J. Otolaryngol.*, *25*(6), 379–384. https://doi.org/10.1016/j.amjoto.2004.04.001

Byers, H. L., Tarelli, E., Homer, K. A., and Beighton, D. (2000). Isolation and characterisation of sialidase from a strain of Streptococcus oralis. *Journal of Medical Microbiology*, *49*(3), 235–244. https://doi.org/10.1099/0022-1317-49-3-235

Caldas, R. R., and Boisramé, S. (2015). Upper aero-digestive contamination by Pseudomonas aeruginosa and implications in Cystic Fibrosis. *J. Cyst. Fibros.*, *14*(1), 6–15. https://doi.org/10.1016/j.jcf.2014.04.008

Callahan, B. J., McMurdie, P. J., Rosen, M. J., Han, A. W., Johnson, A. J. A., and Holmes, S. P. (2016). DADA2: High-resolution sample inference from Illumina amplicon data. *Nat. Methods*, *13*(7), 581–583. https://doi.org/10.1038/nmeth.3869

Carroll, R. K., Weiss, A., and Shaw, L. N. (2014). *RNA-sequencing of Staphylococcus aureus messenger RNA* (pp. 131–141). Springer. ["https://link.springer.com/protocol/10.1007/7651_2014_192", "https://www.researchgate.net/profile/Ronan_Carroll/publication/272083065_RNA-

Sequencing_of_Staphylococcus_aureus_Messenger_RNA/links/59b0153ba6fdcc3f8889a398/RNA-Sequencing-of-Staphylococcus-aureus-Messenger-RNA.pdf"]

Carvalho, S. M., Jong, A. de, Kloosterman, T. G., Kuipers, O. P., and Saraiva, L. M. (2017). The Staphylococcus aureus α-Acetolactate Synthase ALS Confers Resistance to Nitrosative Stress. *Front. Microbiol.*, *8*, 1273. https://doi.org/10.3389/fmicb.2017.01273

Caverly, L. J., and LiPuma, J. J. (2018). Good cop, bad cop: anaerobes in cystic fibrosis airways. *Eur. Respir. J.*, *52*(1). https://doi.org/10.1183/13993003.01146-2018

Chaaban, M. R., Kejner, A., Rowe, S. M., and Woodworth, B. A. (2013). Cystic fibrosis chronic rhinosinusitis: a comprehensive review. *Am. J. Rhinol. Allergy*, *27*(5), 387–395. https://doi.org/10.2500/ajra.2013.27.3919

Charlson, E. S., Bittinger, K., Haas, A. R., Fitzgerald, A. S., Frank, I., Yadav, A., Bushman, F. D., and Collman, R. G. (2011). Topographical Continuity of Bacterial Populations in the Healthy Human Respiratory Tract. *American Journal of Respiratory and Critical Care Medicine*, *184*(8), 957–963. https://doi.org/10.1164/rccm.201104-0655oc

Chester, A. C., Antisdel, J. L., and Sindwani, R. (2008). Symptom-specific outcomes of endoscopic sinus surgery: A systematic review. *Otolaryngology–Head and Neck Surgery*, *140*(5), 633–639. https://doi.org/10.1016/j.otohns.2008.12.048

Choi, K. J., Cheng, T. Z., Honeybrook, A. L., Gray, A. L., Snyder, L. D., Palmer, S. M., Hachem, R. A., and Jang, D. W. (2018). Correlation between sinus and lung cultures in lung transplant patients with cystic fibrosis. *International Forum of Allergy & Rhinology*, *8*(3), 389–393. https://doi.org/10.1002/alr.22067

Choi, Y., Banerjee, A., McNish, S., Couch, K. S., Torralba, M. G., Lucas, S., Tovchigrechko, A., Madupu, R., Yooseph, S., Nelson, K. E., Shanmugam, V. K., and Chan, A. P. (2018). Co-occurrence of Anaerobes in Human Chronic Wounds. *Microbial Ecology*, 1–13. https://doi.org/10.1007/s00248-018-1231-z

Ciofu, O., Johansen, H. K., Aanaes, K., Wassermann, T., Alhede, M., Buchwald, C. von, and Høiby, N. (2013). P. aeruginosa in the paranasal sinuses and transplanted lungs have similar adaptive mutations as isolates from chronically infected CF lungs. *Journal of Cystic Fibrosis*, *12*(6), 729–736. https://doi.org/10.1016/j.jcf.2013.02.004

Coburn, B., Wang, P. W., Caballero, J., Clark, S. T., Brahma, V., Donaldson, S., Zhang, Y., Surendra, A., Gong, Y., Tullis, E. D., Yau, Y. C., Waters, V. J., Hwang, D. M., and

Guttman, D. S. (2015). Lung microbiota across age and disease stage in cystic fibrosis. *Scientific Reports*, *5*, 10241. https://doi.org/10.1038/srep10241

Cook, H. E., and Haber, J. (1987). Bacteriology of the maxillary sinus. *Journal of Oral and Maxillofacial Surgery*, *45*(12), 1011–1014. https://doi.org/10.1016/0278-2391(87)90155-8

Cope, E. K., Goldberg, A. N., Pletcher, S. D., and Lynch, S. V. (2017). Compositionally and functionally distinct sinus microbiota in chronic rhinosinusitis patients have immunological and clinically divergent consequences. *Microbiome*, *5*(1), 53. https://doi.org/10.1186/s40168-017-0266-6

Cox, M. J., Allgaier, M., Taylor, B., Baek, M. S., Huang, Y. J., Daly, R. A., Karaoz, U., Andersen, G. L., Brown, R., Fujimura, K. E., Wu, B., Tran, D., Koff, J., Kleinhenz, M. E., Nielson, D., Brodie, E. L., and Lynch, S. V. (2010). Airway Microbiota and Pathogen Abundance in Age-Stratified Cystic Fibrosis Patients. *PLoS ONE*, *5*(6), e11044. https://doi.org/10.1371/journal.pone.0011044

Cramton, S. E., Gerke, C., Schnell, N. F., Nichols, W. W., and Götz, F. (1999). The Intercellular Adhesion (ica) Locus Is Present in Staphylococcus aureus and Is Required for Biofilm Formation. *Infection and Immunity*, *67*(10), 5427–5433. https://doi.org/10.1128/iai.67.10.5427-5433.1999

Derrien, M., and Passel, M. van. (2010). *Mucin-bacterial interactions in the human oral cavity and digestive tract*. https://doi.org/10.4161/gmic.1.4.12778

Diep, B. A., Gill, S. R., Chang, R. F., Phan, T. H., Chen, J. H., Davidson, M. G., Lin, F., Lin, J., Carleton, H. A., Mongodin, E. F., Sensabaugh, G. F., and Perdreau-Remington, F. (2006). Complete genome sequence of USA300, an epidemic clone of community-acquired meticillin-resistant Staphylococcus aureus. *Lancet*, *367*(9512), 731–739. https://doi.org/10.1016/s0140-6736(06)68231-7

Ding, G., and Zheng, C. (2007). The expression of MUC5AC and MUC5B mucin genes in the mucosa of chronic rhinosinusitis and nasal polyposis. *Am. J. Rhinol.*, *21*(3), 359–366. https://doi.org/10.2500/ajr.2007.21.3037

Douglas, G. M., Maffei, V. J., Zaneveld, J. R., Yurgel, S. N., Brown, J. R., Taylor, C. M., Huttenhower, C., and Langille, M. G. I. (2020). PICRUSt2 for prediction of metagenome functions. *Nature Biotechnology*, *38*(6), 685–688. https://doi.org/10.1038/s41587-020-0548-6

Erkan, M., Asian, T., Ozcan, M., and Ko??, N. (1994). Bacteriology of Antram in Adults With Chronic Maxillary Sinusitis. *The Laryngoscope*, *104*(3), 321???324. https://doi.org/10.1288/00005537-199403000-00013

Erkan, M., Özcan, M., Arslan, S., Soysal, V., Bozdemir, K., and Haghighi, N. (2009). Bacteriology of Antrum in Children with Chronic Maxillary Sinusitis. *Scandinavian Journal of Infectious Diseases*, *28*(3), 283–285. https://doi.org/10.3109/00365549609027174

Escapa, I. F., Chen, T., Huang, Y., Gajare, P., Dewhirst, F. E., and Lemon, K. P. (2018). New Insights into Human Nostril Microbiome from the Expanded Human Oral Microbiome Database (eHOMD): a Resource for the Microbiome of the Human Aerodigestive Tract. *MSystems*, *3*(6). https://doi.org/10.1128/msystems.00187-18

Essack, S., and Pignatari, A. C. (2013). A framework for the non-antibiotic management of upper respiratory tract infections: towards a global change in antibiotic resistance. *International Journal of Clinical Practice*, *67*(s180), 4–9. https://doi.org/10.1111/ijcp.12335

Feazel, L. M., Robertson, C. E., Ramakrishnan, V. R., and Frank, D. N. (2012). Microbiome complexity and Staphylococcus aureus in chronic rhinosinusitis. *The Laryngoscope*, *122*(2), 467–472. https://doi.org/10.1002/lary.22398

Filkins, L. M., Graber, J. A., Olson, D. G., Dolben, E. L., Lynd, L. R., Bhuju, S., and O'Toole, G. A. (2015). Coculture of Staphylococcus aureus with Pseudomonas aeruginosa Drives S. aureus towards Fermentative Metabolism and Reduced Viability in a Cystic Fibrosis Model. *J. Bacteriol.*, *197*(14), 2252–2264. https://doi.org/10.1128/jb.00059-15

Finegold, S. M., Flynn, M. J., Rose, F. V., Jousimies-Somer, H., Jakielaszek, C., McTeague, M., Wexler, H. M., Berkowitz, E., and Wynne, B. (2002). Bacteriologic Findings Associated with Chronic Bacterial Maxillary Sinusitis in Adults. *Clinical Infectious Diseases*, *35*(4), 428–433. https://doi.org/10.1086/341899

Fischer, N., Hentschel, J., Markert, U. R., Keller, P. M., Pletz, M. W., and Mainz, J. G. (2014). Non-invasive assessment of upper and lower airway infection and inflammation in CF patients: UAW and LAW Airway Infection and Inflammation. *Pediatric Pulmonology*, *49*(11), 1065–1075. https://doi.org/10.1002/ppul.22982

Flynn, J. M., Cameron, L. C., Wiggen, T. D., Dunitz, J. M., Harcombe, W. R., and Hunter, R. C. (2020). Disruption of Cross-Feeding Inhibits Pathogen Growth in the Sputa of

Patients with Cystic Fibrosis. *MSphere*, *5*(2). https://doi.org/10.1128/msphere.00343-20

Flynn, J. M., Niccum, D., Dunitz, J. M., and Hunter, R. C. (2016). Evidence and Role for Bacterial Mucin Degradation in Cystic Fibrosis Airway Disease. *PLoS Pathog.*, *12*(8), e1005846. https://doi.org/10.1371/journal.ppat.1005846

Fokkens, W. J., Lund, V. J., Hopkins, C., Hellings, P. W., Kern, R., Reitsma, S., Toppila-Salmi, S., Bernal-Sprekelsen, M., Mullol, J., Alobid, I., Anselmo-Lima, W. T., Bachert, C., Baroody, F., Buchwald, C. von, Cervin, A., Cohen, N., Constantinidis, J., Gabory, L. D., Desrosiers, M., … Zwetsloot, C. P. (2020). European Position Paper on Rhinosinusitis and Nasal Polyps 2020. *Rhinology*, *58*(Suppl S29), 1–464. https://doi.org/10.4193/rhin20.600

Folkesson, A., Jelsbak, L., Yang, L., Johansen, H. K., Ciofu, O., Høiby, N., and Molin, S. (2012). Adaptation of Pseudomonas aeruginosa to the cystic fibrosis airway: an evolutionary perspective. *Nature Reviews. Microbiology*, *10*(12), 841–851. https://doi.org/10.1038/nrmicro2907

Foreman, A., Jervis-Bardy, J., and Wormald, P.-J. J. (2011). Do biofilms contribute to the initiation and recalcitrance of chronic rhinosinusitis? *The Laryngoscope*, *121*(5), 1085–1091. https://doi.org/10.1002/lary.21438

Godoy, J. M., Godoy, A. N., Ribalta, G., and Largo, I. (2011). Bacterial Pattern in Chronic Sinusitis and Cystic Fibrosis. *Otolaryngology–Head and Neck Surgery*, *145*(4), 673–676. https://doi.org/10.1177/0194599811407279

Gohl, D. M., Vangay, P., Garbe, J., MacLean, A., Hauge, A., Becker, A., Gould, T. J., Clayton, J. B., Johnson, T. J., Hunter, R., Knights, D., and Beckman, K. B. (2016). Systematic improvement of amplicon marker gene methods for increased accuracy in microbiome studies. *Nat. Biotechnol.*, *34*(9), 942–949. https://doi.org/10.1038/nbt.3601

Gorwitz, R. J., Kruszon-Moran, D., McAllister, S. K., McQuillan, G., McDougal, L. K., Fosheim, G. E., Jensen, B. J., Killgore, G., Tenover, F. C., and Kuehnert, M. J. (2008). Changes in the Prevalence of Nasal Colonization with Staphylococcus aureus in the United States, 2001–2004. *J. Infect. Dis.*, *197*(9), 1226–1234. https://doi.org/10.1086/533494

Halsey, C. R., Lei, S., Wax, J. K., Lehman, M. K., Nuxoll, A. S., Steinke, L., Sadykov, M., Powers, R., and Fey, P. D. (2017). Amino Acid Catabolism in Staphylococcus aureus and the Function of Carbon Catabolite Repression. *MBio*, *8*(1). https://doi.org/10.1128/mbio.01434-16

Hamad, W. A., Matar, N., Elias, M., Nasr, M., Sarkis-Karam, D., Hokayem, N., and Haddad, A. (2009). Bacterial Flora in Normal Adult Maxillary Sinuses. *American Journal of Rhinology & Allergy*, *23*(3), 261–263. https://doi.org/10.2500/ajra.2009.23.3317

Hamilos, D. L. (2016). Chronic Rhinosinusitis in Patients with Cystic Fibrosis. *The Journal of Allergy and Clinical Immunology: In Practice*, *4*(4), 605–612. https://doi.org/10.1016/j.jaip.2016.04.013

Hansen, S. K., Rau, M. H., Johansen, H. K., Ciofu, O., Jelsbak, L., Yang, L., Folkesson, A., Jarmer, H. Ø., Aanæs, K., Buchwald, C. von, Høiby, N., and Molin, S. (2012). Evolution and diversification of Pseudomonas aeruginosa in the paranasal sinuses of cystic fibrosis children have implications for chronic lung infection. *The ISME Journal*, *6*(1), 31–45. https://doi.org/10.1038/ismej.2011.83

Hardy, B. L., Dickey, S. W., Plaut, R. D., Riggins, D. P., Stibitz, S., Otto, M., and Merrell, S. D. (2019). Corynebacterium pseudodiphtheriticum Exploits Staphylococcus aureus Virulence Components in a Novel Polymicrobial Defense Strategy. *MBio*, *10*(1). https://doi.org/10.1128/mbio.02491-18

Hauser, L. J., Feazel, L. M., Ir, D., Fang, R., Wagner, B. D., Robertson, C. E., Frank, D. N., and Ramakrishnan, V. R. (2015). Sinus culture poorly predicts resident microbiota. *International Forum of Allergy & Rhinology*, *5*(1), 3–9. https://doi.org/10.1002/alr.21428

Hecht, D. W. (2004). Prevalence of Antibiotic Resistance in Anaerobic Bacteria: Worrisome Developments. *Clinical Infectious Diseases*, *39*(1), 92–97. https://doi.org/10.1086/421558

Hibbing, M. E., Fuqua, C., Parsek, M. R., and Peterson, S. B. (2010). Bacterial competition: surviving and thriving in the microbial jungle. *Nature Reviews. Microbiology*, *8*(1), 15–25. https://doi.org/10.1038/nrmicro2259

Hill, M. (1973). Diversity and Evenness: A Unifying Notation and Its Consequences. *Ecology*, *54*(2), 427–432. https://doi.org/10.2307/1934352

Hoeven, J. S. V. der, and Camp, P. J. (1991). Synergistic degradation of mucin by Streptococcus oralis and Streptococcus sanguis in mixed chemostat cultures. *Journal of Dental Research*, *70*(7), 1041–1044.

Hogan, D. A., Willger, S. D., Dolben, E. L., Hampton, T. H., Stanton, B. A., Morrison, H. G., Sogin, M. L., Czum, J., and Ashare, A. (2016). Analysis of Lung Microbiota in

Bronchoalveolar Lavage, Protected Brush and Sputum Samples from Subjects with Mild-To-Moderate Cystic Fibrosis Lung Disease. *PLOS ONE*, *11*(3), e0149998. https://doi.org/10.1371/journal.pone.0149998

Hoggard, M., Biswas, K., Zoing, M., Mackenzie, B. W., Taylor, M. W., and Douglas, R. G. (2017). Evidence of microbiota dysbiosis in chronic rhinosinusitis. *International Forum of Allergy & Rhinology*, *7*(3), 230–239. https://doi.org/10.1002/alr.21871

Hoggard, M., Mackenzie, B. W., Jain, R., Taylor, M. W., Biswas, K., and Douglas, R. G. (2017). Chronic Rhinosinusitis and the Evolving Understanding of Microbial Ecology in Chronic Inflammatory Mucosal Disease. *Clin. Microbiol. Rev.*, *30*(1), 321–348. https://doi.org/10.1128/cmr.00060-16

Homer, K. A., Kelley, S., Hawkes, J., Beighton, D., and Grootveld, M. C. (1996). Metabolism of glycoprotein-derived sialic acid and N-acetylglucosamine by Streptococcus oralis. *Microbiology*, *142*(5), 1221–1230. https://doi.org/10.1099/13500872-142-5-1221

Hsu, J., Avila, P. C., Kern, R. C., Hayes, M. G., Schleimer, R. P., and Pinto, J. M. (2013). Genetics of chronic rhinosinusitis: state of the field and directions forward. *J. Allergy Clin. Immunol.*, *131*(4), 977–993, 993.e1-5. https://doi.org/10.1016/j.jaci.2013.01.028

Huang, A., and Govindaraj, S. (2013). Topical therapy in the management of chronic rhinosinusitis. *Current Opinion in Otolaryngology & Head and Neck Surgery*, *21*(1), 31–38. https://doi.org/10.1097/moo.0b013e32835bc4ab

Huttenhower, C., Gevers, D., Knight, R., Abubucker, S., Badger, J. H., Chinwalla, A. T., Creasy, H. H., Earl, A. M., FitzGerald, M. G., Fulton, R. S., Giglio, M. G., Hallsworth-Pepin, K., Lobos, E. A., Madupu, R., Magrini, V., Martin, J. C., Mitreva, M., Muzny, D. M., Sodergren, E. J., … White, O. (2012). Structure, function and diversity of the healthy human microbiome. *Nature*, *486*(7402), 207–214. https://doi.org/10.1038/nature11234

Illing, E. A., and Woodworth, B. A. (2014). Management of the upper airway in cystic fibrosis. *Current Opinion in Pulmonary Medicine*, *20*(6), 623. https://doi.org/10.1097/MCP.0000000000000107

Jenul, C., and Horswill, A. R. (2018). Regulation of Staphylococcus aureus Virulence. *Microbiol Spectr*, *6*(1). https://doi.org/10.1128/microbiolspec.gpp3-0031-2018

Johansen, H. K., Aanaes, K., Pressler, T., Nielsen, K. G., Fisker, J., Skov, M., Høiby, N., and Buchwald, C. von. (2012). Colonisation and infection of the paranasal sinuses in

cystic fibrosis patients is accompanied by a reduced PMN response. *Journal of Cystic Fibrosis*, *11*(6), 525–531. https://doi.org/10.1016/j.jcf.2012.04.011

Kaiser, J. C., and Heinrichs, D. E. (2018). Branching Out: Alterations in Bacterial Physiology and Virulence Due to Branched-Chain Amino Acid Deprivation. *MBio*, *9*(5). https://doi.org/10.1128/mbio.01188-18

Kaspar, U., Kriegeskorte, A., Schubert, T., Peters, G., Rudack, C., Pieper, D. H., Wos-Oxley, M., and Becker, K. (2015). The culturome of the human nose habitats reveals individual bacterial fingerprint patterns: Human nose culturome. *Environmental Microbiology*, *18*(7), 2130–2142. https://doi.org/10.1111/1462-2920.12891

Kennedy, J. L., and Borish, L. (2013). Chronic rhinosinusitis and antibiotics: the good, the bad, and the ugly. *Am. J. Rhinol. Allergy*, *27*(6), 467–472. https://doi.org/10.2500/ajra.2013.27.3960

Kennedy, J. L., Hubbard, M. A., Huyett, P., Patrie, J. T., Borish, L., and Payne, S. C. (2013). Sino-nasal outcome test (SNOT-22): a predictor of postsurgical improvement in patients with chronic sinusitis. *Ann. Allergy Asthma Immunol.*, *111*(4), 246-251.e2. https://doi.org/10.1016/j.anai.2013.06.033

Kenny, J. G., Ward, D., Josefsson, E., Jonsson, I.-M., Hinds, J., Rees, H. H., Lindsay, J. A., Tarkowski, A., and Horsburgh, M. J. (2009). The Staphylococcus aureus Response to Unsaturated Long Chain Free Fatty Acids: Survival Mechanisms and Virulence Implications. *PLoS ONE*, *4*(2), e4344. https://doi.org/10.1371/journal.pone.0004344

Kiedrowski, M. R., and Bomberger, J. M. (2018). Viral-Bacterial Co-infections in the Cystic Fibrosis Respiratory Tract. *Frontiers in Immunology*, *9*, 3067. https://doi.org/10.3389/fimmu.2018.03067

Kim, D. H., Chu, H.-S. S., Lee, J. Y., Hwang, S. J., Lee, S. H., and Lee, H.-M. M. (2004). Up-regulation of MUC5AC and MUC5B mucin genes in chronic rhinosinusitis. *Archives of Otolaryngology--Head & Neck Surgery*, *130*(6), 747–752. https://doi.org/10.1001/archotol.130.6.747

Kiyohara, M., Tanigawa, K., Chaiwangsri, T., Katayama, T., Ashida, H., and Yamamoto, K. (2010). An exo-α-sialidase from bifidobacteria involved in the degradation of sialyloligosaccharides in human milk and intestinal glycoconjugates. *Glycobiology*, *21*(4), 437–447. https://doi.org/10.1093/glycob/cwq175

Klepac-Ceraj, V., Lemon, K. P., Martin, T. R., Allgaier, M., Kembel, S. W., Knapp, A. A., Lory, S., Brodie, E. L., Lynch, S. V., Bohannan, B. J. M., Green, J. L., Maurer, B. A.,

and Kolter, R. (2010). Relationship between cystic fibrosis respiratory tract bacterial communities and age, genotype, antibiotics and Pseudomonas aeruginosa. *Environmental Microbiology*, *12*(5), 1293–1303. https://doi.org/10.1111/j.1462-2920.2010.02173.x

Klossek, J., Dubreuil, L., Richet, H., Richet, B., and Beutter, P. (1998). Bacteriology of chronic purulent secretions in chronic rhinosinusitis. *J. Laryngol. Otol.*, *112*(12), 1162–1166. https://doi.org/10.1017/s0022215100142732

Krismer, B., Liebeke, M., Janek, D., Nega, M., Rautenberg, M., Hornig, G., Unger, C., Weidenmaier, C., Lalk, M., and Peschel, A. (2014). Nutrient limitation governs Staphylococcus aureus metabolism and niche adaptation in the human nose. *PLoS Pathog.*, *10*(1), e1003862. https://doi.org/10.1371/journal.ppat.1003862

Lam, K., Schleimer, R., and Kern, R. C. (2015). The Etiology and Pathogenesis of Chronic Rhinosinusitis: a Review of Current Hypotheses. *Curr. Allergy Asthma Rep.*, *15*(7), 41. https://doi.org/10.1007/s11882-015-0540-2

Langille, M. G., Zaneveld, J., Caporaso, J. G., McDonald, D., Knights, D., Reyes, J. A., Clemente, J. C., Burkepile, D. E., Thurber, R. L. V., Knight, R., Beiko, R. G., and Huttenhower, C. (2013). Predictive functional profiling of microbial communities using 16S rRNA marker gene sequences. *Nature Biotechnology*, *31*(9), 814–821. https://doi.org/10.1038/nbt.2676

Lavin, J., Bhushan, B., and Schroeder, J. W. (2013). Correlation between respiratory cultures and sinus cultures in children with cystic fibrosis. *International Journal of Pediatric Otorhinolaryngology*, *77*(5), 686–689. https://doi.org/10.1016/j.ijporl.2013.01.018

Lehman, M. K., Nuxoll, A. S., Yamada, K. J., Kielian, T., Carson, S. D., and Fey, P. D. (2019). Protease-Mediated Growth of Staphylococcus aureus on Host Proteins Is opp3 Dependent. *MBio*, *10*(2). https://doi.org/10.1128/mbio.02553-18

Leibig, M., Liebeke, M., Mader, D., Lalk, M., Peschel, A., and Götz, F. (2010). Pyruvate formate lyase acts as a formate supplier for metabolic processes during anaerobiosis in Staphylococcus aureus. *Journal of Bacteriology*, *193*(4), 952–962. https://doi.org/10.1128/jb.01161-10

Liao, Y., Smyth, G. K., and Shi, W. (2013). The Subread aligner: fast, accurate and scalable read mapping by seed-and-vote. *Nucleic Acids Res.*, *41*(10), e108. https://doi.org/10.1093/nar/gkt214

Liao, Y., Smyth, G. K., and Shi, W. (2019). The R package Rsubread is easier, faster, cheaper and better for alignment and quantification of RNA sequencing reads. *Nucleic Acids Res.*, *47*(8), e47. https://doi.org/10.1093/nar/gkz114

Lim, M., Citardi, M. J., and Leong, J.-L. (2008). Topical Antimicrobials in the Management of Chronic Rhinosinusitis: A Systematic Review. *American Journal of Rhinology*, *22*(4), 381–389. https://doi.org/10.2500/ajr.2008.22.3189

Lima, B. P., Hu, L. I., Vreeman, G. W., Weibel, D. B., and Lux, R. (2019). The Oral Bacterium Fusobacterium nucleatum Binds Staphylococcus aureus and Alters Expression of the Staphylococcal Accessory Regulator sarA. *Microb. Ecol.*, *78*(2), 336–347. https://doi.org/10.1007/s00248-018-1291-0

Limoli, D. H., Yang, J., Khansaheb, M. K., Helfman, B., Peng, L., Stecenko, A. A., and Goldberg, J. B. (2016). Staphylococcus aureus and Pseudomonas aeruginosa co-infection is associated with cystic fibrosis-related diabetes and poor clinical outcomes. *European Journal of Clinical Microbiology & Infectious Diseases*, *35*(6), 947–953. https://doi.org/10.1007/s10096-016-2621-0

Lina, G., Boutite, F., Tristan, A., Bes, M., Etienne, J., and Vandenesch, F. (2003). Bacterial competition for human nasal cavity colonization: role of Staphylococcal agr alleles. *Appl. Environ. Microbiol.*, *69*(1), 18–23. https://doi.org/10.1128/aem.69.1.18-23.2003

Loesche, W. J., and Gibbons, R. J. (1968). Amino acid fermentation by Fusobacterium nucleatum. *Archives of Oral Biology*, *13*(2), 191-IN11. https://doi.org/10.1016/0003-9969(68)90051-4

Lombard, V., Ramulu, H., Drula, E., Coutinho, P. M., and Henrissat, B. (2014). The carbohydrate-active enzymes database (CAZy) in 2013. *Nucleic Acids Res.*, *42*(Database issue), D490-5. https://doi.org/10.1093/nar/gkt1178

Love, M. I., Huber, W., and Anders, S. (2014). Moderated estimation of fold change and dispersion for RNA-seq data with DESeq2. *Genome Biol.*, *15*(12), 550. https://doi.org/10.1186/s13059-014-0550-8

Lozupone, C., and Knight, R. (2005). UniFrac: a New Phylogenetic Method for Comparing Microbial Communities. *Applied and Environmental Microbiology*, *71*(12), 8228–8235. https://doi.org/10.1128/aem.71.12.8228-8235.2005

Mackenzie, B. W., Waite, D. W., Hoggard, M., Douglas, R. G., Taylor, M. W., and Biswas, K. (2017). Bacterial community collapse: a meta-analysis of the sinonasal microbiota

in chronic rhinosinusitis. *Environmental Microbiology*, *19*(1), 381–392. https://doi.org/10.1111/1462-2920.13632

Mainz, J. G., Hentschel, J., Schien, C., Cramer, N., Pfister, W., Beck, J., and Tümmler, B. (2012). Sinonasal persistence of Pseudomonas aeruginosa after lung transplantation. *Journal of Cystic Fibrosis*, *11*(2), 158–161. https://doi.org/10.1016/j.jcf.2011.10.009

Mainz, J. G., and Koitschev, A. (2012). Pathogenesis and Management of Nasal Polyposis in Cystic Fibrosis. *Current Allergy and Asthma Reports*, *12*(2), 163–174. https://doi.org/10.1007/s11882-012-0250-y

Mainz, J. G., Naehrlich, L., Schien, M., Käding, M., Schiller, I., Mayr, S., Schneider, G., Wiedemann, B., Wiehlmann, L., Cramer, N., Kahl, B., Beck, J., and Tümmler, B. (2009). Concordant genotype of upper and lower airways P aeruginosa and S aureus isolates in cystic fibrosis. *Thorax*, *64*(6), 535–540. https://doi.org/10.1136/thx.2008.104711

Majima, Y., Masuda, S., and Sakakura, Y. (1997). Quantitative Study of Nasal Secretory Cells in Normal Subjects and Patients With Chronic Sinusitis. *The Laryngoscope*, *107*(11), 1515–1518. https://doi.org/10.1097/00005537-199711000-00017

Malago, J. J. (2015). Contribution of microbiota to the intestinal physicochemical barrier. *Beneficial Microbes*, *6*(3), 295–311. https://doi.org/10.3920/bm2014.0041

Manarey, C. R., Anand, V. K., and Huang, C. (2004). Incidence of methicillin-resistant Staphylococcus aureus causing chronic rhinosinusitis. *Laryngoscope*, *114*(5), 939–941. https://doi.org/10.1097/00005537-200405000-00029

Mantovani, K., Rodrigues, D. de O., Tamashiro, E., Valera, F. C. P., Demarco, R. C., Martinez, R., and Lima, W. T. A. (2010). Comparing different methods used to collect material for a microbiological evaluation of patients with chronic rhinosinusitis. *Brazilian Journal of Otorhinolaryngology*, *76*(3), 321–325. https://doi.org/10.1590/s1808-86942010000300009

Marcus, S., DelGaudio, J. M., Roland, L. T., and Wise, S. K. (2019). Chronic Rhinosinusitis: Does Allergy Play a Role? *Med Sci (Basel)*, *7*(2). https://doi.org/10.3390/medsci7020030

Margolis, E., Yates, A., and Levin, B. R. (2010). The ecology of nasal colonization of Streptococcus pneumoniae, Haemophilus influenzae and Staphylococcus aureus: the role of competition and interactions with host's immune response. *BMC Microbiology*, *10*(1), 59. https://doi.org/10.1186/1471-2180-10-59

Martin, M. (2011). Cutadapt removes adapter sequences from high-throughput sequencing reads. *EMBnet.Journal*, *17*(1), 10–12. https://doi.org/10.14806/ej.17.1.200

McMurdie, P. J., and Holmes, S. (2013). phyloseq: An R Package for Reproducible Interactive Analysis and Graphics of Microbiome Census Data. *PLoS ONE*, *8*(4), e61217. https://doi.org/10.1371/journal.pone.0061217

Mirković, B., Murray, M. A., Lavelle, G. M., Molloy, K., Azim, A. A., Gunaratnam, C., Healy, F., Slattery, D., McNally, P., Hatch, J., Wolfgang, M., Tunney, M. M., Muhlebach, M. S., Devery, R., Greene, C. M., and McElvaney, N. G. (2015). The Role of Short-Chain Fatty Acids, Produced by Anaerobic Bacteria, in the Cystic Fibrosis Airway. *Am. J. Respir. Crit. Care Med.*, *192*(11), 1314–1324. https://doi.org/10.1164/rccm.201505-0943oc

Mondal, M., Nag, D., Koley, H., Saha, D. R., and Chatterjee, N. S. (2014). The Vibrio cholerae Extracellular Chitinase ChiA2 Is Important for Survival and Pathogenesis in the Host Intestine. *PLoS ONE*, *9*(9), e103119. https://doi.org/10.1371/journal.pone.0103119

Muhlebach, M. S., Miller, M. B., Moore, C., Wedd, J. P., Drake, A. F., and Leigh, M. W. (2006). Are lower airway or throat cultures predictive of sinus bacteriology in cystic fibrosis? *Pediatric Pulmonology*, *41*(5), 445–451. https://doi.org/10.1002/ppul.20396

Nadel, D. M., Lanza, D. C., and Kennedy, D. W. (1998). Endoscopically Guided Cultures in Chronic Sinusitis. *American Journal of Rhinology*, *12*(4), 233–241. https://doi.org/10.2500/105065898781390000

Ng, S. K., and Hamilton, I. R. (1971). Lactate metabolism by Veillonella parvula. *Journal of Bacteriology*, *105*(3), 999–1005.

Oksanen, J., Blanchet, F., and Kindt, R. (2013). *Package "vegan."*

Olson, M. E., King, J. M., Yahr, T. L., and Horswill, A. R. (2013). Sialic Acid Catabolism in Staphylococcus aureus. *Journal of Bacteriology*, *195*(8), 1779–1788. https://doi.org/10.1128/jb.02294-12

Ooi, E., Wormald, P.-J., and Tan, L. (2008). Innate immunity in the paranasal sinuses: a review of nasal host defenses. *Am. J. Rhinol.*, *22*(1), 13–19. https://doi.org/10.2500/ajr.2008.22.3127

Orlandi, R. R., Kingdom, T. T., and Hwang, P. H. (2016). International Consensus Statement on Allergy and Rhinology: Rhinosinusitis Executive Summary. *International Forum of Allergy & Rhinology*, *6*(S1), S3–S21. https://doi.org/10.1002/alr.21694

Osborn, A. J., Leung, R., Ratjen, F., and James, A. L. (2011). Effect of Endoscopic Sinus Surgery on Pulmonary Function and Microbial Pathogens in a Pediatric Population With Cystic Fibrosis. *Archives of Otolaryngology–Head & Neck Surgery*, *137*(6), 542. https://doi.org/10.1001/archoto.2011.68

Ou, J., Wang, J., Xu, Y., Tao, Z.-Z., Kong, Y.-G., Chen, S.-M., and Shi, W.-D. (2014). Staphylococcus aureus superantigens are associated with chronic rhinosinusitis with nasal polyps: a meta-analysis. *Eur. Arch. Otorhinolaryngol.*, *271*(10), 2729–2736. https://doi.org/10.1007/s00405-014-2955-0

Petruson, B. (1994). Secretion from Gland and Goblet Cells in Infected Sinuses. *Acta Oto-Laryngologica*, *114*(sup515), 33–37. https://doi.org/10.3109/00016489409124321

Pletcher, S. D., Goldberg, A. N., and Cope, E. K. (2019). Loss of Microbial Niche Specificity Between the Upper and Lower Airways in Patients With Cystic Fibrosis. *The Laryngoscope*, *129*(3), 544–550. https://doi.org/10.1002/lary.27454

Pugliese, G., and Favero, M. S. (2001). Nasal Carriage as a Source of Staphylococcus aureus Bacteremia. *Infection Control & Hospital Epidemiology*, *22*(03), 185. https://doi.org/10.1017/s0195941700069356

Quast, C., Pruesse, E., Yilmaz, P., Gerken, J., Schweer, T., Yarza, P., Peplies, J., and Glöckner, F. O. (2013). The SILVA ribosomal RNA gene database project: improved data processing and web-based tools. *Nucleic Acids Res.*, *41*(Database issue), D590-6. https://doi.org/10.1093/nar/gks1219

Ramakrishnan, V. R., Feazel, L. M., Abrass, L. J., and Frank, D. N. (2013). Prevalence and abundance of Staphylococcus aureus in the middle meatus of patients with chronic rhinosinusitis, nasal polyps, and asthma. *Int. Forum Allergy Rhinol.*, *3*(4), 267–271. https://doi.org/10.1002/alr.21101

Ramakrishnan, V. R., and Frank, D. N. (2015). Impact of cigarette smoking on the middle meatus microbiome in health and chronic rhinosinusitis: Smoking alters the sinonasal microbiome. *International Forum of Allergy & Rhinology*, *5*(11), 981–989. https://doi.org/10.1002/alr.21626

Ramakrishnan, V. R., Gitomer, S., Kofonow, J. M., Robertson, C. E., and Frank, D. N. (2016). Investigation of sinonasal microbiome spatial organization in chronic

rhinosinusitis. *International Forum of Allergy & Rhinology*. https://doi.org/10.1002/alr.21854

Ramakrishnan, V. R., Hauser, L. J., Feazel, L. M., Ir, D., Robertson, C. E., and Frank, D. N. (2015). Sinus microbiota varies among chronic rhinosinusitis phenotypes and predicts surgical outcome. *The Journal of Allergy and Clinical Immunology*, *136*(2), 334-42.e1. https://doi.org/10.1016/j.jaci.2015.02.008

Ramsey, M. M., Freire, M. O., Gabrilska, R. A., Rumbaugh, K. P., and Lemon, K. P. (2016). Staphylococcus aureus shifts toward commensalism in response to Corynebacterium species. *Frontiers in Microbiology*, *7*, 1230.

Cystic Fibrosis Foundation Patient Registry 2018 Annul Data Report. Bethesda, Maryland ©2019 Cystic Fibrosis Foundation.

Rho, J., Wright, D. P., Christie, D. L., Clinch, K., Furneaux, R. H., and Roberton, A. M. (2005). A Novel Mechanism for Desulfation of Mucin: Identification and Cloning of a Mucin-Desulfating Glycosidase (Sulfoglycosidase) from Prevotella Strain RS2. *Journal of Bacteriology*, *187*(5), 1543–1551. https://doi.org/10.1128/jb.187.5.1543-1551.2005

Rice, K. C., Mann, E. E., Endres, J. L., Weiss, E. C., Cassat, J. E., Smeltzer, M. S., and Bayles, K. W. (2007). The cidA murein hydrolase regulator contributes to DNA release and biofilm development in Staphylococcus aureus. *Proceedings of the National Academy of Sciences*, *104*(19), 8113–8118. https://doi.org/10.1073/pnas.0610226104

Robertson, J. M., Friedman, E. M., and Rubin, B. K. (2008). Nasal and sinus disease in cystic fibrosis. *Paediatric Respiratory Reviews*, *9*(3), 213–219. https://doi.org/10.1016/j.prrv.2008.04.003

Roby, B., McNamara, J., and Finkelstein, M. (2008). *Sinus surgery in cystic fibrosis patients: comparison of sinus and lower airway cultures*.

Rosey, E. L., Oskouian, B., and Stewart, G. C. (1991). Lactose metabolism by Staphylococcus aureus: characterization of lacABCD, the structural genes of the tagatose 6-phosphate pathway. *Journal of Bacteriology*, *173*(19), 5992–5998. https://doi.org/10.1128/jb.173.19.5992-5998.1991

Rudkjøbing, V. B., Aanaes, K., Wolff, T. Y., Buchwald, C. von, Johansen, H. K., and Thomsen, T. R. (2014). An exploratory study of microbial diversity in sinus infections of cystic fibrosis patients by molecular methods. *Journal of Cystic Fibrosis*, *13*(6), 645–652. https://doi.org/10.1016/j.jcf.2014.02.008

Rudmik, L., Hoy, M., Schlosser, R. J., Harvey, R. J., Welch, K. C., Lund, V., and Smith, T. L. (2012). Topical therapies in the management of chronic rhinosinusitis: an evidence-based review with recommendations: Topical therapies in the management of CRS. *International Forum of Allergy & Rhinology*, *3*(4), 281–298. https://doi.org/10.1002/alr.21096

Salsgiver, E. L., Fink, A. K., Knapp, E. A., LiPuma, J. J., Olivier, K. N., Marshall, B. C., and Saiman, L. (2016). Changing Epidemiology of the Respiratory Bacteriology of Patients With Cystic Fibrosis. *Chest*, *149*(2), 390–400. https://doi.org/10.1378/chest.15-0676

Sanders, N. N., Eijsink, V. G. H., Pangaart, P. S. van den, Neerven, R. J. J. van, Simons, P. J., Smedt, S. C. D., and Demeester, J. (2007). Mucolytic activity of bacterial and human chitinases. *Biochimica et Biophysica Acta (BBA) - General Subjects*, *1770*(5), 839–846. https://doi.org/10.1016/j.bbagen.2007.01.011

Satiaputra, J., Eijkelkamp, B. A., McDevitt, C. A., Shearwin, K. E., Booker, G. W., and Polyak, S. W. (2018). Biotin-mediated growth and gene expression in Staphylococcus aureus is highly responsive to environmental biotin. *Applied Microbiology and Biotechnology*, *102*(8), 3793–3803. https://doi.org/10.1007/s00253-018-8866-z

Schliep, K. (2011). phangorn: phylogenetic analysis in R. *Bioinformatics*, *27*(4), 592–593. https://doi.org/10.1093/bioinformatics/btq706

Schoenfelder, S. M. K., Marincola, G., Geiger, T., Goerke, C., Wolz, C., and Ziebuhr, W. (2013). Methionine biosynthesis in Staphylococcus aureus is tightly controlled by a hierarchical network involving an initiator tRNA-specific T-box riboswitch. *PLoS Pathogens*, *9*(9), e1003606. https://doi.org/10.1371/journal.ppat.1003606

Smith, K. A., Orlandi, R. R., and Rudmik, L. (2015). Cost of adult chronic rhinosinusitis: A systematic review. *Laryngoscope*, *125*(7), 1547–1556. https://doi.org/10.1002/lary.25180

Smith, S., Evans, C. T., Tan, B. K., Chandra, R. K., Smith, S. B., and Kern, R. C. (2013). National burden of antibiotic use for adult rhinosinusitis. *J. Allergy Clin. Immunol.*, *132*(5), 1230–1232. https://doi.org/10.1016/j.jaci.2013.07.009

Smith, T. L., Schlosser, R. J., Mace, J. C., Alt, J. A., Beswick, D. M., DeConde, A. S., Detwiller, K. Y., Mattos, J. L., and Soler, Z. M. (2019). Long-term outcomes of endoscopic sinus surgery in the management of adult chronic rhinosinusitis. *International Forum of Allergy & Rhinology*, *9*(8), 831–841. https://doi.org/10.1002/alr.22369

Sobin, J., Engquist, S., and Nord, C. E. (2009). Bacteriology of the Maxillary Sinus in Healthy Volunteers. *Scandinavian Journal of Infectious Diseases*, *24*(5), 633–635. https://doi.org/10.3109/00365549209054650

Sobin, L., Kawai, K., Irace, A. L., Gergin, O., Cunningham, M., Sawicki, G. S., and Adil, E. A. (2017). Microbiology of the Upper and Lower Airways in Pediatric Cystic Fibrosis Patients. *Otolaryngology–Head and Neck Surgery*, *157*(2), 302–308. https://doi.org/10.1177/0194599817702332

Soret, P., Vandenborght, L.-E., Francis, F., Coron, N., Enaud, R., Avalos, M., Schaeverbeke, T., Berger, P., Fayon, M., Thiebaut, R., Delhaes, L., Chabe, M., Audebert, C., Durand-Joly, I., Boldron, A., Pin, I., Cognet, O., Pelloux, H., Prevotat, A., … Turck, D. (2020). Respiratory mycobiome and suggestion of inter-kingdom network during acute pulmonary exacerbation in cystic fibrosis. *Scientific Reports*, *10*(1), 3589. https://doi.org/10.1038/s41598-020-60015-4

Spahich, N. A., Vitko, N. P., Thurlow, L. R., Temple, B., and Richardson, A. R. (2016). Staphylococcus aureus lactate- and malate-quinone oxidoreductases contribute to nitric oxide resistance and virulence. *Mol. Microbiol.*, *100*(5), 759–773. https://doi.org/10.1111/mmi.13347

National Center for Health Statistics. (2019). Selected respiratory diseases among adults aged 18 and over, by selected characterisics: United States, National Health Interview Survey, 2018. Hyattsville, Maryland. https://www.cdc.gov/nchs/nhis/data-questionnaires-documentation.htm.

Stevens, W. W., Lee, R. J., Schleimer, R. P., and Cohen, N. A. (2015). Chronic rhinosinusitis pathogenesis. *Journal of Allergy and Clinical Immunology*, *136*(6), 1442–1453. https://doi.org/10.1016/j.jaci.2015.10.009

Syed, S. A., Whelan, F. J., Waddell, B., Rabin, H. R., Parkins, M. D., and Surette, M. G. (2016). Reemergence of Lower-Airway Microbiota in Lung Transplant Patients with Cystic Fibrosis. *Annals of the American Thoracic Society*, *13*(12), 2132–2142. https://doi.org/10.1513/annalsats.201606-431oc

Tailford, L. E., Crost, E. H., Kavanaugh, D., and Juge, N. (2015). Mucin glycan foraging in the human gut microbiome. *Frontiers in Genetics*, *6*.

Terra, V. S., Homer, K. A., Rao, S. G., Andrew, P. W., and Yesilkaya, H. (2010). Characterization of Novel β-Galactosidase Activity That Contributes to Glycoprotein Degradation and Virulence in Streptococcus pneumoniae. *Infection and Immunity*, *78*(1), 348–357. https://doi.org/10.1128/iai.00721-09

Tos, M., and Mogensen, C. (1984). Mucus Production in Chronic Maxillary Sinusitis: A Quantitative Histopathological Study. *Acta Oto-Laryngologica*, *97*(1–2), 151–159. https://doi.org/10.3109/00016488409130975

Valm, A., Welch, J., and Rieken, C. (2011). *Systems-level analysis of microbial community organization through combinatorial labeling and spectral imaging*. https://doi.org/10.1073/pnas.1101134108

Vickery, T. W., Ramakrishnan, V. R., and Suh, J. D. (2019). The Role of Staphylococcus aureus in Patients with Chronic Sinusitis and Nasal Polyposis. *Curr. Allergy Asthma Rep.*, *19*(4), 21. https://doi.org/10.1007/s11882-019-0853-7

Vitko, N. P., Grosser, M. R., Khatri, D., Lance, T. R., and Richardson, A. R. (2016). Expanded Glucose Import Capability Affords Staphylococcus aureus Optimized Glycolytic Flux during Infection. *MBio*, *7*(3). https://doi.org/10.1128/mbio.00296-16

Wagner, C. E., Wheeler, K. M., and Ribbeck, K. (2018). Mucins and Their Role in Shaping the Functions of Mucus Barriers. *Annu. Rev. Cell Dev. Biol.*, *34*, 189–215. https://doi.org/10.1146/annurev-cellbio-100617-062818

Wang, Q., Garrity, G. M., Tiedje, J. M., and Cole, J. R. (2007). Naive Bayesian classifier for rapid assignment of rRNA sequences into the new bacterial taxonomy. *Appl. Environ. Microbiol.*, *73*(16), 5261–5267. https://doi.org/10.1128/aem.00062-07

Wang, X., Kim, J., McWilliams, R., and Cutting, G. R. (2005). Increased prevalence of chronic rhinosinusitis in carriers of a cystic fibrosis mutation. *Arch. Otolaryngol. Head. Neck Surg.*, *131*(3), 237–240. https://doi.org/10.1001/archotol.131.3.237

Wang, Y., Dai, A., Huang, S., Kuo, S., Shu, M., Tapia, C. P., Yu, J., Two, A., Zhang, H., Gallo, R. L., and Huang, C.-M. (2014). Propionic acid and its esterified derivative suppress the growth of methicillin-resistant Staphylococcus aureus USA300. *Benef. Microbes*, *5*(2), 161–168. https://doi.org/10.3920/bm2013.0031

Ward, T., Larson, J., Meulemans, J., Hillmann, B., Lynch, J., Sidiropoulos, D., Spear, J. R., Caporaso, G., Blekhman, R., Knight, R., Fink, R., and Knights, D. (2017). BugBase Predicts Organism Level Microbiome Phenotypes. *BioRxiv*, 133462. https://doi.org/10.1101/133462

Wertheim, H. F. L., Vos, M. C., Ott, A., Belkum, A. van, Voss, A., Kluytmans, J. A. J. W., Keulen, P. H. J. van, Vandenbroucke-Grauls, C. M. J. E., Meester, M. H. M., and Verbrugh, H. A. (2004). Risk and outcome of nosocomial Staphylococcus aureus

bacteraemia in nasal carriers versus non-carriers. *Lancet*, *364*(9435), 703–705. https://doi.org/10.1016/s0140-6736(04)16897-9

Wertheim, H. F., Melles, D. C., Vos, M. C., Leeuwen, W. van, Belkum, A. van, Verbrugh, H. A., and Nouwen, J. L. (2005). The role of nasal carriage in Staphylococcus aureus infections. *Lancet Infect. Dis.*, *5*(12), 751–762. https://doi.org/10.1016/s1473-3099(05)70295-4

Wickström, C., Herzberg, M. C., Beighton, D., and Svensäter, G. (2009). Proteolytic degradation of human salivary MUC5B by dental biofilms. *Microbiology (Reading, England)*, *155*(Pt 9), 2866–2872. https://doi.org/10.1099/mic.0.030536-0

Wolcott, R. D., Hanson, J. D., Rees, E. J., Koenig, L. D., Phillips, C. D., Wolcott, R. A., Cox, S. B., and White, J. S. (2016). Analysis of the chronic wound microbiota of 2,963 patients by 16S rDNA pyrosequencing. *Wound Repair and Regeneration*, *24*(1), 163–174. https://doi.org/10.1111/wrr.12370

Wollenberg, M. S., Claesen, J., Escapa, I. F., Aldridge, K. L., Fischbach, M. A., and Lemon, K. P. (2014). Propionibacterium-produced coproporphyrin III induces Staphylococcus aureus aggregation and biofilm formation. *MBio*, *5*(4), e01286-14. https://doi.org/10.1128/mbio.01286-14

Wright, D. P., Rosendale, D. I., and Roberton, A. M. (2000). Prevotella enzymes involved in mucin oligosaccharide degradation and evidence for a small operon of genes expressed during growth on mucin. *FEMS Microbiology Letters*, *190*(1), 73–79. https://doi.org/10.1111/j.1574-6968.2000.tb09265.x

Wright, E. S. (2016). Using DECIPHER v2. 0 to analyze big biological sequence data in R. *R J.*, *8*(1). https://journal.r-project.org/archive/2016-1/wright.pdf

Yan, M., Pamp, S. J., Fukuyama, J., Hwang, P. H., Cho, D.-Y., Holmes, S., and Relman, D. A. (2013). Nasal microenvironments and interspecific interactions influence nasal microbiota complexity and S. aureus carriage. *Cell Host Microbe*, *14*(6), 631–640. https://doi.org/10.1016/j.chom.2013.11.005

Zanin, M., Baviskar, P., Webster, R., and Webby, R. (2016). The Interaction between Respiratory Pathogens and Mucus. *Cell Host Microbe*, *19*(2), 159–168. https://doi.org/10.1016/j.chom.2016.01.001

Zhang, H., Yohe, T., Huang, L., Entwistle, S., Wu, P., Yang, Z., Busk, P. K., Xu, Y., and Yin, Y. (2018). dbCAN2: a meta server for automated carbohydrate-active enzyme

annotation. *Nucleic Acids Res.*, *46*(W1), W95–W101. https://doi.org/10.1093/nar/gky418

Zhao, J., Schloss, P. D., Kalikin, L. M., Carmody, L. A., Foster, B. K., Petrosino, J. F., Cavalcoli, J. D., VanDevanter, D. R., Murray, S., Li, J. Z., Young, V. B., and LiPuma, J. J. (2012). Decade-long bacterial community dynamics in cystic fibrosis airways. *Proceedings of the National Academy of Sciences of the United States of America*, *109*(15), 5809–5814. https://doi.org/10.1073/pnas.1120577109

Appendices

Appendix A: Supplementary Information for Chapter 2 - 16S rRNA gene sequencing reveals site-specific signatures of the upper and lower airways of cystic fibrosis patients †

---

† Reprinted from *Journal of Cystic Fibrosis*. Sarah K. Lucas, Robert Yang, Jordan M. Dunitz, Holly C. Boyer, and Ryan C. Hunter. "16S rRNA gene sequencing reveals site-specific signatures of the upper and lower airways of cystic fibrosis patients." **© European**

Cystic Fibrosis Society. Originally published by Elsevier B.V. in *Journal of Cystic Fibrosis* 17 (2018) 204-212.

Table S1. Summary of subject clinical data

Patient	Sex	Age	CFTR Genotype	FEV1/FVC (FEV1%)	SNOT-22	Prior FESS (#)	Polyposis
1	M	25	ΔF508/P553X	60	21		Yes
2	M	31	ΔF508/ΔF508	54	41	Yes(2)	Yes
3	M	28	ΔF508/ΔF508	77	21		Yes
4	M	42	ΔF508/ΔF508	50		Yes(4)	Yes
5	M	31	ΔF508/ΔF508	76	20	Yes(2)	Yes
6	M	26	G551D/2789+5G>A	86	8		Yes
7	F	19	ΔF508/1717−1G>A	71	50	Yes(4)	
8	F	26	ΔF508/1717−1G>A	72	59	Yes(1)	Yes
9	F	32	ΔF508/ΔF508	51	34	Yes(1)	Yes
10	M	41	1717-1G-7A/3849+10kbc-T1	76	23	Yes(1)	Yes
11	F	36	ΔF508/ΔF508	70	36	Yes(1)	
12	M	31	ΔF508/394delTT	54	58	Yes(3)	Yes
Avg. +/- s.d.		30.5 +/- 6.5		66.4 +/- 12.1	35 +/- 17.2		

Table S2. Sinus and Sputum clinical culture results.

Sinus Cultures								
Patient	Dominant 16S OTU	*Pseudomonas aeruginosa (mucoid strain)*	*Pseudomonas aeruginosa*	*Staphylococcus aureus*	*Coagulase Negative Staphylococcus (CONS)*	*Streptococcus pneumoniae*	*Burkholderia cepacia complex*	*Achromobacter xylosoxidans*
1	*Streptococcus*	-	-	-	-	-	-	-
2	*Staphylococcus*	-	+	-	+	-	-	-
3	*Pseudomonas*	-	++	-	+	-	-	-
4	*Pseudomonas*	-	++	++	-	-	-	-
5	*Staphylococcus*	-	-	-	-	-	-	++
6	*Staphylococcus*	-	-	+++	-	-	-	-
7	*Staphylococcus*	NA	NA	NA	NA	NA	NA	NA
8	*Pseudomonas*	+	-	+	-	-	-	-
9	*Pseudomonas*	-	+	-	+	-	-	-
10	*Burkholderia*	-	-	-	-	-	++	-
11	*Staphylococcus*	-	+	+++ (MRSA)	-	-	-	-
12	*Pseudomonas*	-	+++	+++ (MRSA)	-	-	-	+++
Lung Sputum Cultures								
Patient	Dominant 16S OTU	*Pseudomonas aeruginosa (mucoid strain)*	*Pseudomonas aeruginosa*	*Staphylococcus aureus*	*Coagulase Negative Staphylococcus (CONS)*	*Streptococcus pneumoniae*	*Burkholderia cepacia complex*	*Achromobacter xylosoxidans*
1	NA	++	++	-	-	-	-	-
2	*Pseudomonas*	+	+	+++	-	-	-	-
3	*Pseudomonas*	+++	+	-	-	-	-	-

4	NA	++	-	+++	-	-	-	-
5	NA	-	-	-	-	-	-	-
6	NA	NA	NA	NA	NA	NA	NA	NA
7	*Staphylococcus*	-	-	+	-	-	-	-
8	NA	-	-	+++	-	-	-	-
9	NA	++	-	-	-	-	-	-
10	NA	-	-	-	-	-	++	-
11	NA	-	++	+++ (MRSA)	-	-	-	-
12	*Pseudomonas*	-	+	+++ (MRSA)	-	-	-	++

(+) Light growth, (++) Moderate Growth, (+++) Heavy Growth

Table S3. Spearman correlations between bacterial genera in sample pairs

Sample Pair	Correlation coefficient	Nonparametric p-value	CI (lower)	CI (upper)
1	0.3422	0.014	0.0736	0.5646
2	0.2542	0.065	-0.023	0.4951
3	0.6692	0.001	0.4826	0.7977
4	0.7089	0.001	0.5385	0.8236
5	0.3489	0.012	0.0811	0.5697
6	0.1056	0.473	-0.1751	0.3704
7	0.4129	0.003	0.155	0.6181
8	0.6026	0.001	0.3921	0.7531
9	0.2869	0.027	0.0123	0.5213
10	0.2862	0.043	0.0116	0.5207
11	0.3089	0.022	0.0364	0.5386
12	0.5761	0.001	0.3573	0.735

Table S4. Antibiotics and route of delivery prescribed three days prior to FESS surgery.

Patient	Azithromycin	Cayston	Colistin	Tobramycin	Doxycycline	Gentamicin	Ciprofloxacin	Bactrim	Amoxicillin
1	Oral	Inhalation	-	-	-	-	Oral	-	-
2	Oral	Inhalation	-	-	-	-	-	-	-
3	Oral	-	-	Oral	-	-	-	-	-
4	-	-	-	-	-	-	-	-	-
5	-	-	Inhalation	-	-	-	-	-	Oral
6	-	-	-	-	-	Intravenous	-	-	-
7	Oral	-	-	Inhalation	-	-	-	Oral	-
8	Oral	Inhalation	Inhalation	-	-	-	-	-	-
9	Oral	Inhalation	-	Inhalation	-	-	-	-	-
10	Oral	-	-	Inhalation	-	-	-	-	-
11	Oral	Inhalation	-	-	Oral	-	-	-	-
12	-	Inhalation	-	-	-	-	-	-	-

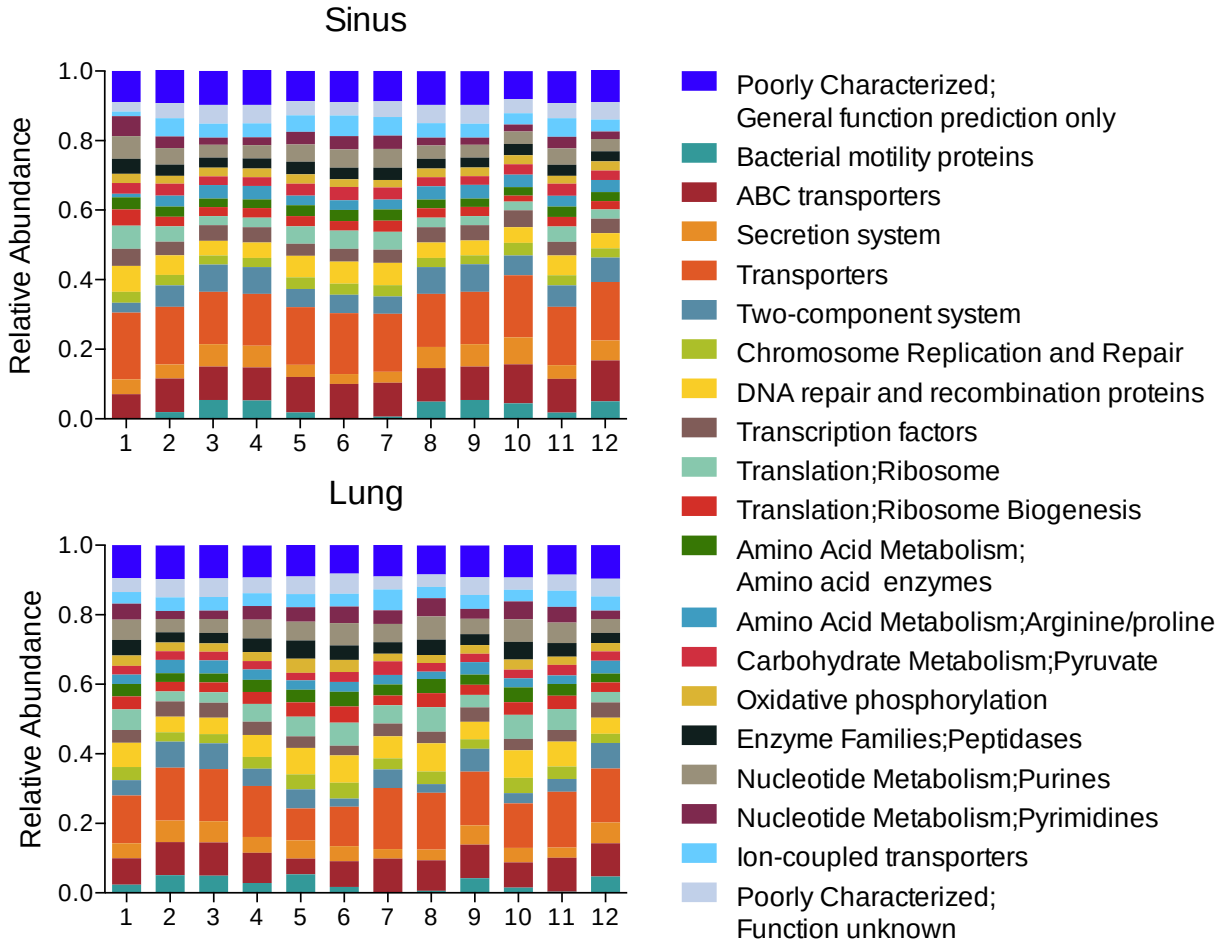

Figure S1. KEGG Pathways identified in sinus and lung samples through PICRUSt analysis. KEGG pathways represented in PICRUSt predicted metagenomes (>1%) exhibited similar composition and abundance between sinus and lung samples. Common predicted pathways between sinus and lung niches belong to bacterial secretion systems, and ABC transporters.

SUPPLEMENTAL METHODS

Quantitative PCR. Bacterial burden was estimated by quantifying 16S copy number from DNA extracted from clinical specimens using qPCR. Universal 16S rRNA qPCR primers 338F and 518R were used (36, 37). QuantiTect SYBR Green (Qiagen, Valencia, CA) was used according to manufacturer's instructions. Reactions were prepared in triplicate as described previously, with adjustments to the amplification protocol (22). Briefly, reactions (25 µL) each contained 12.5 µL 2X QuantiTect SYBR Green Master Mix, 2.5 µL each of 3 µM forward and reverse primers, and 6.5 µL H_2O. Each sample was diluted to 10ng/µl and 1 µl of each of these dilutions was added to their respective reactions. Amplification was done using a CFX96 Real-Time PCR System (Bio-Rad, Hercules, CA) with the following cycling conditions: 95˚C for 15 min followed by 40 cycles of 94˚C for 15 s, 55˚C for 30 s, 72˚C for 30 s with data acquisition at 72˚C. Quantification cycle (Cq) values were calculated using instrument software (CFX Manager, v.3.1). A standard curve with a range from $5x10_6$ to $5x10_2$ 16S rDNA gene copies was used for quantification of 16S copy number and prepared using serial dilutions of DNA extracted from a pure culture of *Escherichia coli* MG1655 (ATCC 47076), known to have seven 16S rDNA gene copies per genome.

DNA extraction, Library Preparation, and Sequencing. The Powersoil DNA Isolation Kit (MoBio, Carlsbad, CA) was used to extract genomic DNA from 300 µL of mucus, following the manufacturer's protocol. Purified DNA was submitted to the UMN Genomics Center (UMGC) for 16S library preparation using a two-step PCR protocol (23). The V4 region of the 16S gene was amplified and sequenced on an Illumina MiSeq using TruSeq version 3 2x300 paired-end technology. Water and reagent control samples were also submitted for sequencing and did not pass quality control steps due to 16S rRNA gene content below detection thresholds. Raw 16S rRNA gene sequence data were deposited as fastq files in the NCBI Sequence Read Archive under accession number PRJNA374847.

Sequence analysis. Sequence data were obtained from UMGC and analyzed using a pipeline developed by the UMN Informatics Institute in collaboration with the UMGC and the Research Informatics Solutions (RIS) group at the UMN Supercomputing Institute (38). Briefly, this pipeline implements Trimmomatic (39) to trim Illumina TruSeq adapter sequences using default options, followed by PANDAseq (40) to align paired-end reads. Consensus sequences were then clustered into operational taxonomic units (OTUs) at 97% identity to the Greengenes database (v.13.8) (41), through implementation of the pick_open_reference_otus.py script with the usearch61 algorithm provided through the Quantitative Insights Into Microbial Ecology (QIIME) software (v.1.9.1) (42).

The OTU table was then filtered such that only OTUs present in the Greengenes database were evaluated. OTUs representing less than 0.005% relative abundance in each sample were excluded as were OTUs representing mitochondrial and plastid sequences. The median number of sequences/sample at this stage was 59774 (interquartile range (IQR)=25002-124256). For calculation of alpha diversity metrics and ordination for principal coordinates analysis, sequences were subsampled to 1674 reads per sample. For principal coordinates analysis, count data in the OTU table was transformed to proportions of the total sequences in each sample. Permutational analysis of variance (PERMANOVA) and homogeneity of dispersion tests were carried out using the 'adonis', 'betadisper', and 'permutest' functions in the 'vegan' R package (43).

Prediction of sinus and lung metagenomes based on 16S rRNA data. Metagenomes were inferred from 16S rRNA data using Phylogenetic Investigation of Communities by Reconstruction

of Unobserved States (PICRUSt) (v. 1.0.0) (24). PICRUSt uses marker gene survey data to predict metagenome functional content of microorganisms through ancestral state reconstruction. We implemented PICRUSt scripts to infer metagenomes from the quality filtered OTU table. Briefly, OTUs were normalized by 16S copy number using the script normalize_copy_number.py. Normalized OTUs were used to predict KEGG orthology (KO)-based metagenomes of our samples through input into the script predict_metagenomes.py with an additional per-sample Nearest Sequenced Taxon Index (NTSI) calculation. Finally, predicted metagenomes were further categorized by KEGG pathways using the categorize_by_function.py script. Output of this script was filtered to only include those pathways that accounted for ≥1% of count data in each sample.

We then used BugBase (https://bugbase.cs.umn.edu) to summarize predicted metagenomes by bacterial phenotype. BugBase combines functionalities of PICRUSt, Integrated Microbial Genome comparative analysis system (IMG4) (44), the PATRIC bacterial bioinformatics database (45), and the KEGG database (46), to identify specific OTUs that contribute to a community-wide phenotype. The main script was run with default settings using the same filtered OTU table as used in PICRUSt. BugBase implements the non-parametric Wilcoxon matched-pairs signed rank test to assess significance. Within-patient and between-sample type taxonomy correlations were calculated using the QIIME script compare_taxa_summaries.py using Spearman correlation with 999 permutations (42).

SUPPLEMENTAL REFERENCES

36. Lane DJ. 16S/23S rRNA sequencing. In: Stackebrandt E, Goodfellow M, editors. Nucleic Acid Techniques in Bacterial Systematics. New York: John Wiley & Sons; 1991, p. 115-148.

37. Muyzer G, de Waal EC, Uitterlinden AG. Profiling of complex microbial populations by denaturing gradient gel electrophoresis analysis of polymerase chain reaction-amplified genes coding for 16S rRNA. *Appl Environ Microbiol* 1993; 59(3):695-700. doi:

38. Garbe JR, Gould T, Knights D, Beckman K. Gopher-Pipelines: Metagenomics-Pipeline Version 1.4 [Computer software]. 2016; https://bitbucket.org/jgarbe/gopher-pipelines/wiki/metagenomics-pipeline.rst.

39. Bolger AM, Lohse M, Usadel B. Trimmomatic: a flexible trimmer for Illumina sequence data. *Bioinformatics* 2014;30(15):2114-20. doi: 10.1093/bioinformatics/btu170.

40. Masella AP, Bartram AK, Truszkowski JM, Brown DG and Neufeld JD. PANDAseq: paired-end assembler for illumina sequences. *BMC Bioinformatics* 2012; 13:31. doi: 10.1186/1471-2105-13-31.

41. DeSantis TZ, Hugenholtz P, Larsen N, Rojas M, Brodie EL, Keller K, Huber T, Dalevi D, Hu P, Anderson GLl. Greengenes, a chimera-checked 16S rRNA gene database and workbench compatible with ARB. *Appl Environ Microbiol* 2006; 72(7):5069-72.

42. Caporaso GJ, Kuczynski J, Stombaugh J, Bittinger K, Bushman FD, Costello EK, Fierer N, Pena A, Goodrich JK, Gordon JI. QIIME allows analysis of high-throughput community sequencing data. *Nat methods* 2010;7(5):335–336. doi: 10.1038/nmeth.f.303.

43. Oksanen J, Blanchet G, Friendly M, Kindt R, Legendre P, McGlinn D, Minchin PR, O'Hara RB, Simpson GL, Solymos P, Stevens MHH, Szoecs E and Wagner H. vegan: Community Ecology Package 2017; R package version 2.4-3. https://CRAN.R-project.org/package=vegan.

44. Markowitz VM, Chen I, Palaniappan K, Chu K, Szeto E, Pillay M, Ratner A, Huang J, Woyke T, Huntermann M, Anderson I, Billis K, Varghese N, Mavromatis K, Pati A, Ivanova NN, Kyrpides NC. IMG 4 version of the integrated microbial genomes comparative analysis system. *Nucleic Acids Res* 2013; 42:D560-D567. doi:10.1093/nar/gkt963.

45. Wattam AR, Abraham D, Dalay O, Disz TL, Driscoll T, Gabbard JL, Gillespie JJ, Gough R, Hix D, Kenyon R, Machi D. PATRIC, the bacterial bioinformatics database and analysis resource. *Nucleic acids Res* 2014; 42: D581-91. doi: 10.1093/nar/gkt1099.

46. Kanehisa M, Sato Y, Kawashima M, Furumichi M and Tanabe M. KEGG as a reference resource for gene and protein annotation. *Nucleic acids research* 2015; 44:D457-D462. doi:10.1093/nar/gkv107

Appendix B: Bioorthogonal non-canonical amino acid tagging reveals translationally active subpopulations of the cystic fibrosis lung microbiota†

† Reprinted from *Nature Communications*. (2020) 11:2287. Talia D. Valentini, Sarah K. Lucas, Kelsey A. Binder, Lydia C. Cameron, Jason A. Motl, Jordan M. Dunitz, and Ryan C. Hunter. "Bioorthogonal non-canonical amino acid tagging reveals translationally active subpopulations of the cystic fibrosis lung microbiota."

Abstract

Culture-independent studies of cystic fibrosis lung microbiota have provided few mechanistic insights into the polymicrobial basis of disease. Deciphering the specific contributions of individual taxa to CF pathogenesis requires comprehensive understanding of their ecophysiology at the site of infection. We hypothesize that only a subset of CF microbiota are translationally active and that these activities vary between subjects. Here, we apply bioorthogonal non-canonical amino acid tagging (BONCAT) to visualize and quantify bacterial translational activity in expectorated sputum. We report that the percentage of BONCAT labeled (i.e. active) bacterial cells varies substantially between subjects (6-56%). We use fluorescence-activated cell sorting (FACS) and genomic sequencing to assign taxonomy to BONCAT-labeled cells. While many abundant taxa are indeed active, most bacterial species detected by conventional molecular profiling show a mixed population of both BONCAT labeled and unlabeled cells, suggesting heterogeneous growth rates in sputum. Differentiating translationally active subpopulations adds to our evolving understanding of CF lung disease and may help guide antibiotic therapies targeting bacteria most likely to be susceptible.

Introduction

The increased viscosity and impaired clearance of mucus secretions in cystic fibrosis (CF) airways creates a favorable environment for chronic microbial colonization, the primary cause of morbidity and mortality (1). *Pseudomonas aeruginosa* and *Staphylococcus aureus* have long been recognized as primary CF pathogens and are the targets of common therapeutic regimens (2), though recent culture-independent studies have revealed a more complex polymicrobial community harboring facultative and obligately anaerobic bacteria that are relatively understudied (3–5). While the specific contributions of individual community members to disease progression remain poorly understood and at times controversial (6), cross-sectional studies of both pediatric and adult cohorts have revealed compelling relationships between bacterial community composition and disease stage, antibiotic use, age, and other phenotypes (7–12). These data have challenged the field to reconsider therapeutic strategies in a polymicrobial community context (13,14).

Relatively fewer studies have identified within-subject perturbations in bacterial community structures that coincide with acute and complex disease flares known as pulmonary exacerbations (PEx). Though no standardized definition of PEx is broadly accepted (15), these episodes are generally characterized by increased respiratory symptoms (e.g., shortness of breath, sputum production) and acute decreases in lung function that can, but not always, be resolved in response to antibiotic therapy. While this would suggest a bacterial etiology, sputum cultures generally demonstrate that airway pathogens are recovered at similar densities before, during, and after disease flares (16–19). Culture independent studies show similar trends; with exceptions (9,20–22), longitudinal sequencing analyses of sputum from individual subjects frequently reveal unique, subject-specific bacterial communities whose diversity and composition remain stable during PEx onset and upon resolution of disease symptoms (16,23,24). This lack of association between lung microbiota and disease dynamics may reflect the inability of both culture-based and sequencing approaches to capture changes in bacterial activity, which likely have a critical impact on disease progression and therapeutic effectiveness.

To date, there have been few studies of bacterial growth and metabolism within the CF airways (25–30). RNA-based profiling of stable CF subjects has shown consistencies between RNA

and DNA signatures suggesting that many bacterial taxa identified by 16S rRNA gene sequencing are metabolically active, though these data have also corroborated that bacterial community membership is not necessarily predictive of growth activity (25,26). Further, rRNA/DNA ratio methods are inherently constrained for use on complex bacterial communities with varying growth strategies (i.e., human microbiota) (31,32). Interactions between respiratory pathogens and the host and/or co-colonizing microbiota can influence growth rates, metabolism, virulence factor production, and antimicrobial susceptibility without an accompanying change in bacterial abundance (33–38). And finally, growth rates of respiratory pathogens can vary substantially between subjects and even within a single sputum sample (27,28), the heterogeneity of which is not captured using conventional molecular profiling. There remains a need for novel methods to characterize bacterial activity and its role in disease progression.

Bioorthogonal non-canonical amino-acid tagging (BONCAT) has been used to characterize the activity of uncultured microbes in soil and marine samples (39–43). BONCAT relies on the cellular uptake of a non-canonical amino-acid (e.g., L-azidohomoalanine (AHA), a L-methionine analog) carrying a chemically-modifiable azide group (44). After uptake, AHA exploits the substrate promiscuity of methionyl-tRNA synthetase and is incorporated into newly synthesized proteins. Translationally active cells can then be identified through a bioorthogonal azide-alkyne click reaction in which a fluorophore-tagged alkyne is covalently ligated to AHA, resulting in a fluorescently labeled population of translationally active cells that can be further studied using a variety of microscopy and analytical methods.

BONCAT has been shown to correlate with other established methods of quantifying microbial activity (40,43) and represents a robust tool for characterization of bacterial communities and a range of other organisms in their native growth environment. BONCAT has also recently been used to study bacterial pathogens in vitro (45–48), though it has seen limited use in the study of host-associated bacterial communities (40,49). Samples derived from the CF airways provide a unique opportunity to do so, as the site of infection is amenable to longitudinal studies and the bacterial growth environment is relatively stable upon removal from the host (50). Exploiting these advantages, here we use BONCAT together with imaging, fluorescence-activated cell sorting (FACS) and 16S rRNA gene sequencing to characterize the translational activity of bacterial communities within sputum derived from a cohort of seven clinically stable CF subjects. We reveal that active bacteria represent only a subset of microbiota captured using conventional 16S rRNA gene sequencing and discuss these results in the context of progression and treatment of chronic airway disease.

Results

BONCAT differentiates translationally active bacteria

To optimize the BONCAT experimental approach, we first grew *P. aeruginosa*, a canonical CF pathogen, to mid-log phase followed by supplementation with 6 mM L-azidohomoalanine (AHA) for 3h. Post-AHA treatment, azide-alkyne click chemistry using Cy5-labeled dibenzocyclooctyne (Cy5–DBCO), permitted fluorescent detection of translationally active cells (Fig. 1a). Quantification of average Cy5 pixel intensity per cell revealed active protein synthesis in ~98% of the population. By contrast, supplementation of the growth medium with 6 mM L-methionine (MET) or pretreatment of *P. aeruginosa* with tobramycin, chloramphenicol, and tetracycline (to arrest de novo protein synthesis) prior to AHA resulted in negligible fluorescence

(Fig. 1b, c). These data were also confirmed by SDS-PAGE (Supplementary Fig. 1). Finally, when two AHA-labeled cultures (one treated with antibiotics, one without) were combined in a 1:1 ratio prior to Cy5–DBCO labeling, a bimodal distribution of fluorescence intensities were observed, representing a mix of active and inactive cells (Fig.1d). Together, these data demonstrate the utility of BONCAT for characterizing *P. aeruginosa* translational activity in an amino-acid-rich growth environment.

To assess whether BONCAT is broadly suitable for labeling polymicrobial communities found in the airways, we then performed mixed activity labeling as described above on representative isolates of common CF-associated microbiota;(51) *Achromobacter xylosoxidans, Burkholderia cenocepacia, Escherichia coli, Fusobacterium nucleatum, Prevotella melaninogenica, Rothia mucilaginosa, Staphylococcus aureus, Stenotrophomonas maltophilia, Streptococcus parasanguinis,* and *Veillonella parvula* (Fig. 2). Each mixed culture (+/−antibiotics in a 1:1 ratio) exhibited a similar labeling pattern to *P. aeruginosa*, suggesting that BONCAT can be used to characterize translational activity among diverse bacterial taxa associated with the CF airways. Notably, all species tested demonstrated BONCAT labeling. In addition, AHA did not affect the growth phenotype of any species under our experimental conditions (Supplementary Fig. 2), consistent with previous studies showing that BONCAT permits labeling of microbiota without concomitant changes in growth rate or protein expression (40,52).

BONCAT identification of active CF microbiota

The BONCAT protocol optimized for lab-grown cultures was then modified for analysis of CF bacterial communities in sputum. To do so, sputum was collected from clinically stable subjects and immediately supplemented with cycloheximide to reduce AHA incorporation by host cells (Supplementary Fig. 3). Samples were then divided into three equal-volume aliquots, supplemented with either 6 mM AHA, 6 mM methionine, or antibiotics (30 μg mL−1 chloramphenicol, 200 μg mL−1 tetracycline, and 10 μg mL−1 tobramycin) plus 6 mM AHA, and incubated at 37°C under oxic conditions for 3 h. Incubation time was chosen to maximize labeling while minimizing changes in bacterial growth conditions such that they closely reflected the in vivo chemical environment. AHA concentration (6 mM) was based on average methionine content in CF sputum (0.6 mM) (53) and a 10:1 AHA:MET ratio (or greater) required for effective labeling (Supplementary Fig. 4).

Representative micrographs (Fig. 3a) reveal BONCAT-labeled sputum obtained from three individual CF subjects (Supplementary Table 1, subjects 1–3). Consistent with previous reports of heterogeneous growth rates (27,28,54), notable differences in Cy5 fluorescence are apparent at higher magnification (Fig. 3b); several individual cells and cell aggregates show moderate to intense labeling whereas others are unlabeled. Treatment with methionine instead of AHA did not result in fluorescent signal, ruling out non-specific labeling and residual dye that could not be removed by washing (Supplementary Fig. 5). Similarly, treatment of sputum with antibiotics prior to AHA addition also resulted in a significant reduction in fluorescence intensity. However, this reduction was incomplete, which may reflect the development of antimicrobial tolerance that arises among CF pathogens. Finally, though cycloheximide treatment results in a significant reduction in AHA uptake by macrophages (Supplementary Fig. 3), we note that host-cell contributions to BONCAT fluorescence cannot be ruled out. Despite this possibility, average pixel intensity per cell (Fig. 3c) further emphasizes the range of bacterial translational activity and the likely slower growth

rates of CF microbiota in sputum compared to cultures grown in vitro (compare Fig. 3c and Fig. 1a). These analyses demonstrate that BONCAT labeling can be used to characterize bacterial activity within complex sputum samples. Moreover, these data suggest that translationally active bacteria represent only a subpopulation of the CF lung microbiota.

Flow cytometric analysis of BONCAT-labeled CF microbiota

BONCAT combined with fluorescence-activated cell sorting (FACS) has previously been used to study microbial activity within soils and marine sediments (39,42). We therefore sought to use FACS to characterize and isolate BONCAT-labeled (i.e., active) cells and bacterial aggregates within sputum samples derived from clinically stable CF subjects (Supplementary Table 1, Subjects 4–6). Our experimental workflow is shown in Fig. 4. Upon sputum collection, a small aliquot (original) was removed and stored at −80°C prior to conventional 16S rRNA gene amplicon analysis. Remaining sputum was then treated with cycloheximide and divided into four aliquots, three of which were supplemented with AHA (6 mM). As a control, the remaining aliquot was treated with 6 mM methionine, and all samples were then incubated under oxic conditions at 37 °C for 3h. Samples were subjected to Cy5–DBCO labeling and counterstaining, followed by removal of another aliquot (sort input) to determine community profile changes as a result of chemical fixation and sputum incubation ex vivo. Remaining samples were homogenized and filtered to remove host cells, followed by FACS to isolate Cy5− (sort-negative) and Cy5+ (sort-positive) cells.

Given the potential heterogeneity of a single sputum plug, triplicate aliquots from each CF sputum sample were BONCAT-labeled and analyzed by FACS and 16 S rRNA gene sequencing to assess the consistency of results (Supplementary Figs. 7 and 8). Representative FACS plots are shown in Fig.5a. Cy5−and Cy5+ gates were sample-specific and were established first by using an AHA−(MET+) aliquot to define the negative gate for each sample. Positive gates were then conservatively assigned by comparing the AHA+ aliquots to the AHA− control (see Supplementary Fig. 9 for gating scheme). AHA+ samples underwent notable shifts along the Cy5+ axis (Fig. 5a) and cells that fell within the Cy5+ gate exhibited a higher geometric mean off fluorescence intensity in the Cy5 channel (Supplementary Fig.10). These data confirm BONCAT labeling and are reflective of translational activity (Fig. 5a). Sort specificity was validated by immunostaining using an anti-Cy5 antibody, which revealed estimated false-negative and false-positive rates of 6.8% and 12%, respectively (Supplementary Fig. 6). Based on total events (~6.5 million counts per sample, on average; Supplementary Table 2), we consistently found that only a subset of the overall bacterial population was Cy5+. For the three individuals surveyed, replicate averages of the Cy5-labeled population were 6.2% (+/−1.21), 42.6% (+/−5.62), and 56.1% (+/−9.57) for subjects 4,5, and 6, respectively. These data reflect labeling patterns shown by microscopy (Fig. 3) and suggest that expectorated sputum harbors bacterial communities with a range of translational activity.

Taxonomic identities of active sputum microbiota

16S rRNA gene sequencing was applied to original, sort input, sort-negative, and sort-positive fractions from each sample to determine bacterial community composition. Sequence data were analyzed using the DADA2 pipeline (55) to reduce potential loss of biological sequence variation due to clustering by similarity and to improve observation of fine-scale variation (including species-level resolution) in bacterial populations. Using this approach, sequence data derived from AHA-labeled samples (sort input, sort-negative, and sort-positive) were compared to

their paired original sample to characterize translationally active subpopulations. For each subject, sample replicates were compared by proportions of the top-ranking taxa (Supplementary Fig. 8a), and variation related to sample type was visualized using a double principle coordinates analysis (DPCoA) (Supplementary Fig. 8b). Replicate samples showed considerable agreement, thus, relative abundances were averaged for further analysis.

Each subject harbored lung microbiota of low to moderate complexity (Fig. 5b), and community profiles were consistent with prior 16S rRNA gene surveys of CF sputum in which *Pseudomonas* and *Streptococcus* were dominant genera (3–5,9–12). We also achieved species-level resolution for less abundant taxa, including several obligate and facultative anaerobes (e.g., *Prevotella* sp., *Rothia* sp.). In general, AHA labeling did not result in substantial changes in bacterial membership; for the most abundant taxa (>1%), community composition was comparable before (original) and after (sort input) BONCAT labeling, demonstrating that AHA treatment and chemical fixation had minimal effect on relative bacterial abundance. Interestingly, bacterial populations recovered from BONCAT–FACS analysis (sort-negative, sort-positive) also showed similarities among the most abundant community members relative to the original sample (i.e., those detected by conventional 16S rRNA gene sequencing). Notable exceptions were *Staphylococcus aureus* and *Rothia* sp. for subject 4, which despite efficient labeling in laboratory culture, were of negligible abundance in the positive fraction, suggesting low translational activity. Less abundant taxa (Supplementary Fig. 11), showed greater variation between fractions, but most were also generally detectable in both sort-negative and sort-positive gates. Together, these data suggest that a subset of most taxa detected by conventional 16 S rRNA gene sequencing are translationally active. Moreover, each taxon appears to exhibit heterogeneous growth activity, which may have important implications for the progression and treatment of CF disease.

To better observe changes in the relative abundances of translationally active bacterial taxa, we calculated fold-change differences between sort-negative, sort-positive, and sort input fractions for each subject (Fig. 5c and Supplementary Figs. 12 and 13). Some genera/species present in fold-change plots do not appear in taxa plots (Fig. 5b) because they were less than 1% relative abundance, but we note that activity among these less abundant populations may also be determinants of CF pathogenesis. In general, ranks of relative abundance were not appreciably different between sort-positive and sort-negative fractions (denoted by heatmaps in Fig. 5c). The most abundant organism in all subjects, *Pseudomonas* (ASV1/ASV4), was always in greater relative abundance in the positive sort (Fig. 5c), reflecting its active growth in sputum and underscoring its recognized importance as a CF pathogen. However, this trend of agreement between relative abundance and fold-change did not always hold. For example, *Leptotrichia* (ASV5) in subject 6 was high in rank abundance (see heatmaps), but its fold difference between positive and negative fractions was 0.22 (~4.5-fold greater in the negative sort), indicating lower relative translational activity than its co-colonizing microbiota. This was also observed for *Streptococcus* (ASV2) in subject 4, which was the second most abundant taxon yet showed low translational activity. Conversely, some low abundance organisms were in higher relative abundance in the positive sort. Most notably, *Streptococcus* (ASV12) and *Rothia dentocariosa* (ASV37) in subject 5 had average relative abundances of 1.3% and 2.3%, respectively, in the negative sort, but were 4.5- and 5.25-fold more prominent in the positive fraction. Other low abundance ASVs assigned as *Actinomyces*, *Enterococcus*, *Peptostreptococcus*, and *Capnocytophaga sputigena* showed similar trends, which were also confirmed by additional comparisons between sort-input/sort-positive and sort-input/sort-negative fractions (Supplemental Figs. 12 and 13).

Taken together, these BONCAT data reveal the extensive heterogeneity of translational activity among CF microbiota. Each individual harbors a unique bacterial community, though community membership and relative abundance are not necessarily predictive of translational activity. Ultimately, profiling of bacterial communities in this manner may help guide therapeutic strategies by identifying subpopulations of translationally active bacteria.

Discussion

16S rRNA gene sequencing has become the gold standard for culture-independent characterization of CF airway bacterial communities. Despite the wealth of data that have emerged regarding the complexity of lung microbiota, we have little understanding of bacterial activity at the site of infection and the specific contributions of individual species to pathogenesis. Expanding on recent studies employing BONCAT as a means of characterizing the ecophysiology of microbial communities in their natural growth environment (39–43), we use this approach in combination with FACS and 16 S rRNA gene sequencing to shed light on bacterial activity in CF sputum. We demonstrate that only a subset of each taxon is detectable by metabolic labeling. Identification and characterization of this subpopulation is not achievable using conventional sequencing approaches and may provide a more precise representation of relevant microbiota within the CF lung.

BONCAT-based studies of translationally active bacteria challenge our thinking on the microbial ecology of the CF airways. Each subject harbored a unique bacterial community consisting primarily of canonical lung pathogens (e.g., *Pseudomonas*). Consistent with previous studies using RNA-based methods (25,26), BONCAT–FACS-based sequencing data indicate these most abundant taxa are also active in situ, reinforcing a probable role for these genera in CF pathogenesis. However, we also revealed that low abundance community members not commonly associated with CF lung disease comprise many taxa that exhibited increased abundance in the positive sort, indicating that community membership is not always predictive of translational activity. In conventional 16S rRNA datasets, rare taxa (i.e., <1%) can be challenging to detect among high abundance organisms (or they are commonly grouped into an ‘other’ category). Moreover, longitudinal dynamics among low abundance taxa can be masked in standard taxa plots and may explain why observed within-subject differences in bacterial community composition rarely track with disease symptoms (9,16,23). While we cannot rule out that some AHA-negative cells are a result of impaired AHA uptake or instrument detection limits, our data suggest that dead and/or dormant biomass comprise a substantial proportion of sequence reads generated via 16S rRNA gene sequencing of CF sputum. We hypothesize that low abundance organisms represent keystone members of the lung microbiota, whose activity dynamics are determinants of acute inflammation, either by directly impacting the host, or indirectly through modulating the growth and virulence of higher abundance pathogens.

BONCAT imaging of sputum and fold-change plots between sort-positive and sort-negative fractions demonstrated both population-wide and taxon-specific translational heterogeneity. This spectrum of metabolic states may confer a significant advantage for bacteria and optimize their fitness in the complex environment of the CF lung. In vivo, airway microbiota face a dynamic milieu shaped by microbial competitors, antimicrobials, the host immune response, nutrient limitation, and other chemical stimuli that can be unfavorable to growth. Under these conditions, adopting a bet-hedging strategy in which only a subpopulation of cells is active may ensure that a given bacterial species is prepared to contend with environmental stress (56). In addition, the transition between translationally active and dormant states may help to explain the

periodicity of PEx, faced with a favorable growth environment, more cells of a given taxon (or taxa) may be induced into active growth and elicit a heightened host response.

The balance between growth states may also be a critical determinant of host response to therapy. By adopting a persister-like strategy in which reduced cellular activity confers a temporary multidrug-resistant phenotype, a dormant subpopulation could ensure persistence during an antibiotic challenge. Once antibiotic-selective pressure is relieved, antimicrobial tolerant populations may emerge. This heterogeneity may also help explain instances in which a subject's clinical response is not predicted by the in vitro drug susceptibility of a given pathogen. We posit that clinical sensitivity panels are poorly predictive of antibiotic efficacy because, among other limitations, they do not account for the heterogeneous translational activity described here.

While active cells are likely more responsible for pathogenesis, inactive cells (Cy5−) are also of importance to CF lung disease as bacteria do not necessarily have to be translationally active to influence their greater community. For example, it is known that largely dormant populations can drive geochemical processes in their growth environment (e.g., mineralizing organic carbon to CO2) (57–59). Translationally inactive cells can also shape their growth environment through nutrient exchange, secretion of virulence factors and small metabolites, electrostatic interactions, and stimulation of the host immune response. Further characterization of activity heterogeneity, the contributions of both active and dormant populations to disease, the frequency of transition between states and the factors that stimulate those transitions will help us to better understand disease dynamics and nature of these.

Though BONCAT represents a useful tool for the study of CF microbiota, we note limitations, several of which have been described previously (39,40,60). First, bacterial cell sorting by flow cytometry is imperfect, as each species has characteristic sort properties. When defining our gating scheme, Cy5+and Cy5−gates were conservatively chosen (requiring a gap in between gates) such that the selection of inactive cells in the positive gate was minimized, and vice versa. However, with this gap a subset of the active population is not collected. Similarly, there is a high probability of selecting active cells in the negative gate due to flow migration characteristics (e.g., *F. nucleatum* shifts differently than a much smaller *V. parvula* cell). Finally, bacterial aggregates, in which only some cells are active (see Fig. 3b) could be pulled into the negative gate by the inactive population of that aggregate. We are currently exploring alternative approaches, including optimization of gating strategies, to improve upon the sorting efficiency of BONCAT-labeled cells.

It is also possible that our experimental conditions were selective against certain taxa. As an example, the 3h AHA incubation is performed under oxic conditions, which may induce an aerobe bloom or inhibit less aero-tolerant bacteria ex vivo. Electrode analyses have shown that steep oxygen gradients are retained in expectorated mucus plugs and are stable over time (50), but it is notable that after AHA treatment, *Rothia mucilaginosa* (ASV8), *Prevotella salivae* (ASV30), *Veillonella* (ASV13), and other anaerobes were far more prevalent in the negative sort. However, this was not always the case (e.g., *R. dentocariosa* and *S. wiggsiae* increased in subjects 5 and 6) making it difficult to determine whether the observed fold-differences reflect growth constraints during BONCAT labeling or a true slow growth (or dormant) phenotype. Though each bacterium tested *in vitro* demonstrated the ability to uptake AHA (Fig.2), it is also expected that each species will incorporate AHA into new proteins at different rates. Similarly, it is possible that catabolism of AHA may skew bacterial composition or induce metabolic changes (61). Future work will be aimed at optimizing reaction conditions and incubation times to minimize the effect of the experimental approach biasing FACS and sequencing data.

Despite these limitations, BONCAT can be used to extend our understanding of the role of specific microbiota in chronic lung disease. Here we focused on a cross-sectional cohort of stable CF subjects, but the approach can be used to address important questions about microbial community dynamics over time. For example, (i) how do active populations vary with disease state? Future studies will focus on longitudinal analyses of within-subject microbial dynamics and how active species correlate with disease symptoms. By identifying bacterial sub-populations most active either preceding or during an acute disease flare (i.e., PEx), more effective therapeutic strategies are likely to be identified. (ii) Why are only some subjects responsive to antimicrobial therapy? As mentioned above, in vivo drug efficacy is often inconsistent with clinical sensitivity panels. By obtaining sputum and amending small aliquots with different classes of antibiotics, BONCAT analysis of the ensuing changes in bacterial activity can be used to predict how CF subjects might respond to treatment. (iii) How do specific taxa respond to environmental stimuli? It is known that bacteria are dynamically responsive to their growth environment, yet how CF microbiota adapt to perturbations in the sputum milieu is poorly understood. BONCAT characterization of sputum samples amended with specific nutrients or incubation under varying environmental conditions (e.g., low pH) will help to shed light on parameters that constrain or potentiate bacterial growth in vivo. (iv) How is translational activity spatially arranged? With the exception of small bacterial aggregates (Fig.3), the approach described here offers limited insight on the spatial distribution of bacterial activity. As an alternative to FACS-based sequencing, BONCAT could be combined with species-specific fluorescence in situ hybridization (FISH) probes and histological analysis of sputum (or lung tissue) to visualize spatial relationships between translationally active bacteria (39,40,62).

In summary, we demonstrate that BONCAT is a powerful tool for the visualization and identification of translationally active bacteria and provides a measure of microbial activity not captured by conventional molecular profiling. Our use of BONCAT lays the foundation for a more detailed understanding of the ecophysiology of CF microbiota and has important implications for the development of new therapeutic strategies and improved clinical outcomes. In addition, the approach is broadly applicable to other airway diseases (e.g., COPD, ventilator associated pneumonias, and sinusitis) where the activity of complex bacterial communities is central to disease states. We are currently using this approach to study microbial community dynamics in a variety of infectious disease contexts.

Methods

Bacterial strains and culture conditions

Bacterial strains are listed in Table 1. *Fusobacterium nucleatum*, *Prevotella melaninogenica*, *Veillonella parvula*, and *Streptococcus parasanguinis* were derived from the American Tissue Type Collection and obtained from Microbiologics (St. Cloud, MN). *Rothia mucilaginosa* was obtained from the Japan Collection of Microorganisms (Riken, Tokyo). *Staphylococcus aureus*, *Escherichia coli* and *Pseudomonas aeruginosa* were obtained from D. K. Newman (California Institution of Technology), and *Burkholderia cenocepacia* was obtained from C.H. Mohr (University of Minnesota). *Achromobacter xylosoxidans* and *Stenotrophomonas maltophilia* were isolated from individuals undergoing treatment at the UMN Adult CF Center. Aerobes were maintained on Luria-Bertani (LB) agar, while anaerobes were maintained on Brain-Heart Infusion (BHI) agar supplemented with a 5% vitamin K-hemin solution (Hardy Diagnostics

#Z237) in an anaerobic chamber (Coy) under a 90% N2/5% CO2/5% H2 atmosphere. Bacterial growth curves were performed in triplicate in BHI broth containing either 6 mM L-azidohomoalanine (AHA) or 6 mM L-methionine (MET).

Bioorthogonal non-canonical amino-acid tagging (BONCAT)

BONCAT labeling was performed as described by Hatzenpichler (40) with modifications. Briefly, for imaging of lab-grown cultures (see below), *P. aeruginosa, B. cenocepacia, A. xylosoxidans, S. maltophilia, R. mucilaginosa, E. coli,* and *S. aureus* were grown aerobically in LB, while *S. parasanguinis, V. parvula, P. melaninogenica,* and *F. nucleatum* were cultured under anaerobic conditions in BHI broth supplemented with hemin and vitamin K. Cultures were grown overnight and diluted 1/100 in 10 mL of fresh medium. Upon reaching mid-log phase, cultures were supplemented with either 6 mM AHA or 6 mM methionine (MET) and incubated for 3 h at 37 °C. When indicated, an antibiotic cocktail consisting of chloramphenicol (30 μg mL^{-1}), tetracycline (200 μg mL^{-1}), and tobramycin (10 μg mL^{-1}) was added 30 min prior to AHA addition to arrest protein synthesis. After incubation, cultures were pelleted via centrifugation (5 min at 10,000 × g), fixed in 4% paraformaldehyde (PFA) for 2 h at 4 °C, resuspended in phosphate buffered saline (PBS, pH 7.4) and stored at 4 °C. All growth curves were performed in triplicate (n = 3).

Sputum samples used for imaging were treated with cycloheximide (100 μg mL^{-1}) upon expectoration and divided into three equal volumes. Aliquots were supplemented with either AHA (6 mM), methionine (6 mM), or AHA (6 mM) with chloramphenicol/tetracycline/tobramycin as described above, incubated at 37 °C for 3 h, followed by fixation in 4% PFA overnight at 4 °C. Samples collected for flow cytometry were divided into five 300−500 μL aliquots. One control aliquot was immediately frozen at −80 °C and later used for conventional 16 S rRNA gene sequencing. Cycloheximide (100 μg mL^{-1}) was added to the remaining four aliquots, three of which were supplemented with AHA (6 mM). One was also supplemented with MET (6 mM), followed by incubation of all samples at 37 °C for 3 h. Labeled samples (and unlabeled controls) were then fixed in 4% PFA for 2 h, pelleted via centrifugation (5 min at 10,000 × g), resuspended in PBS, and stored at 4 °C.

Click Chemistry

For each bacterial culture and sputum sample, strain-promoted azide-alkyne cycloaddition (click chemistry)63 was also performed as described previously (40). Briefly, fixed biomass was pelleted, resuspended in freshly prepared 2chloroacetamide (100 mM) and incubated for 1 h at 46 °C, shaking at 450 r.p.m. in the dark. Cy5-dibenzocyclooctyne (Cy5–DBCO) (Click Chemistry Tools) was then added to a final concentration of 10 μM followed by incubation for 30 min at 46 °C. Samples were washed three times in PBS and further processed for imaging and flow cytometry (see below).

SDS-PAGE

P. aeruginosa was grown to late-exponential phase as described above and supplemented with varying concentrations of AHA (100 μM^{-1} mM) for 1 h prior to fixation. Similarly, *P. aeruginosa* was grown in the presence of varying ratios of MET:AHA. Bacterial pellets were resuspended in extraction buffer (1% sodium dodecyl sulfate, 50 mM NaCl, 100 mM EDTA, 1 mM

MgCl2 at pH 8.4) and boiled for 30 min. After boiling, samples underwent click chemistry as described above. A mixture of methanol:chloroform:water (12:3:8) was then added to each sample followed immediately by centrifugation for 5 min at 16,000 × g. The water/ methanol phase was then carefully removed, and protein recovered from the interface was washed three times in 100% methanol. After the final wash, supernatant was removed and pellets were air dried. Protein was resuspended in 100 µl 1X LDS (lithium dodecyl sulfate) sample buffer and denatured at 70 °C for 10 min. Ten microliter of protein was run on an 8% Bis-Tris gel with MOPS (3-(N-morpholino)propanesulfonic acid)-sodium dodecyl sulfate (SDS) running buffer to which sodium bisulfite had been freshly added. Gels were run at 150 V, fixed for 30 min in a 1:2:7 acetate:methanol:water mix, and imaged with a Typhoon FLA 9500 scanner (GE Healthcare) using an excitation wavelength of 635 nm.

Fluorescence microscopy

BONCAT-labeled bacterial cultures and sputum were spotted on Superfrost Plus microscope slides and counterstained using 1.6 µM STYO64 in PBS. Slides were then washed twice in PBS, mounted using Prolong Diamond Antifade and imaged using an Olympus IX83 microscope with a transmitted Koehler illuminator and a ×60 oil objective lens (NA 1.42). Images were captured on a Hamamatsu ORCA-Flash4.0 V2 digital CMOS camera, and post-acquisition image analysis was performed using cellSens software (v.1.14, Olympus). SYTO64 and Cy5 were visualized using excitation/emission wavelengths of 562 nm/583 nm and 628/640 nm, respectively.

Image analysis was performed using FIJI (64). Briefly, images were subjected to background subtraction using a rolling ball radius of 150 pixels. Individual cells were identified by adjusting thresholds of SYTO64 images using Huang's fuzzy thresholding method (65). Images were also segmented using a watershedding algorithm that assumes each maximum belongs to a discrete particle. The Analyze Particles operation was used to detect and record locations of individual bacterial cells in a given image. For clinical samples, particles were constrained between 100 and 1000 pixels to minimize detection of host cells and sputum debris. Mean pixel intensity at 647 nm (Cy5) was then quantified for each assigned particle. Imaging experiments were performed in triplicate for each bacterial species, and ten images for each sample were captured (n > 1000 particles per sample).

Flow cytometry

Prior to sorting, Cy5–DBCO-labeled sputum was collected by centrifugation and counterstained with 1.6 µM SYTO9 (Invitrogen) in PBS for 30 min. Sputum samples were also stained with 1 µg ml−1 of phycoerythrin (PE) antihuman CD45RO in PBS (BioLegend) for 30 min to stain activated and memory T cells, some B-cell subsets, activated monocytes/macrophages, and granulocytes. All samples were washed in PBS containing 1% BSA and 1 mM EDTA, homogenized using 16- and 22-gauge needles and filtered through a 40 µm cell strainer. To separate AHA + and AHA- bacterial populations, clinical samples were analyzed and sorted on a FACSAriaIIu Cell Sorter (Beckton Dickinson) with a 70µm nozzle at 70 psi. Contaminating human leukocytes staining positive for PE antihuman CD45RO were excluded from bacterial populations of interest in the initial sorting gate (Supplementary Fig. 9). An AHA- control was then matched to each sample to determine the level of non-specific Cy5–DBCO binding and was used to establish Cy5+ (i.e., active) and Cy5− (i.e., inactive) sorting gates. Forward scatter and side scatter gates

were then applied to remove large particulates and debris, and liberal doublet discrimination was used to minimize loss of bacterial aggregates. Collected samples were stored at 4 °C and processed within 24 h. FlowJo software (v.10.5.0) was used for data analysis and presentation.

Cy5+ and Cy5− sorted populations were assessed for post-sort purity by flow cytometry, while collected fractions were visualized by anti-Cy5 immunostaining. To do so, BONCAT-labeled sputum samples were spread across Superfrost Plus microscope slides using a sterile pipette tip and allowed to air dry for 30 min. Slides were washed 3X in PBS and blocked using 1% goat serum in PBS for 1 h, followed by treatment with an anti-Cy5 monoclonal antibody (C1117, Sigma–Aldrich) (1:100 dilution) in incubation buffer (1% goat serum, 0.3% Triton X100 and 10 mg mL^{-1} bovine serum albumin) overnight at 4 °C. Slides were washed 3×, and incubated with Cy3 goat anti-mouse secondary antibody (1:250) in incubation buffer for 45 min. Slides were washed 2×, counterstained using 0.1% Hoescht in PBS and mounted using Prolong Diamond Antifade. Slides were imaged as described above.

DNA extraction

Genomic DNA (gDNA) was extracted using a modified phenolchloroform method previously described (66). Briefly, FACS-sorted samples were collected onto 0.22 µm polycarbonate membranes (EMD Millipore), which were then transferred to 1 mL of TENS buffer (50 mM Tris-HCl [pH 8.0], 20 mM EDTA, 100 mM NaCl, 1% SDS) containing lysozyme (0.2 mg mL^{-1}) and lysostaphin (0.02 µg mL^{-1}) and incubated at 37 °C for 30 min. Sodium dodecyl sulfate (SDS) and proteinase K were added to final concentrations of 1% and 1.2 mg mL^{-1}, respectively, and samples were incubated overnight at 55 °C. Enzymes were deactivated by incubating samples at 90 °C for 30 min, and sample liquid (including membrane) was transferred to a 5 mL conical tube containing an equal volume of phenol:chloroform:isoamyl alcohol (P:C:I, 25:24:1, pH 7.9), which dissolved the membrane. The resulting sample was then split into two Lysing Matrix E tubes (MP Biomedicals) and processed twice by bead beating for 30 seconds. Contents of both tubes were recombined and centrifuged at 3200 × g for 20 min. The aqueous layer was transferred to a new tube and P:C:I extraction was repeated, followed by a chloroform:isoamyl alcohol (24:1) extraction. A 1/10th volume of sodium acetate (3 M, pH 5.2) was then added and nucleic acid was precipitated using one volume of isopropanol followed by centrifugation at 21,130 × g for 20 min. Supernatant was removed, the pellet was washed with 80% ethanol, and centrifuged at 21,130 × g for 10 min. Finally, the gDNA pellet was air dried, resuspended in 10 mM Tris buffer (pH 8.0), and stored at −80 °C until sequencing.

DNA sequencing and analysis

gDNA derived from sputum samples was submitted to the University of Minnesota Genomics Center (UMGC) for 16 S rRNA gene library preparation using a two-step PCR protocol (67). The V4 variable region was amplified using V4_515F and V4_806R primers with common adapter sequences (5'-TCGTCGGCAGCGTCAGATGTGTATAAGAGACAGGTGCCAG CMGCCGCGGTAA-3', 5'-GTCTCGTGGGCTCGGAGATGTGTATAAGAGACA GGGACTACHVGGGTWTCTAAT-3'), followed by the addition of dual indices and Illumina flow cell adaptors in a secondary amplification using primers 5'-AAT GATACGGCGACCACCGAGATCTACACXXXXXXXXTCGTCGGCAGCGTC-3' and 5'-CAAGCAGAAGACGGCATACGAGATXXXXXXXXGTCTCGTGGGCT CGG-3'. Amplicons

were sequenced on an Illumina MiSeq using TruSeq (v.3) 2 × 300 paired-end technology. FACS sheath fluid and DNA extraction reagent control samples were also submitted for sequencing. These control samples did not pass quality control steps due to DNA content below detection thresholds but were incorporated into downstream analyses. An average of 67,793 sequences per sample were obtained. Sequence data are available at NCBI sequence read archive under Bioproject ID PRJNA604587.

Sequence quality was assessed using the DADA2 R package (v.1.2.1) (55). Cutadapt (68) was used to remove primer and Illumina adapter sequences, with size filtering set to a minimum and maximum of 215 bp and 285 bp, respectively. DADA2 functions were used to trim and filter sequences, model and correct Illumina sequence errors, align paired-end sequences, and filter chimeric reads. Specifically, forward and reverse sequences were trimmed to 250 bp and 200 bp, respectively, and a post-trimming minimum length filter of 175 bp was applied. All other DADA2 pipeline parameters were run using default options. Resulting amplicon sequence variants (ASVs) were assigned taxonomy using RDP classifier (69) and the SILVA SSU database (Release 132, December 2017) (70,71). Species-level taxonomy was assigned using the DADA2 addSpecies function only if an ASV unambiguously matched a sequence in the SILVA-132 database. A phylogenetic tree was approximated using the phangorn R package (72) and sequences were aligned using DECIPHER. The phangorn package was then used to construct a neighbor-joining tree, which was then used to fit a GTR + G + I maximum likelihood tree.

The Decontam package (v.1.2.0) (73) was used to reproducibly filter out contaminant sequences. The function isContaminant was used with method = “either” and a probability threshold set to 0.5. Frequency was determined from 16 S qPCR data obtained from UMGC. A total of 28 taxa were removed from the dataset based on frequency and prevalence in the sample when compared with DNA extraction control. An average of 40,773 sequences were recovered from DADA2/Decontam analysis corresponding to 357 ASVs. 79.55% of ASVs were assigned to the genus level, and 22.97% had an unambiguous species assignment.

ASV count data, taxonomic assignment, and the phylogenetic tree were used within the analysis framework of the Phyloseq R package (v.1.26.0)(74–80). ASVs were filtered when they did not belong to the domain Bacteria, or when not assigned taxonomy at the phylum level. Phyla that had low prevalence and abundance (including Acidobacteria, Chloroflexi, Dependentiae, Planctomycetes, and Synergistetes) were removed from the dataset, as were singleton ASVs or those that did not belong to the original or input samples. Finally, ASVs at a relative abundance below 0.001 (0.1%) were removed. After filtering there remained 45 unique taxonomic assignments with 22 assigned at the species level. Fold-change in relative abundance for each ASV were calculated between sort input and sort-positive fractions for each study subject. For all figures, a specific epithet was used when assigned exactly from the SILVA database.

Data availability

Raw 16 S rRNA gene sequence data (Fig. 5 and Supplementary Figs. 8, 11-13) that support the findings of this study were deposited and are available as fastq files in the NCBI sequence read archive under Bioproject ID PRJNA604587. Source data and full gel scans underlying Figs. 1, 3, 5, and Supplementary Figs. 1, 2, 4, 6, 12, and 13 are provided in the Source Data file**.**

Code availability

Previously published software packages and versions used to analyze 16 S rRNA sequence data are cited in the methods above. The custom R function used in sequence analysis is available on Github: https://github.com/hunterlabumn/Valentini_et_al_2020

Acknowledgements

We thank Roland Hatzenpichler (Montana State University) for technical advice, Alex Vitti for figure design, the care team at the UMN Adult CF Treatment Center and their patients for participating in the research. This work was supported by a Gilead Sciences Investigator Sponsored Research Award and a Cystic Fibrosis Foundation Research Grant (HUNTER16G0) to R.C.H. K.A.B. was supported by a NIH Lung Sciences T32 fellowship (#2T32HL007741-21) awarded through the National Heart, Lung, and Blood Institute. S.K.L. received support from T32 (#T90 DE0227232) and F31 (#F31 DE027602) fellowships through the National Institute of Dental and Craniofacial Research.

Author contributions

T.D.V., S.K.L., and K.A.B. contributed equally to this work. T.D.V., S.K.L., K.A.B., and R. C.H. were responsible for study design and wrote the manuscript. T.D.V., K.A.B., and R. C.H. performed BONCAT labeling and imaging experiments. T.D.V., K.A.B., and J.A.M. performed and optimized flow cytometry and FACS. L.C.C. and J.M.D. were responsible for recruitment, sample collection, and data management. S.K.L. performed sequencing and analysis.

References

1. Rajan, S. & Saiman, L. Pulmonary infections in patients with cystic fibrosis. *Semin. Respir. Infect.***17**,47–56 (2002).
2. Cystic Fibrosis Foundation. Patient registry 2017 annual data report.https://cff.org/research/researcher-resources/patient-registry/2017-patient-registry-annual-data-report.pdf(2018).
3. Rogers, G. B. et al. Characterization of bacterial community diversity in cystic fibrosis lung infections by use of 16S ribosomal DNA terminal restriction fragment length polymorphism profiling. *J. Clin. Microbiol*. **42**, 5176–5183(2004).
4. Harris, J. K. et al. Molecular identification of bacteria in bronchoalveolar lavage fluid from children with cystic fibrosis. *Proc. Natl Acad. Sci*. USA**104**,20529–20533 (2007).
5. Filkins, L. M. & O'Toole, G. A. Cystic fibrosis lung infections: polymicrobial, complex, and hard to treat. *PLoS Pathog.* **11**, e1005258 (2015).
6. Caverly, L. J. & LiPuma, J. J. Good cop, bad cop: anaerobes in cystic fibrosis airways. *Eur. Resp. J*. **52**, 1801146 (2018).
7. Cox, M. J. et al. Airway microbiota and pathogen abundance in age-stratified cystic fibrosis patients. *PLoS ONE.* **5**, e11044 (2010).
8. Klepac-Ceraj, V. et al. Relationship between cystic fibrosis respiratory tract bacterial communities and age, genotype, antibiotics and *Pseudomonas aeruginosa*. *Environ. Microbiol.* **12**, 1293–1303 (2010).
9. Carmody, L. A. et al. Changes in cystic fibrosis airway microbiota at pulmonary exacerbation. *Ann. Am. Thorac. Soc.* **10**, 179–187 (2013).
10. Carmody, L. A. et al. Fluctuations in airway bacterial communities associated with clinical states and disease stages in cystic fibrosis. *PLoS ONE*. **13**, e0194060 (2018).

11. Stressmann, F. A. et al. Long-term cultivation-independent microbial diversity analysis demonstrates that bacterial communities infecting the adult cystic fibrosis lung show stability and resilience. *Thorax.* **67**, 867–873 (2012).
12. Muhlebach, M. S. et al. Initial acquisition and succession of the cystic fibrosis lung microbiome is associated with disease progression in infants and preschool children. *PLoS Pathog.* **14**, e1006798 (2018).
13. Caverly, L. J., Zhao, J. & LiPuma, J. J. Cystic fibrosis lung microbiome: opportunities to reconsider management of airway infection. *Pediatr. Pulmonol.* **50**, S31–S38 (2015).
14. Conrad, D. et al. Cystic fibrosis therapy: a community ecology perspective. Am. J. Respir. Cell. *Mol. Biol.* **48**, 150–156 (2013).
15. Van Devanter, D. R. et al. Changing thresholds and incidence of antibiotic treatment of cystic fibrosis pulmonary exacerbations, 1995–2005. *J. Cyst.Fibros.***12**, 332–337 (2013).
16. Fodor, A. A. et al. The adult cystic fibrosis airway microbiota is stable overtime and infection type, and highly resilient to antibiotic treatment of exacerbations. *PloS ONE.* **7**, e45001 (2012).
17. Stressmann, F. A. et al. Does bacterial density in cystic fibrosis sputum increase prior to pulmonary exacerbation? *J. Cyst. Fibros*. **10**, 357–365 (2011).
18. Reid, D. W., Latham, R., Lamont, I. L., Camara, M. & Roddam, L. F. Molecular analysis of changes in *Pseudomonas aeruginosa* load during treatment of a pulmonary exacerbation in cystic fibrosis. *J. Cyst. Fibros.* 1**2**, 688–699 (2013).
19. Lam, J. C., Somayaji, R., Surette, M. G., Rabin, H. R. & Parkins, M. D. Reduction in *Pseudomonas aeruginosa* sputum density during a cystic fibrosis pulmonary exacerbation does not predict clinical response. *BMC Infect. Dis.* **15**, 145 (2015).
20. Sibley, C. D. et al. A polymicrobial perspective of pulmonary infections exposes an enigmatic pathogen in cystic fibrosis patients. *Proc. Natl Acad. Sci. USA* **105**, 15070–15075 (2008).
21. Carmody, L. A. et al. The daily dynamics of cystic fibrosis airway microbiota during clinical stability and at exacerbation. *Microbiome* **3,** 12 (2015).
22. Sherrard, L. J. et al. Assessment of stability and fluctuations of cultured lower-airway bacterial communities in people with cystic fibrosis. *J. Cyst. Fibros.* **18**,808–816 (2019).
23. Price, K. E. et al. Unique microbial communities persist in individual cystic fibrosis patients throughout a clinical exacerbation. *Microbiome* **1**, 27 (2013).
24. Whelan, F. J. et al. Longitudinal sampling of the lung microbiota in individuals with cystic fibrosis. *PLoS ONE* **12**, e0172811 (2017).
25. Grahl, N. et al. Profiling of bacterial and fungal microbial communities in cystic fibrosis sputum using RNA. *mSphere* **3**, e00292–18 (2018).
26. Rogers, G. B. et al. Bacterial activity in cystic fibrosis lung infections. *Respir. Res.* **6**, 49 (2005).
27. Kopf, S. H. et al. Trace incorporation of heavy water reveals slow and heterogeneous pathogen growth rates in cystic fibrosis sputum. *Proc. Natl. Acad. Sci. USA* **113**, E110–E116 (2016).
28. DePas, W. H. et al. Exposing the three-dimensional biogeography and metabolic states of pathogens in cystic fibrosis sputum via hydrogel embedding, clearing, and rRNA labeling. *mBio* **7**, e00796–16 (2016).
29. Yang, L. et al. In situ growth rates and biofilm development of *Pseudomonas aeruginosa* populations in chronic lung infections. *J. Bacteriol.* **190**, 2767–2776(2008).
30. Kragh, K. N. et al. Polymorphonuclear leukocytes restrict the growth of *Pseudomonas aeruginosa* in the lungs of cystic fibrosis patients. *Infect. Immun.* **82**, 4477–4486 (2014).
31. Steven, B., Hesse, C., Soghigian, J., Gallegos-Graves, L. V. & Dunbar, J. Simulated rRNA/DNA ratios show potential to misclassify active populations as dormant. *Appl. Environ. Microbiol.* **83**, e00696–17 (2017).
32. Papp, K., Hungate, B. A. & Schwartz, E. Microbial rRNA synthesis and growth compared through quantitative stable isotope probing with $H_2{}^{18}O$. *Appl. Environ. Microbiol.* **84**, e02441–17 (2018).
33. Radlinski, L. et al. *Pseudomonas aeruginosa* exoproducts determine antibiotic efficacy against *Staphylococcus aureus*. *PLoS Biol.* **15**, e2003981(2017).

34. Korgaonkar, A., Trivedi, U., Rumbaugh, K. P. & Whiteley, M. Community surveillance enhances *Pseudomonas aeruginosa* virulence during polymicrobial infection. *Proc. Natl Acad. Sci. USA* **110**, 1059–1064 (2013).
35. Duan, K., Dammel, C., Stein, J., Rabin, H. & Surette, M. G. Modulation of *Pseudomonas aeruginosa* gene expression by host microflora through interspecies communication. *Mol. Microbiol.* **50**, 1477–1491 (2003).
36. Hoffman, L. R. et al. Selection for *Staphylococcus aureus* small-colony variants due to growth in the presence of *Pseudomonas aeruginosa*. *Proc. Natl Acad. Sci. USA* **103**, 19890–19895 (2006).
37. Sibley, C. D. et al. A polymicrobial perspective of pulmonary infections exposes an enigmatic pathogen in cystic fibrosis patients. *Proc. Natl Acad. Sci. USA* **105**, 15070–15075 (2008).
38. Venkataraman, A., Rosenbaum, M. A., Werner, J. J., Winans, S. C. & Angenent, L. T. Metabolite transfer with the fermentation product 2,3butanediol enhances virulence by *Pseudomonas aeruginosa*. *ISME J.* **8**, 1210–1220 (2014).
39. Hatzenpichler, R. et al. Visualizing in situ translational activity for identifying and sorting slow-growing archaeal-bacterial consortia. *Proc. Natl Acad. Sci. USA* **113**, E4069–E4078 (2016).
40. Hatzenpichler, R. et al. In situ visualization of newly synthesized proteins in environmental microbes using amino acid tagging and click chemistry. *Environ. Microbiol.* **16**, 2568–2590 (2014).
41. Pasulka, A. L. et al. Interrogating marine virus-host interactions and elemental transfer with BONCAT and nanoSIMS-based methods. *Environ. Microbiol.* **20**, 671–692 (2018).
42. Couradeau, E. et al. Probing the active fraction of soil microbiomes using BONCAT-FACS. *Nat. Commun.* **10**, 2770 (2019).
43. Samo, T. J. et al. Broad distribution and high proportion of protein synthesis active marine bacteria revealed by click chemistry at the single cell level. *Front. Mar. Sci.* **1**, 48 (2014).
44. Kiick, K. L. et al. Incorporation of azides into recombinant proteins for chemoselective modification by the Staudinger ligation. *Proc. Nat. Acad. Sci. USA* **99**, 19–24 (2002).
45. Babin, B. M. et al. SutA is a bacterial transcription factor expressed during slow growth in *Pseudomonas aeruginosa*. *Proc. Natl Acad. Sci. USA* **113**, E597–E605 (2016).
46. Grammel, M., Zhang, M. M. & Hang, H. C. Orthogonal alkynyl amino acid reporter for selective labeling of bacterial proteomes during infection. *Angew. Chem. Int. Ed. Engl.* **122**, 6106–6110 (2010).
47. Mahdavi, A. et al. Identification of secreted bacterial proteins by noncanonical amino acid tagging. *Proc. Natl Acad. Sci. USA* **111**, 433–438 (2014).
48. Chande, A. G. et al. Selective enrichment of mycobacterial proteins from infected host macrophages. *Sci. Rep.* **5**, 13430 (2015).
49. Geva-Zatorsky, N. et al. In vivo imaging and tracking of host-microbiota interactions via metabolic labeling of gut anaerobic bacteria. *Nat. Med.* **21**, 1091 (2015).
50. Cowley, E. S., Kopf, S. H., LaRiviere, A., Ziebis, W. & Newman, D. K. Pediatric cystic fibrosis sputum can be chemically dynamic, anoxic, and extremely reduced due to hydrogen sulfide formation. *mBio* **6**, e00767–15 (2015).
51. Bevinino, A. et al. Deciphering the ecology of cystic fibrosis bacterial communities: towards systems-level integration. *Trends. Mol. Med.* **25**, 1110–1122 (2019).
52. Bagert, J. D. et al. Quantitative, time-resolved proteomic analysis by combining bioorthogonal noncanonical amino acid tagging and pulsed stable isotope labeling by amino acids in cell culture. *Mol. Cell. Proteom.* **13**, 1352–1358 (2014).
53. Palmer, K. L., Mashburn, L. M., Singh, P. K. & Whiteley, M. Cystic fibrosis sputum supports growth and cues key aspects of *Pseudomonas aeruginosa* physiology. *J. Bacteriol.* **187**, 5267–5277 (2005).
54. Neubauer, C. et al. Refining the application of microbial lipids as tracers of *Staphylococcus aureus* growth rates in cystic fibrosis sputum. *J. Bacteriol.* **200**, e00365–18 (2018).
55. Callahan, B. J. et al. DADA2: high-resolution sample inference from Illumina amplicon data. *Nat. Methods* **13**, 581–583 (2016).
56. Acar, M., Mettetal, J. T. & Van Oudenaarden, A. Stochastic switching as a survival strategy in fluctuating environments. *Nat. Genet.* **40**, 471–475 (2008).

57. Anderson, T. H. & Domsch, K. H. Application of eco-physiological quotients (qCO2 and qD) on microbial biomasses from soils of different cropping histories. *Soil Biol. Biochem*. **22**, 251–255 (1990).
58. Pester, M., Bittner, N., Deevong, P., Wagner, M. & Loy, A. A 'rare biosphere' microorganism contributes to sulfate reduction in a peatland. *ISME J.* **4**, 1591–1602 (2010).
59. Hausmann, B., Pelikan, C., Rattei, T., Loy, A. & Pester, M. Long-term transcriptional activity at zero growth of a cosmopolitan rare biosphere member. *mBio* **10**, e02189–18 (2019).
60. Hatzenpichler, R. & Orphan, V.J. in Hydrocarbon and Lipid Microbiology Protocols (eds. T. McGenity, K. Timmis & B. Nogales) 145–157 (Springer, Berlin, 2015).
61. Steward, K. F. et al. Metabolic implications of using biorthogonal noncanonical amino acid tagging (BONCAT) for tracking protein synthesis. *Front. Microbiol.* **11**, 197 (2020).
62. Leizeaga, A. et al. Using Click-Chemistry for visualizing in situ changes of translational activity in planktonic marine bacteria. *Front. Microbiol.* **8**, 2360 (2017).
63. Agard, N. J., Prescher, J. A. & Bertozzi, C. R. A strain-promoted [3 + 2] azidealkyne cycloaddition for covalent modification of biomolecules in living systems. *J. Am. Chem. Soc.* **126**, 15046–15047 (2004).
64. Schindelin, J. et al. Fiji: an open-source platform for biological-image analysis. *Nat. Methods* **9**, 676–682 (2012).
65. Huang, L. & Wang, M. J. Image thresholding by minimizing the measure of fuzziness. *Pattern Recognit*. **28**, 41–51 (1995)
66. Urakawa, H., Martens-Habbena, W. & Stahl, D. A. High abundance of ammonia-oxidizing Archaea in coastal waters, determined using a modified DNA extraction method. *Appl. Environ. Microbiol*. **76**, 2129–2135 (2010).
67. Gohl, D. et al. Systematic improvement of amplicon marker gene methods for increased accuracy in microbiome studies. *Nat. Biotechnol.* **34**, 942–949 (2016).
68. Martin, M. Cutadapt removes adapter sequences from high-throughput sequencing reads. *EMBnet. J.* **1**, 10–12 (2011).
69. Wang, Q., Garrity, G. M., Tiedje, J. M. & Cole, J. R. Naive Bayesian classifier for rapid assignment of rRNA sequences into the new bacterial taxonomy. *Appl. Environ. Microbiol.* **73**, 5261–5267 (2007).
70. Yilmaz, P. et al. The SILVA and "all-species living tree project (LTP)" taxonomic frameworks. *Nucleic Acids Res.* **42**, D643–D648 (2014).
71. Quast, C. et al. The SILVA ribosomal RNA gene database project: improved data processing and web-based tools. *Nucleic Acids Res*. **41**, D590–D596 (2012).
72. Schliep, K. P. phangorn: phylogenetic analysis in R. *Bioinformatics* **27**, 592–593 (2011).
73. Davis, N. M., Proctor, D., Holmes, S. P., Relman, D. A. & Callahan, B. J. Simple statistical identification and removal of contaminant sequences in marker-gene and metagenomics data. *Microbiome* **6**, 226 (2018).
74. McMurdie, P. J. & Holmes, S. phyloseq: an R package for reproducible interactive analysis and graphics of microbiome census data. *PLoS ONE* **8**, e61217 (2013).
75. Badalamenti, J. P. & Hunter, R. C. Complete genome sequence of *Achromobacter xylosoxidans* MN001, a cystic fibrosis airway isolate. *Genome Announc* **3**, ee00947–15 (2015).
76. Lewenza, S., Conway, B., Greenberg, E. P. & Sokol, P. A. Quorum sensing in *Burkholderia cepacia*: identification of the luxRI homologs cepRI. *J. Bacteriol*. **181**, 748–756 (1999).
77. Saltikov, C. W. & Newman, D. K. Genetic identification of a respiratory arsenate reductase. *Proc. Natl Acad. Sci. USA* **100**, 10983–10988 (2003).
78. Rahme, L. G. et al. Common virulence factors for bacterial pathogenicity in plants and animals. *Science* **268**, 1899–1902 (1995).
79. Collins, M. D., Hutson, R. A., Båverud, V. & Falsen, E. Characterization of a *Rothia*-like organism from a mouse: description of *Rothia nasimurium* sp. nov. and reclassification of *Stomatococcus mucilaginosus* as *Rothia mucilaginosa* comb. nov. *Int. J. Syst. Evol. Microbiol.* **50**, 1247–1251 (2000).
80. Blomster-Hautamaa, D. A. & Schlievert, P. M. Preparation of toxic shock syndrome toxin-1. *Methods Enzymol*. **165**, 37–43 (1988).

Tables

Table 1. Bacterial strains used in this study

Bacterial Species	Comment	Source
Achromobacter xylosoxidans	CF clinical isolate MN001	75
Burkholderia cenocepacia	CF Clinical isolate K56-2	76
Escherichia coli	UQ950	77
Fusobacterium nucleatum	ATCC 25586	ATCC
Prevotella melaniniogenica	ATCC 25845	ATCC
Pseudomonas aeruginosa	Clincial isolate UCBPP-PA14	78
Rothia mucilaginosa	JCM 10910	79
Staphylococcus aureus	Clinical isolate MN8	80
Stenotrophomonas maltophilia	CF clinical isolate CHB83-1	This study
Streptococcus parasanguinis	ATCC 15912	ATCC
Veillonella parvula	ATCC 10790	ATCC

Figures

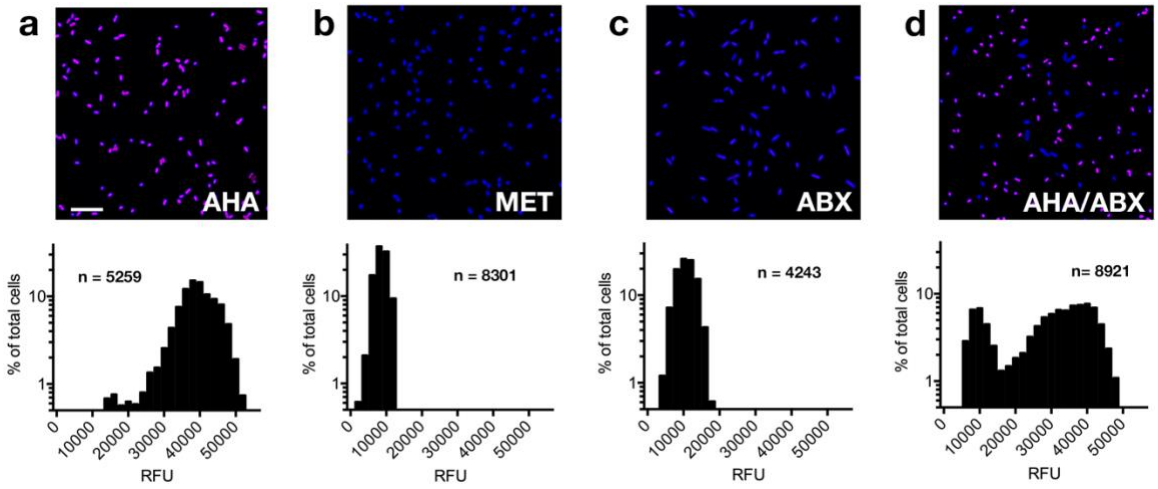

Figure 1. BONCAT labeling of P. aeruginosa differentiates translationally active and inactive cells. P. aeruginosa was incubated in the presence of a AHA, b methionine (MET), and c antibiotics prior to AHA (ABX). Actively growing cells were identified via strain-promoted click chemistry (Cy5, magenta; SYTO64, blue). Histograms associated with each image represent average Cy5 pixel intensity (relative fluorescence units, RFU) per cell. d Two AHAtreated cultures (one with antibiotics, one without) were mixed in a 1:1 ratio prior to Cy5–DBCO labeling. These data demonstrate that BONCAT can differentiate translationally active and inactive bacterial cells in a complex nutritional milieu. Scale bar = 10 μm. n refers to the number of cells examined over ten images from each of three independent experiments. Source data are provided as a Source Data file.

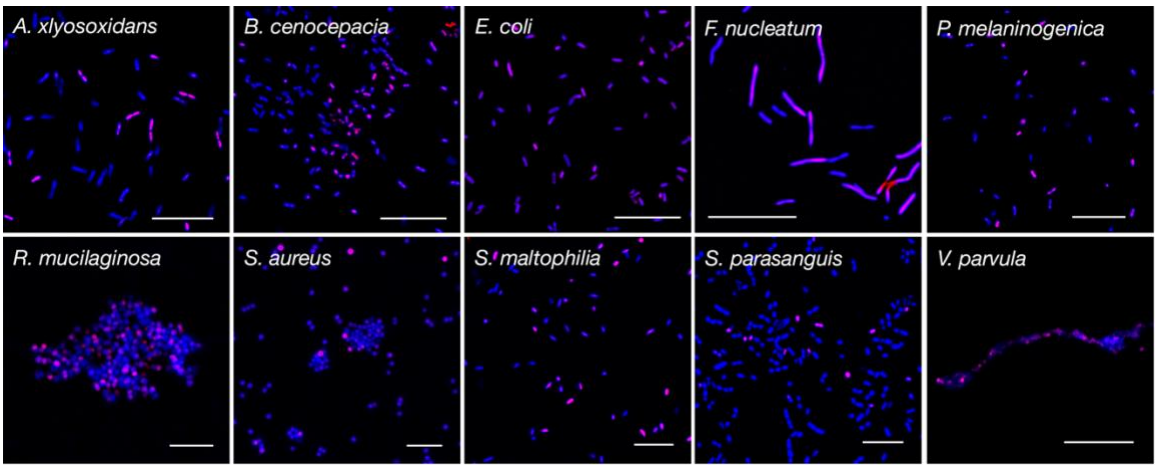

Figure 2. BONCAT can identify active cells among diverse CF microbiota. Two cultures (one treated with antibiotics, one without) of each species were grown in the presence of AHA and mixed 1:1 prior to Cy5–DBCO (magenta) labeling and SYTO64 counterstaining (blue). These data demonstrate that BONCAT can differentiate between active and inactive bacterial cells among diverse CF microbiota. Scale bars; Ax, Bc, Fn, Ec, Pm, Rm = 20 µm; Sa, Sm, Sp = 10 µm; Vp = 5 µm. Images are representative of ten images from each of three biologically independent experiments for each organism.

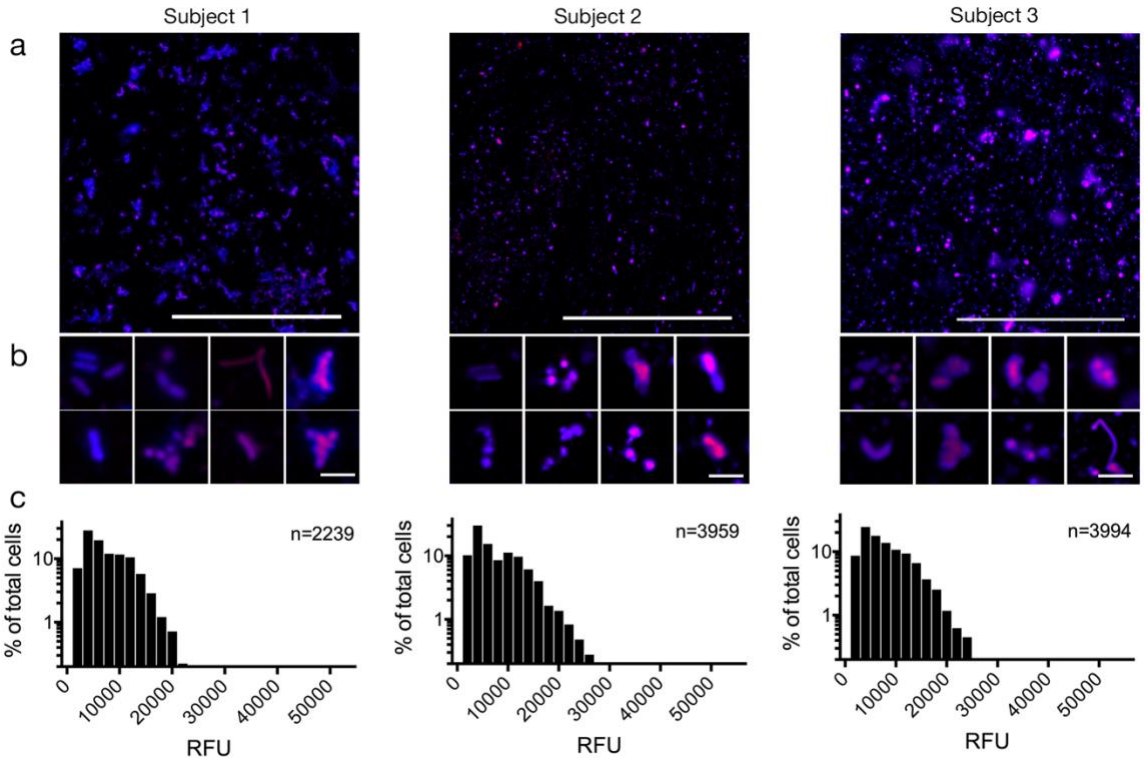

Figure 3. CF microbiota exhibit heterogeneous translational activity within sputum. a Sputum was incubated in the presence of 6 mM AHA immediately upon expectoration. BONCAT labeling with Cy5–DBCO (magenta) and counterstaining with SYTO64 (blue) reveals heterogeneous AHA incorporation (i.e., translational activity). b Higher magnification images further emphasize the range of bacterial activity at the single-cell level. c Average Cy5 pixel intensity per cell suggests slow and heterogeneous translational activity among bacterial cells in situ. Scale bars; a = 100 µm, b = 5 µm. Source data are provided as a Source Data file.

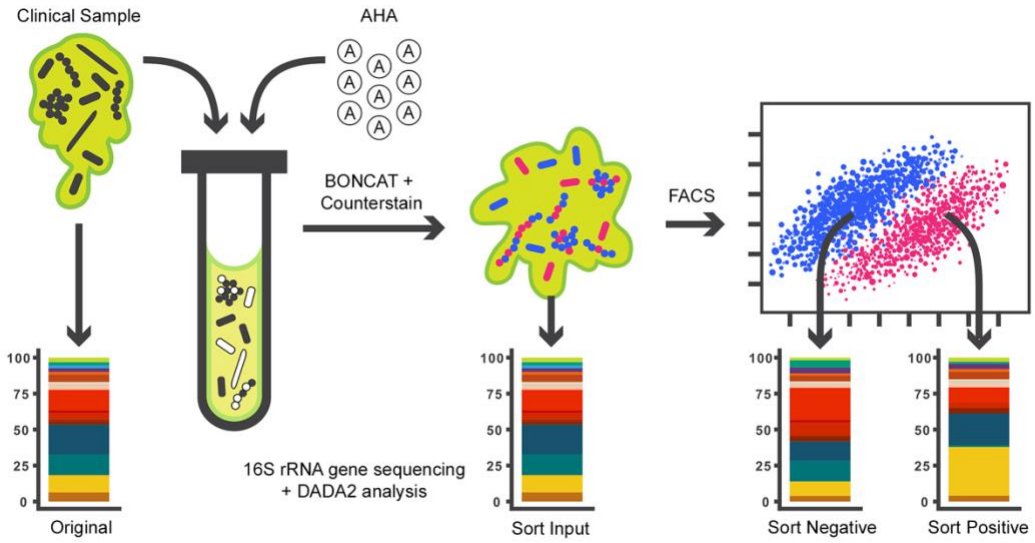

Figure 4. Experimental workflow for BONCAT. Analysis of CF sputum.

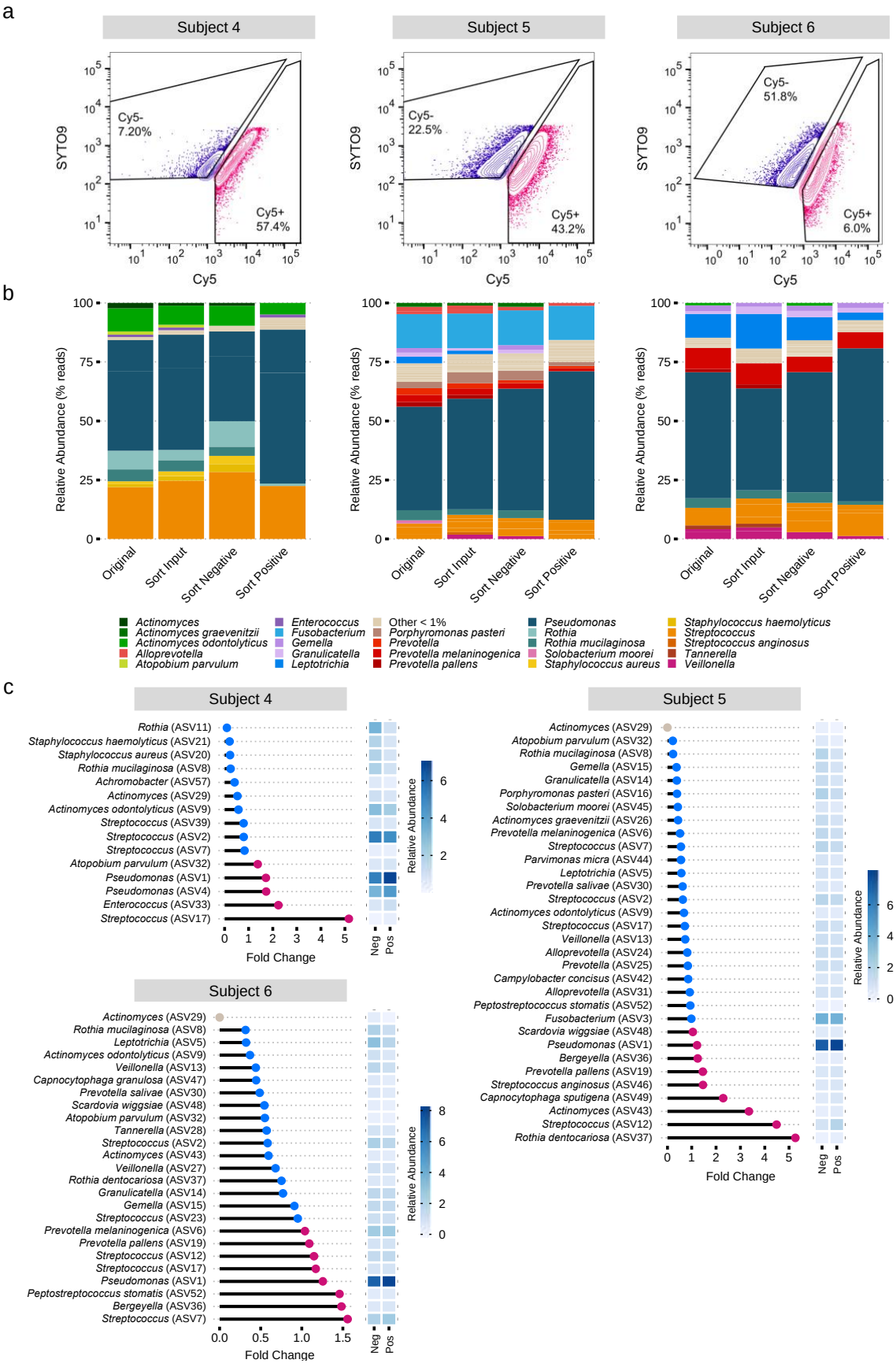
a
Subject 4
Subject 5
Subject 6
SYTO9
Cy5
Cy5-
7.20%
Cy5+
57.4%
Cy5-
22.5%
Cy5+
43.2%
Cy5-
51.8%
Cy5+
6.0%
b
Relative Abundance (% reads)
Original
Sort Input
Sort Negative
Sort Positive
Actinomyces
Actinomyces graevenitzii
Actinomyces odontolyticus
Alloprevotella
Atopobium parvulum
Enterococcus
Fusobacterium
Gemella
Granulicatella
Leptotrichia
Other < 1%
Porphyromonas pasteri
Prevotella
Prevotella melaninogenica
Prevotella pallens
Pseudomonas
Rothia
Rothia mucilaginosa
Solobacterium moorei
Staphylococcus aureus
Staphylococcus haemolyticus
Streptococcus
Streptococcus anginosus
Tannerella
Veillonella
c
Subject 4
Rothia (ASV11)
Staphylococcus haemolyticus (ASV21)
Staphylococcus aureus (ASV20)
Rothia mucilaginosa (ASV8)
Achromobacter (ASV57)
Actinomyces (ASV29)
Actinomyces odontolyticus (ASV9)
Streptococcus (ASV39)
Streptococcus (ASV2)
Streptococcus (ASV7)
Atopobium parvulum (ASV32)
Pseudomonas (ASV1)
Pseudomonas (ASV4)
Enterococcus (ASV33)
Streptococcus (ASV17)
Fold Change
Relative Abundance
Neg
Pos
Subject 5
Actinomyces (ASV29)
Atopobium parvulum (ASV32)
Rothia mucilaginosa (ASV8)
Gemella (ASV15)
Granulicatella (ASV14)
Porphyromonas pasteri (ASV16)
Solobacterium moorei (ASV45)
Actinomyces graevenitzii (ASV26)
Prevotella melaninogenica (ASV6)
Streptococcus (ASV7)
Parvimonas micra (ASV44)
Leptotrichia (ASV5)
Prevotella salivae (ASV30)
Streptococcus (ASV2)
Actinomyces odontolyticus (ASV9)
Streptococcus (ASV17)
Veillonella (ASV13)
Alloprevotella (ASV24)
Prevotella (ASV25)
Campylobacter concisus (ASV42)
Alloprevotella (ASV31)
Peptostreptococcus stomatis (ASV52)
Fusobacterium (ASV3)
Scardovia wiggsiae (ASV48)
Pseudomonas (ASV1)
Bergeyella (ASV36)
Prevotella pallens (ASV19)
Streptococcus anginosus (ASV46)
Capnocytophaga sputigena (ASV49)
Actinomyces (ASV43)
Streptococcus (ASV12)
Rothia dentocariosa (ASV37)
Fold Change
Relative Abundance
Neg
Pos
Subject 6
Actinomyces (ASV29)
Rothia mucilaginosa (ASV8)
Leptotrichia (ASV5)
Actinomyces odontolyticus (ASV9)
Veillonella (ASV13)
Capnocytophaga granulosa (ASV47)
Prevotella salivae (ASV30)
Scardovia wiggsiae (ASV48)
Atopobium parvulum (ASV32)
Tannerella (ASV28)
Streptococcus (ASV2)
Actinomyces (ASV43)
Veillonella (ASV27)
Rothia dentocariosa (ASV37)
Granulicatella (ASV14)
Gemella (ASV15)
Streptococcus (ASV23)
Prevotella melaninogenica (ASV6)
Prevotella pallens (ASV19)
Streptococcus (ASV12)
Streptococcus (ASV17)
Pseudomonas (ASV1)
Peptostreptococcus stomatis (ASV52)
Bergeyella (ASV36)
Streptococcus (ASV7)
Fold Change
Relative Abundance
Neg
Pos

Fig. 5 BONCAT, FACS, and sequencing of CF sputum reveals the taxonomic identities of translationally active microbiota. a FACS of BONCAT-labeled sputum reveals Cy5− and Cy5+ subpopulations. Percentages shown reflect % of parent population post-CD45RO gating. b Original, sort input, sortnegative (Cy5−), and sort-positive (Cy5+) fractions were analyzed by 16 S rRNA gene sequencing. Taxa plots summarize sequencing data by subject and averaged relative abundances between triplicate-positive and -negative sorted fractions. c Fold-changes between relative abundances of taxa in the sortpositive compared to the negative fraction. Point color indicates taxa that were increased (pink) and decreased (blue) in relative abundance in the sortpositive fraction, representing translationally active microbiota. The single gray points indicate ASVs seen only in the negative sample. Heatmap sidebars represent square root transformed relative abundances.

Supplementary Figures

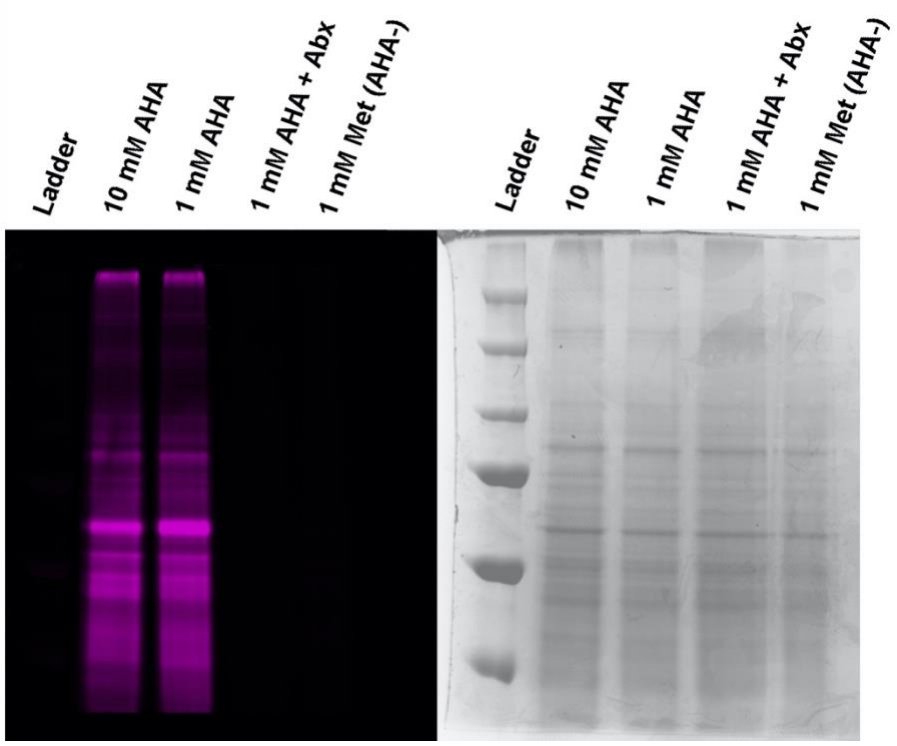

Figure S1. BONCAT labeling of P. aeruginosa is specific for AHA and translational activity. SDSPAGE visualization of BONCAT labeling of laboratory cultures of P. aeruginosa PA14. Labeling is specific for AHA and inhibited by antibiotics (Abx = chloramphenicol, tetracycline, tobramycin). Full gel scans are provided as a Source Data file.

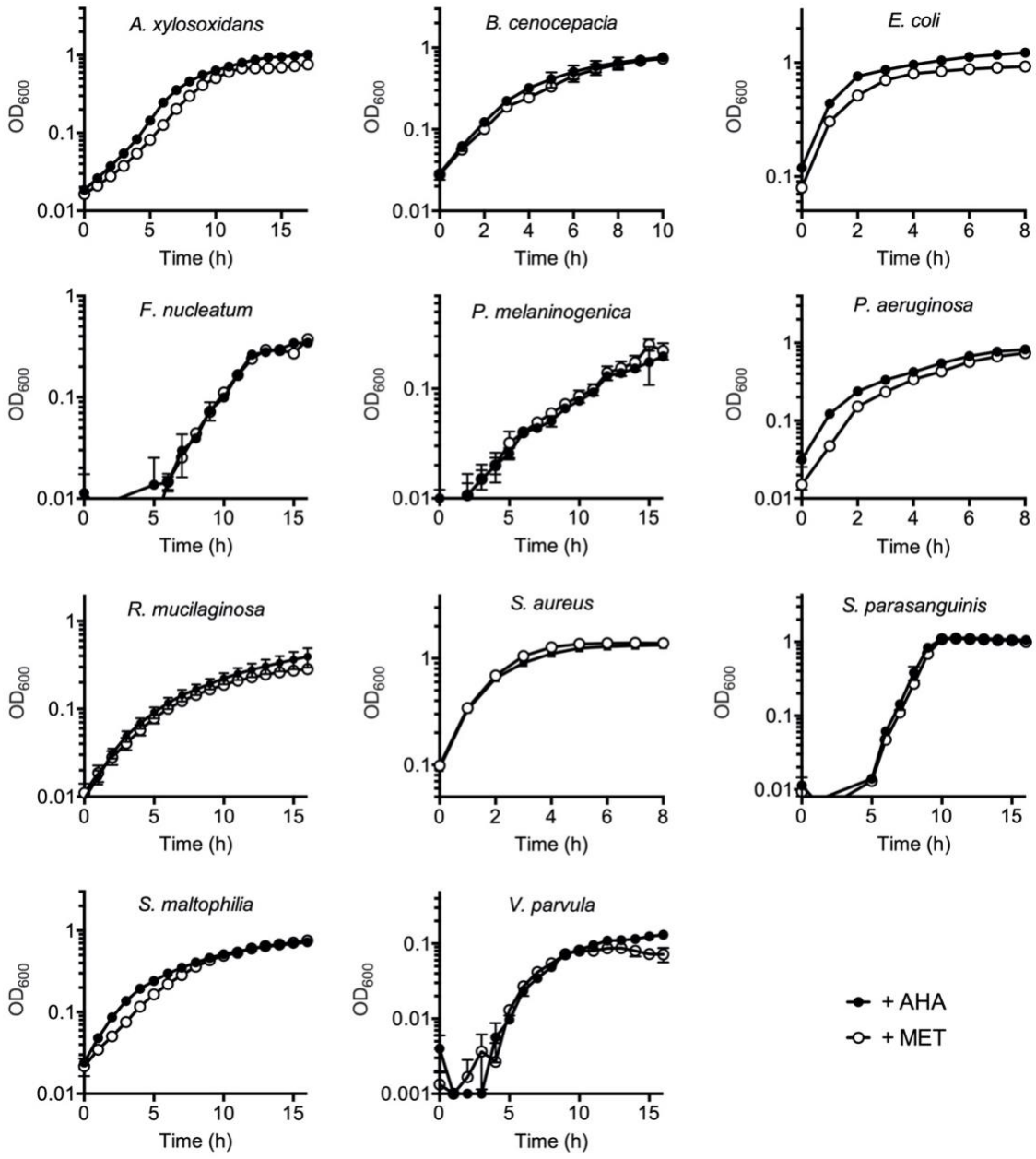

Figure S2. AHA-incubation has negligible effect on bacterial growth. Growth curves were performed in triplicate for each species under each growth condition (6mM L-azidohomoalanine (AHA) or 6mM methionine (MET)). Error bars represent standard deviation of the mean of three biological replicates. Source data are provided as a Source Data file.

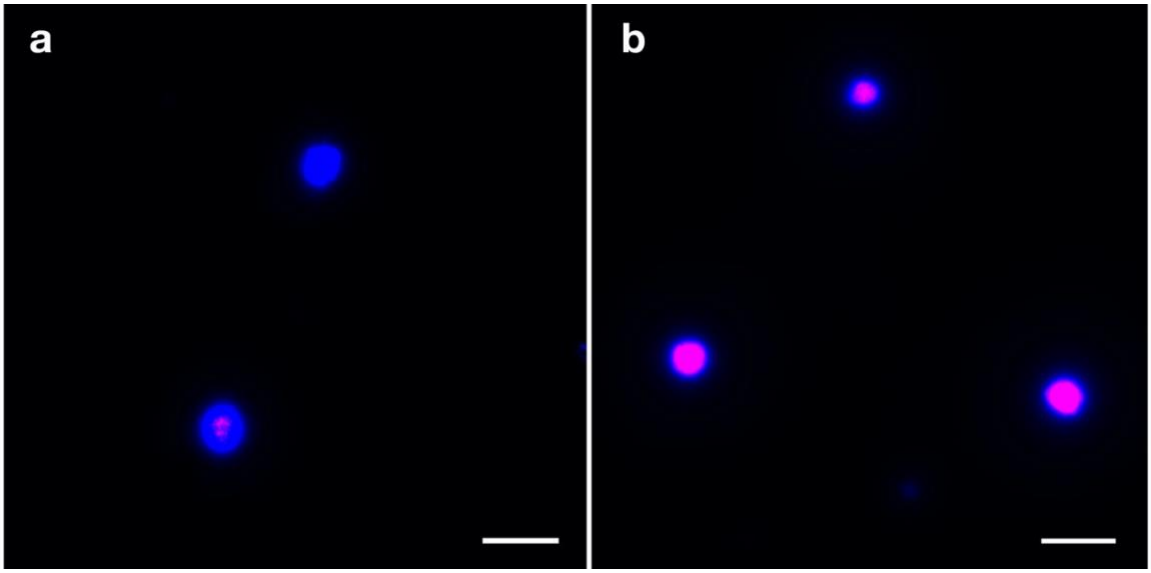

Figure S3. Cycloheximide Inhibition of host cell BONCAT labeling. RAW 264.7 macrophages (Sigma Aldrich 91062702) were cultured in T25 flasks containing high glucose Dulbecco's Modified Eagle's Medium supplemented with GlutaMAX and pyruvate (Thermo, 10569044). Cycloheximide was added to one flask at a final concentration of 100 µg/mL, and another was left untreated. AHA was then added to a final concentration of 6mM to both flasks and incubated for 3h. Cells were detached using 0.25% trypsin solution in EDTA (Sigma T4049) and fixed in 1mL of 4% PFA in PBS for 2 h prior to imaging. Imaging was performed as described in the main text. Representative images of two biologically independent experiments are shown. (a) BONCAT labeling of macrophages to which cycloheximide was added were inhibited relative to (b) untreated (i.e. AHA+ cells). Bar = 20 µM.

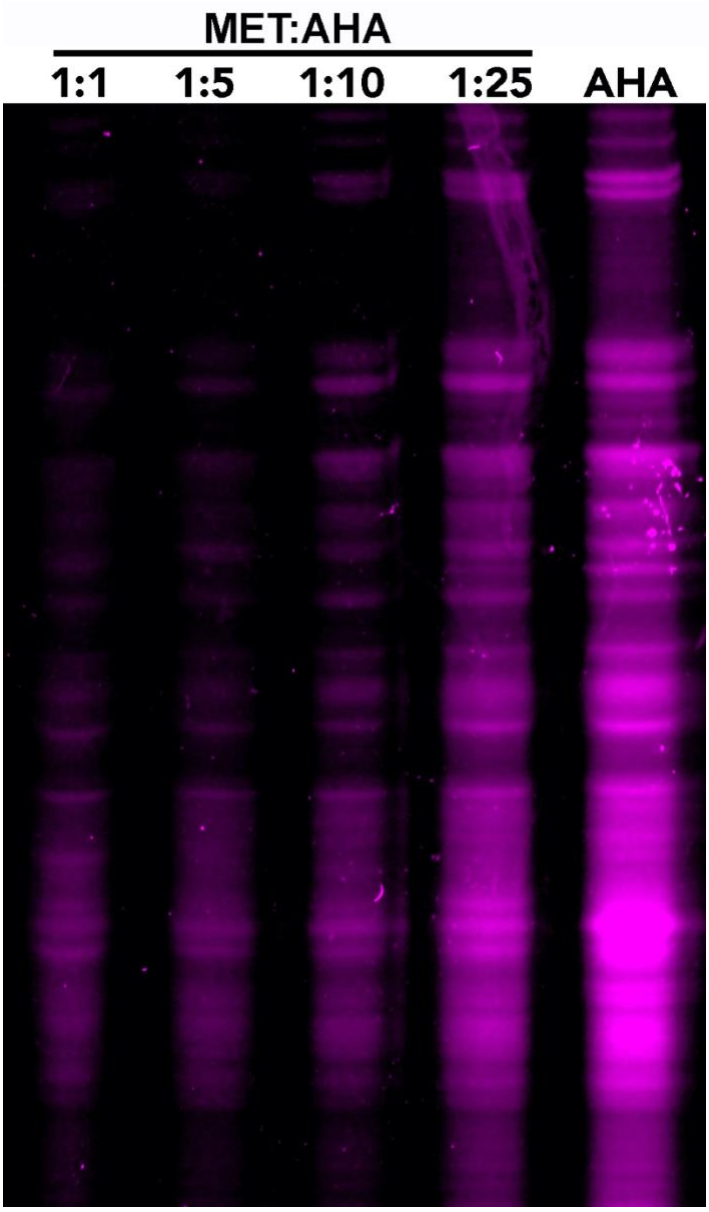

Figure S4. Supplementary Figure 4. SDS-PAGE determination of MET:AHA ratio required for BONCAT labeling of P. aeruginosa. Cells were grown in varying concentrations of MET:AHA prior to labeling with Cy5-DBCO. Based on these profiles, a 1:10 ratio was selected for labeling of in vitro bacterial cultures and expectorated sputum samples. These data are representative of three independent experiments. Full gel scans are provided as a Source Data file.

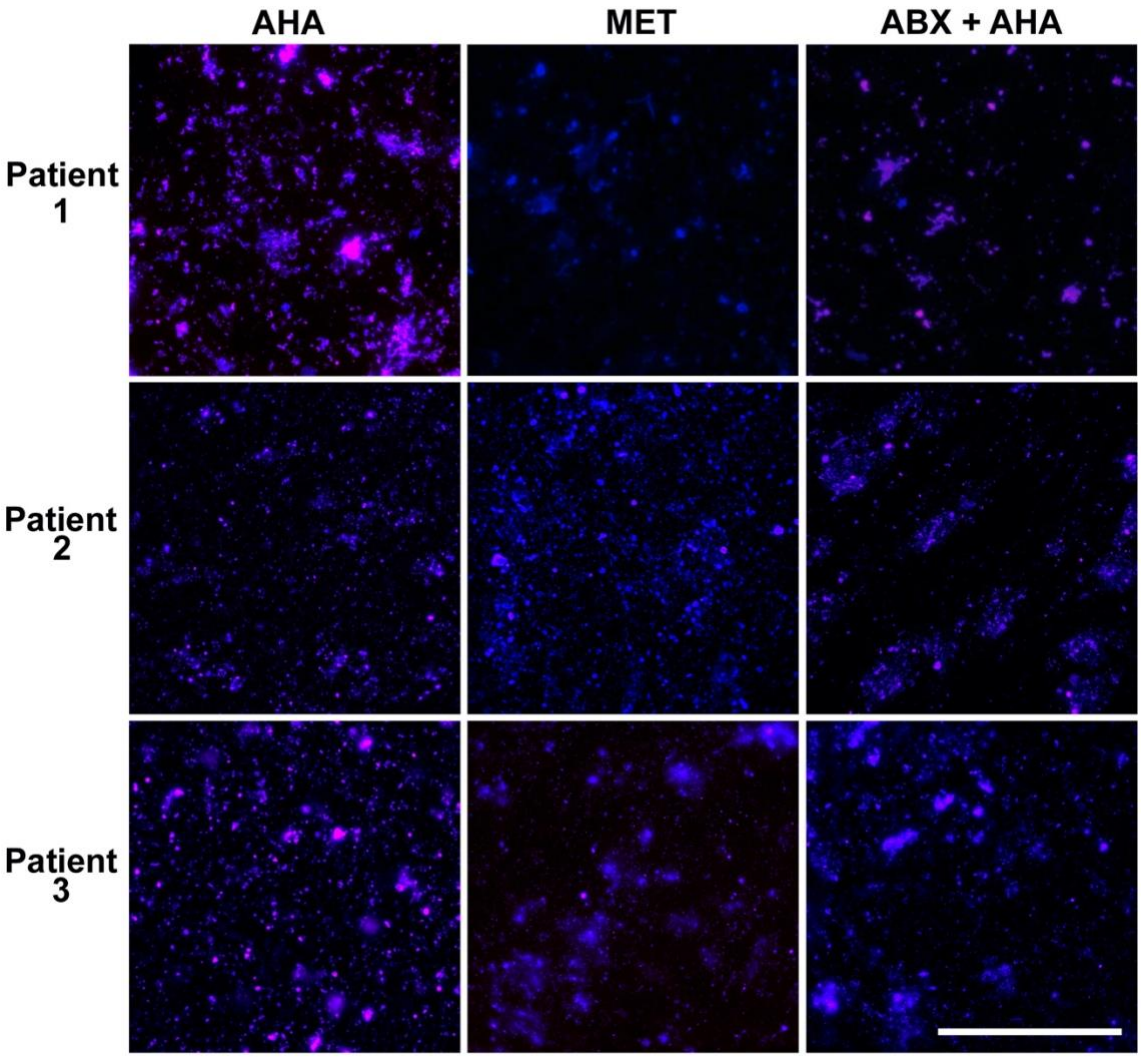

Figure S5. BONCAT labeling of sputum microbiota is specific for AHA. Expectorated sputum samples were supplemented with 6mM AHA and incubated for 3h prior to Cy5-DBCO labeling (Cy5; magenta) and counterstaining (SYTO64; blue). Negligible background fluorescence was observed in paired sputum samples incubated with methionine (MET). Incubation with antibiotics prior to AHA labeling (ABX+AHA) resulted in a moderate decrease in fluorescence that may reflect antimicrobial tolerance among airway microbiota. Bar = 100 μm. Abx = chloramphenicol, tetracycline, tobramycin. Data are representative of ten images from each patient sample.

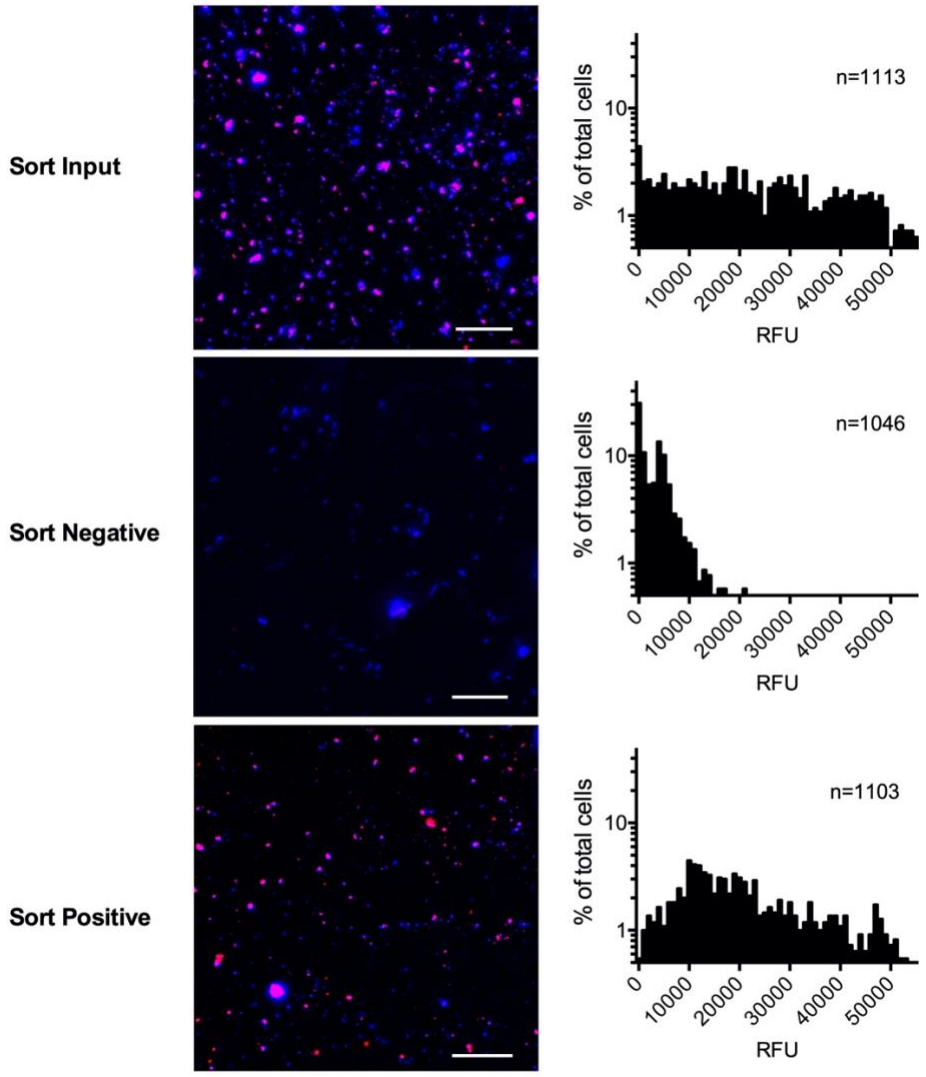

Figure S6. Supplementary Figure 6. Validation of BONCAT-FACS. During sorting, the Cy5 label is subject to photobleaching; we therefore used immunostaining (Cy3 anti-Cy5 antibody), fluorescence microscopy and quantitative image analysis in FIJI to validate FACS sort integrity. Pixel intensity was calculated as described in Methods. Anti-Cy5 labeling of sort input, sort negative and sort positive fractions demonstrates that BONCAT-FACS effectively removes host cells and translationally inactive bacteria from downstream 16S rRNA gene sequencing analysis. As expected, more cells in the positive fraction were anti-Cy5 reactive, confirming AHA uptake and translational activity among this bacterial subpopulation. However, some collected cells appeared unlabeled by the Cy3-labeled antibody. If we assume a mean pixel intensity of 10,000 as the cutoff between AHA-/AHA+ cells, these data suggest false negative and false positive sort rates of 6.8% and 12.0%, respectively. Bar = 10 µm. Source data are provided as a Source Data file.

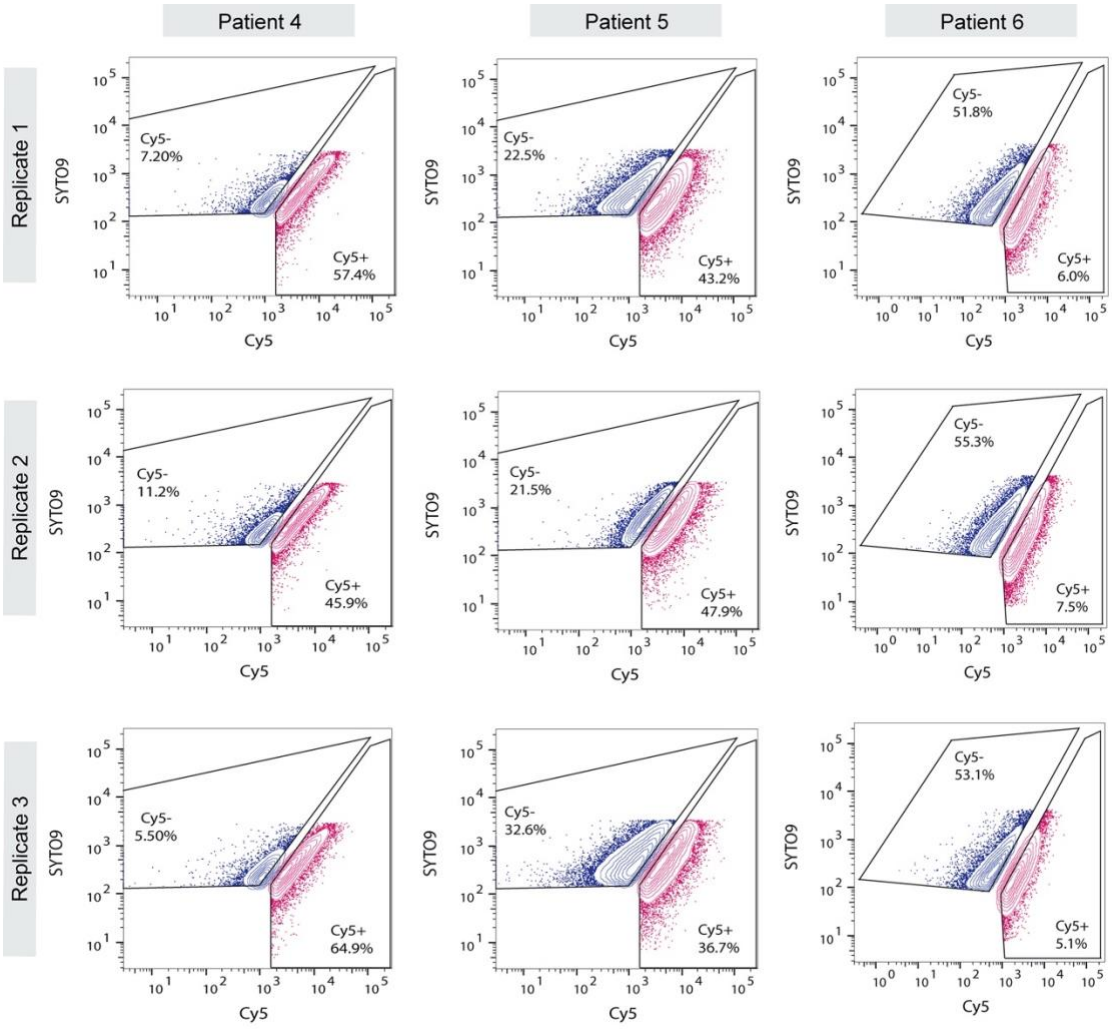

Figure S7. FACS of BONCAT-labeled sputum reveals consistency of Cy5- and Cy5+ subpopulations between replicates. Percentages shown reflect % of parent population post-CD45RO gating.

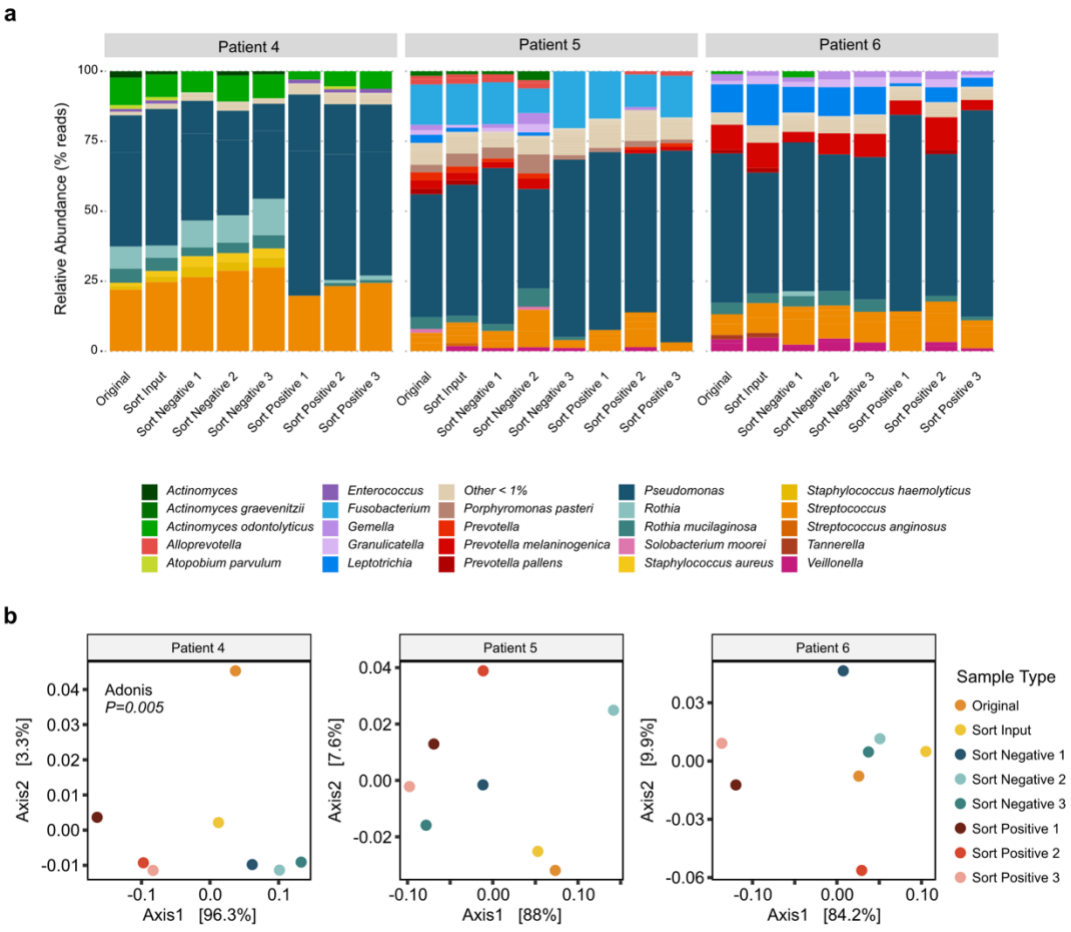

Figure S8. 16s rRNA gene sequencing reveals concordance of sort positive and sort negative replicates. (a) Stacked bar graphs of taxa relative abundance including all samples in analysis (triplicate positive and negative sort). (b) Double Principle Coordinate Analysis (DPCoA) shows grouping of samples by sample type.

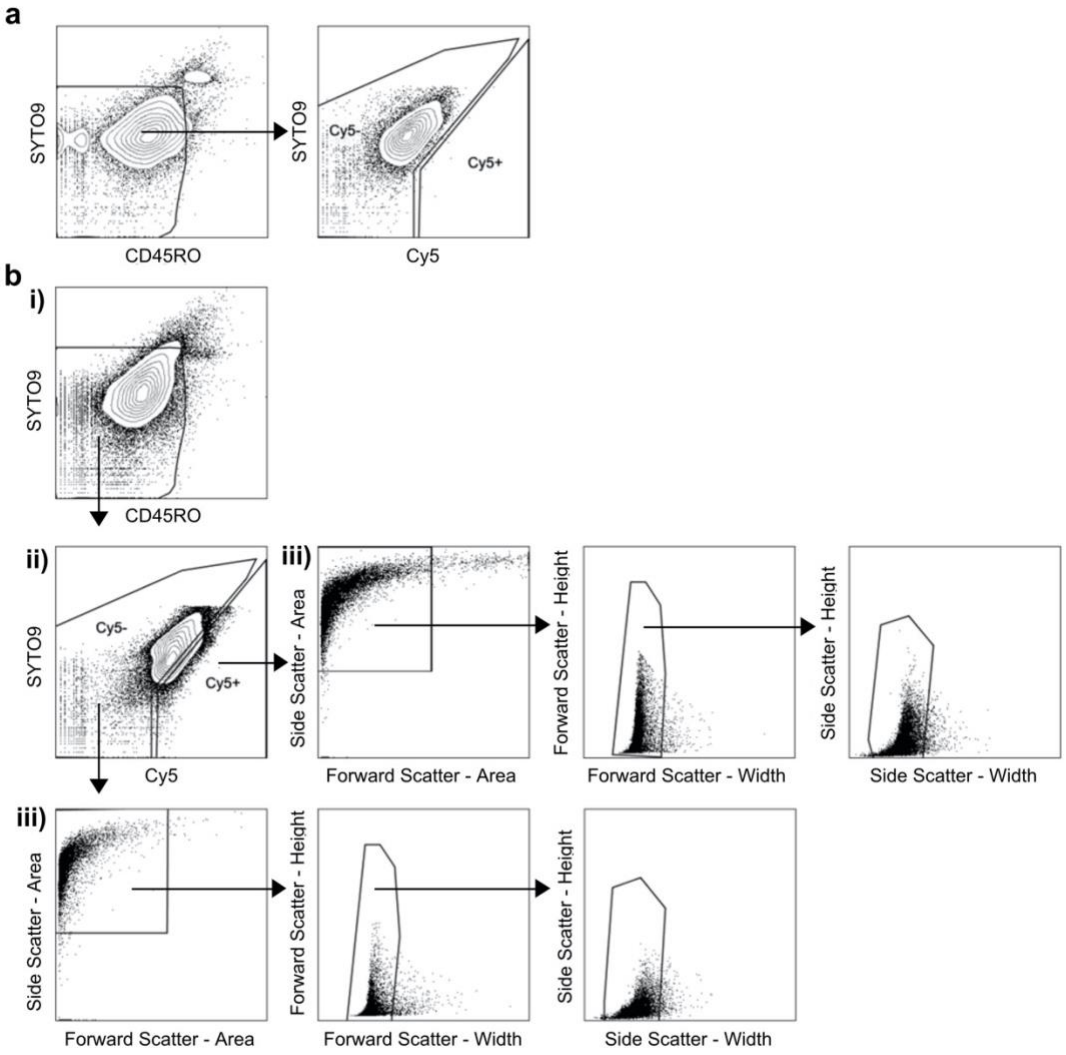

Figure S9. Representative gating scheme for AHA+ and AHA- populations. (a) AHA- control samples were first gated based on PE anti-human CD45RO staining to remove human leukocytes. Next, the negative control was used to measure background Cy5 fluorescence to define Cy5+ (i.e. active) and Cy5- (i.e. inactive) sorting gates. (b) shows a subject-matched AHA+ sample and the gating used to isolate populations of interest. The gating strategy involved, i) excluding human leukocytes using PE anti-human CD45RO, ii) using Cy5+ and Cy5- gates based on the subject-matched AHA- control, iii) creating forward scatter and side scatter plots to remove large, complex particulates and debris, and liberal doublet discrimination to minimize the loss of bacterial aggregates. The gating shown in panel ii corresponds to FACS data panels shown in Figures 5, S7, and S10.

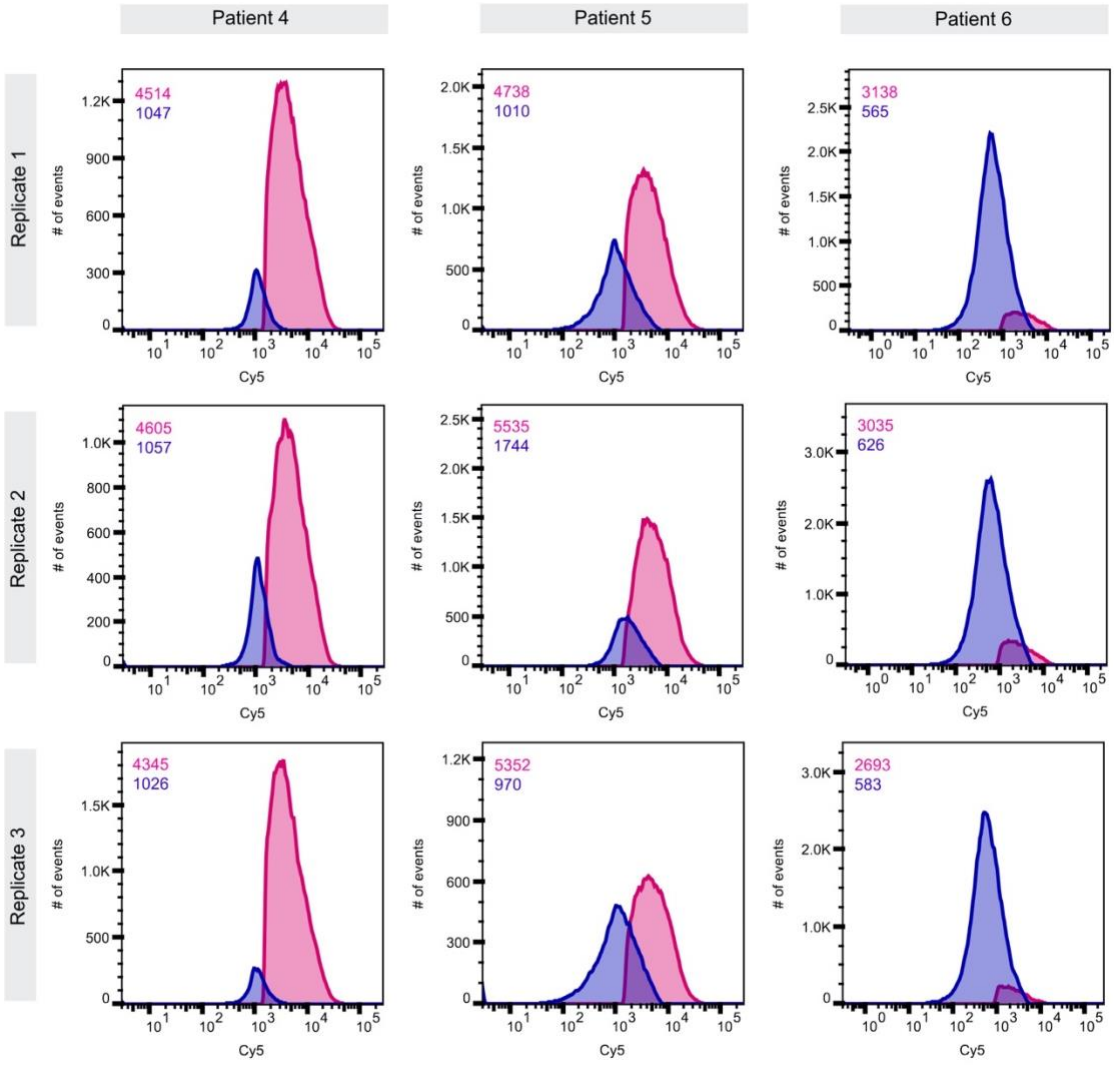

Figure S10. Confirmation of BONCAT Labeling. Flow cytometry histograms represent the number of events (cell counts) versus the log fluorescent intensity of Cy5 (blue = Cy5- population, magenta = Cy5+ population). Numbers in the upper left-hand corner represent the geometric means of Cy5 intensity. The Cy5+ population exhibited a higher geometric mean of fluorescent intensity validating AHA uptake and BONCAT labeling of the active subpopulation from CF sputum samples.

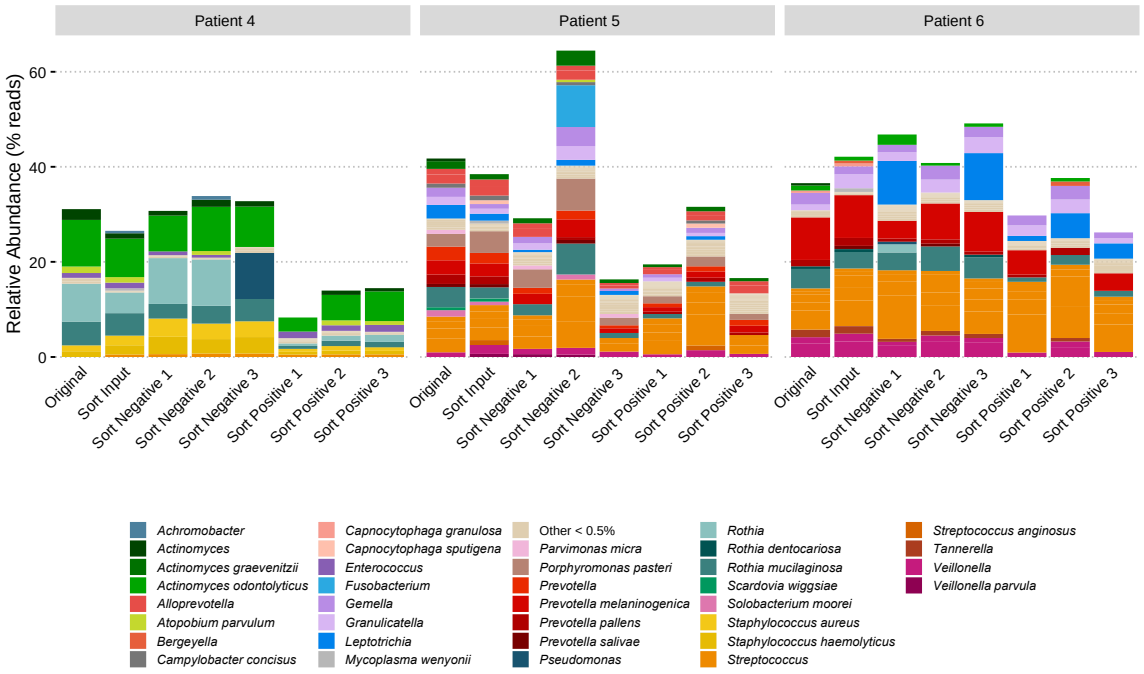

Figure S11. Low abundance community members are translationally active. Bacterial community membership of taxa with relative abundances less than 10% exhibit notable differences between "sort positive" community composition (i.e. translational activity) relative to the "original" fraction.

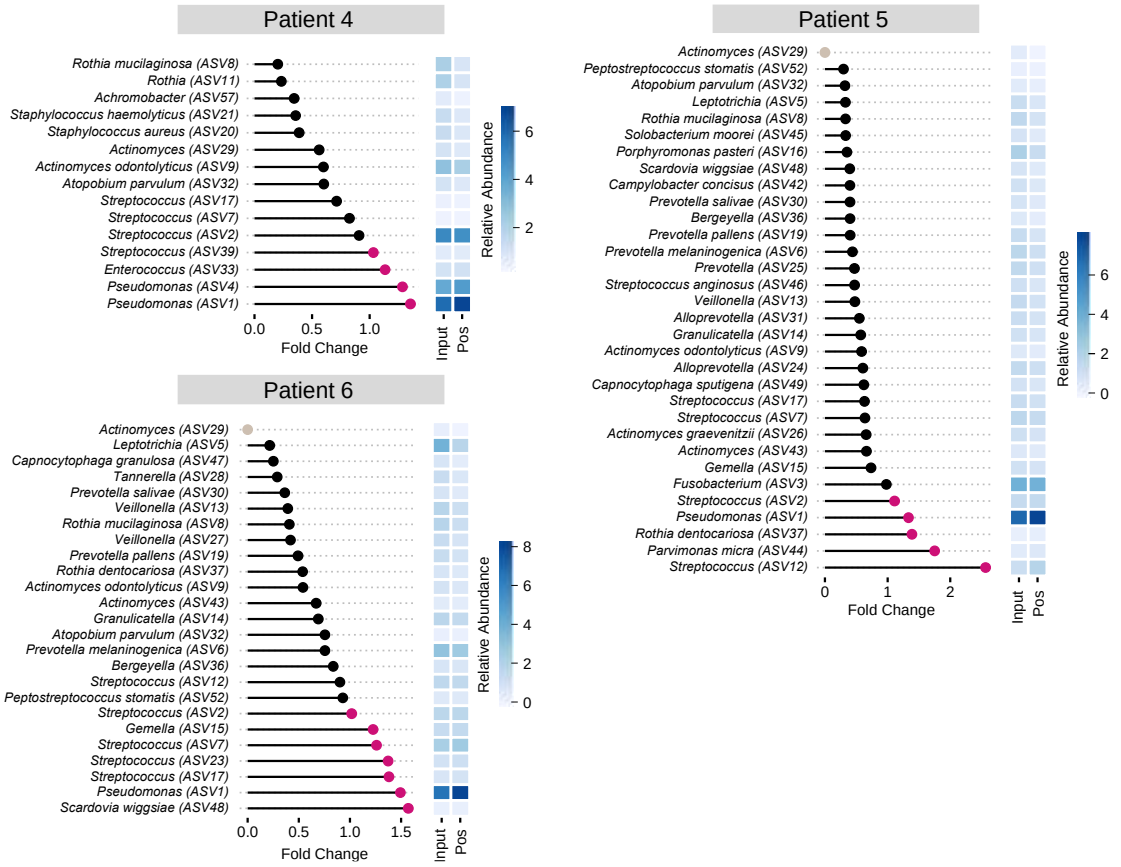

Figure S12. Fold difference in taxon relative abundance between "sort input" and "sort positive" fractions. Pink and black markers indicate taxa that were higher in relative abundance in the positive and input fractions, respectively. Source data are provided as a Source Data file.

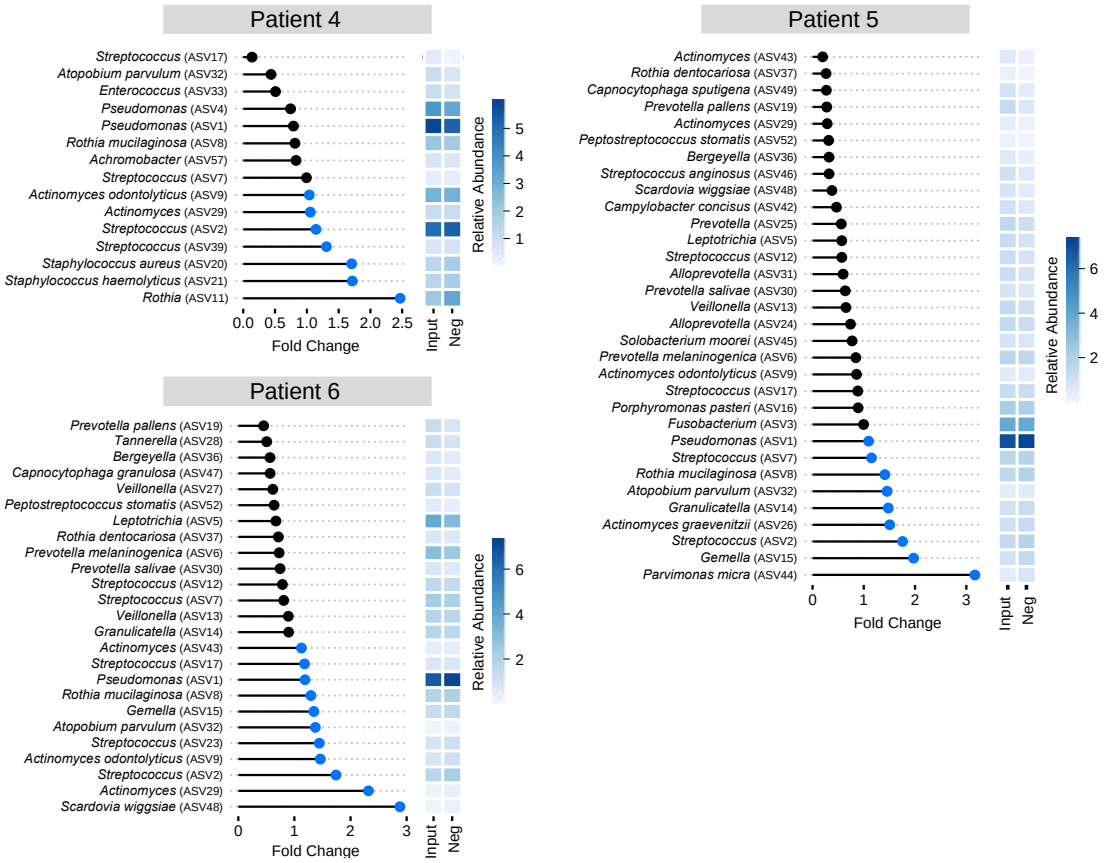

Figure S13. . Fold difference in taxon relative abundance between "sort input" and "sort negative" fractions. Black and blue markers indicate taxa that were higher in relative abundance in the input and negative fractions, respectively. Source data are provided as a Source Data file.

Supplementary Tables

Table S1. Cohort clinical data

Subject	Age	Sex	FEV1%	CFTR genotype	Bacterial Cultures	Current Antibiotics
1	23	F	38	ΔF508/ΔF508	*A. xylosoxidans*	azithromycin, colistin, doxycycline
2	38	M	31	ΔF508/ΔF508	*A. xylosoxidans*, *B. cepacia complex*, *P. aeruginosa*	azithromycin, aztreonam, doxycycline, meropenem, sulfamethoxazole-trimethoprim, zosyn
3	23	M	56	ΔF508/ΔI507	*P. aeruginosa*, *S. aureus*	azithromycin, aztreonam, tobramycin
4	26	F	42	ΔF508/N1303K	*S. aureus*, *P. aeruginosa*, *A. xylosoxidans*	azithromycin, colistin, gentamicin, sulfamethoxazole-trimethoprim
5	40	F	39	1898+1g>a/3849+10kbC>t	*P. aeruginosa*	azithromycin, aztreonam, ciprofloxacin
6	42	M	38	F508del/621+1G->T	*P. aeruginosa*	azithromycin, aztreonam, doxycyline

Table S2. BONCAT-FACS summary

Subject	Replicate	# of Cy5- events collected	# of Cy5+ events collected	% of Parent population[a] in Cy5- gate	% of Parent population[a] in Cy5+ gate	Geometric mean of fluorescent intensity (Cy5)[b] in Cy5- gate	Geometric mean of fluorescent intensity (Cy5)[b] in Cy5+ gate
4	1	1,632,712	4,000,000	7.2	57.4	1047	4514
	2	3,061,496	4,010,359	11.2	45.9	1057	4605
	3	1,329,894	4,000,000	5.5	64.9	1026	4345
5	1	1,983,509	4,001,293	22.5	43.2	1010	4738
	2	2,770,068	4,003,957	21.5	47.9	1744	5535
	3	4,000,000	4,003,615	32.6	36.7	970	5352
6	1	4,000,000	2,144,345	51.8	6	565	3138
	2	4,000,000	3,845,123	55.3	7.5	626	3035
	3	4,000,000	1,717,276	53.1	5.1	583	2693

[a] Percentages reflect % of parent population post-CD45RO gating. Remaining counts fell outside Cy5-/Cy5+ gates.
[b] Histograms are shown in Supplementary Figure 8.